

Draft Final Report

**Rheology Limits for Grout Materials
used for Precast Bent Cap Pile Pockets
in Hot Weather**

Contract Number BDV30 TWO 977-16

FSU Project ID: 037124

Submitted to:

Florida Department of Transportation

Research Center
605 Suwannee Street
Tallahassee, Florida 32399-0450

Steven Nolan, P.E.

Project Manager
FDOT Structures Design Office



Prepared by:

Raphael Kampmann, Ph.D.

Principal Investigator

Michelle Roddenberry, Ph.D., P.E.

Co-Principal Investigator

Stefan Oertker and Christoph Ebbing

Graduate Research Assistant

FAMU-FSU College of Engineering

Department of Civil and Environmental Engineering

2525 Pottsdamer Street

Tallahassee, FL 32310

2/28/2017

Disclaimer

The opinions, findings, and conclusions expressed in this publication are those of the authors, who are responsible for the facts and accuracy of the data presented herein. The contents do not necessarily reflect the views or policies of the Florida Department of Transportation or the Research and Special Programs Administration. This report does not constitute a standard, specification, or regulation.

The report is prepared in cooperation with the State of Florida Department of Transportation and the U.S. Department of Transportation.

Approximate conversion to SI units

Symbol	When you know	Multiply by	To find	Symbol
Length				
in.	inches	25.4	millimeters	mm
ft	feet	0.305	meters	m
yd	yards	0.914	meters	m
mi	miles	1.61	kilometers	km
Area				
in ²	square inches	645.2	square millimeters	mm ²
ft ²	square feet	0.093	square meters	m ²
yd ²	square yard	0.836	square meters	m ²
ac	acres	0.405	hectares	ha
mi ²	square miles	2.59	square kilometers	km ²
Volume				
fl oz	fluid ounces	29.57	milliliters	mL
gal	gallons	3.785	liters	L
ft ³	cubic feet	0.028	cubic meters	m ³
yd ³	cubic yards	0.765	cubic meters	m ³
Mass				
oz	ounces	28.35	grams	g
lb	pounds	0.454	kilograms	kg
T	short tons (2000 lb)	0.907	megagrams	Mg
Temperature				
°F	Fahrenheit	$\frac{5}{9}(F - 32)$	Celsius	°C
Illumination				
fc	foot-candles	10.76	lux	lx
fl	foot-Lamberts	3.426	$\frac{\text{candela}}{\text{m}^2}$	$\frac{\text{cd}}{\text{m}^2}$
Stress/Pressure				
lbf	poundforce	4.45	newtons	N
$\frac{\text{lbf}}{\text{in}^2}$ (or psi)	$\frac{\text{poundforce}}{\text{square inch}}$	6.89	kilopascals	kPa

Approximate conversion to imperial units

Symbol	When you know	Multiply by	To find	Symbol
Length				
mm	millimeters	0.039	inches	in.
m	meters	3.28	feet	ft
m	meters	1.09	yards	yd
km	kilometers	0.621	miles	mi
Area				
mm ²	square millimeters	0.0016	square inches	in ²
m ²	square meters	10.764	square feet	ft ²
m ²	square meters	1.195	square yards	yd ²
ha	hectares	2.47	acres	ac
km ²	square kilometers	0.386	square miles	mi ²
Volume				
mL	milliliters	0.034	fluid ounces	fl oz
L	liters	0.264	gallons	gal
m ³	cubic meters	35.314	cubic feet	ft ³
m ³	cubic meters	1.307	cubic yards	yd ³
Mass				
g	grams	0.035	ounces	oz
kg	kilograms	2.202	pounds	lb
Mg	megagrams	1.103	short tons (2000 lb)	T
Temperature				
°C	Celsius	$\frac{9}{5}C + 32$	Fahrenheit	°F
Illumination				
lx	lux	0.0929	foot-candles	fc
$\frac{cd}{m^2}$	$\frac{\text{candela}}{m^2}$	0.2919	foot-Lamberts	fl
Stress/Pressure				
N	newtons	0.225	poundforce	lbf
kPa	kilopascals	0.145	$\frac{\text{poundforce}}{\text{square inch}}$	$\frac{\text{lbf}}{\text{in}^2}$ (or psi)

Technical Report Documentation Page

1. Report No. BDV30 TWO 977-16		2. Government Accession No.		3. Recipient's Catalog No.	
4. Title and Subtitle Rheology Limits for Grout Materials used for Precast Bent Cap Pile Pockets in Hot Weather				5. Report Date February 2017	
				6. Performing Organization Code	
7. Author(s) Raphael Kampmann, Ph.D. Michelle Roddenberry, Ph.D., P.E. Stefan Oertker, and Christoph Ebbing				8. Performing Organization Report No.	
9. Performing Organization Name and Address Florida State University 600 W. College Avenue Tallahassee, FL 32306				10. Work Unit No. (TRAVIS)	
				11. Contract or Grant No. 037124	
12. Sponsoring Agency Name and Address Florida Department of Transportation 605 Suwannee Street Tallahassee, Florida 32399-0450				13. Type of Report and Period Covered Technical Report December 2015 – February 2017	
				14. Sponsoring Agency Code	
15. Supplementary Notes					
16. Abstract While prefabricated bridge elements and systems (PBES) have been used for many years in Florida, The Florida Department of Transportation (FDOT) is currently developing local specifications for PBES to address the Federal Highway Administration (FHWA) Every Day Count (EDC) initiative. The construction on the first designated PBES project in Florida started in 2013 on the US90 between Tallahassee and Quincy. Individual pre-fabricated elements were pieced together and – if needed – grouted to complete the connection details. During the pilot project, grout material was wasted due to the restrictive temperature range and flow rate limitations, specified by the grout manufacturer, or due to inadequate sealing of the connection point. This research aimed to evaluate grouted pile pocket connections to assist the standardization process. Information was gathered through simulating different flow spaces (grout gaps) as well as varying grout consistencies and temperatures, while documenting the flow, final air voids, the temperature development during the hardening process, and final grout strength. For acceptance testing, contractors generally model the structural elements from plywood. Therefore, the pile head for the mockup specimens was made from plywood as well. However, to allow for grout flow observations, the pile pocket was constructed from acrylic glass. PVC pipes were installed on top of the pile-pocket model to aid the filling and ventilation process, simulating ducts used in field construction. Throughout the research, it was determined that the fresh grout temperature, the viscosity of the material and the thickness of the gap between the pile head and the bent cap does not significantly affect the quality of the grout flow and fillability. However, it was found that a tapered roof (7%) inside the pile pocket promotes proper ventilation for the displaced air and helps to avoid air entrapment above the pile head corners. Additionally, it was noted that the current construction tolerances may lead to critical hydration temperatures for massive (high volume-to-surface ratio) grout volumes under hot weather conditions. The research suggests more rigorous construction tolerances to achieve a desired maximum gap size opening of less than 4 in. (100 mm).					
17. Key Word Rheology Limits, Grout, pile head-to-bent cap, pile-pocket, ABC connection, Accelerated Bridge Construction, hot weather grouting,				18. Distribution Statement	
19. Security Classif. (of this report)		20. Security Classif. (of this page)		21. No. of Pages 93 (108)	22. Price

Acknowledgments

The authors would like to thank the Florida Department of Transportation (FDOT) for providing the funding for this research. In particular, Steven Nolan, William A. Potter, David J. Wagner, Bruno Vasconcelos, and Stephen Eudy provided helpful comments and valuable discussions throughout the project. The staff at the FDOT Structures Research Center was very supportive and contributed to the success of this research.

Executive Summary

While prefabricated bridge elements and systems (PBES) have been used for many years in Florida, The Florida Department of Transportation (FDOT) is currently developing local specifications for PBES to address the Federal Highway Administration (FHWA) Every Day Count (EDC) initiative. The construction on the first designated PBES project in Florida started in 2013 on the US 90 between Tallahassee and Quincy. Individual pre-fabricated elements were pieced together and — if needed — grouted to complete the connection details. During the pilot project, grout material was wasted due to the restrictive temperature range and flow rate limitations, specified by the grout manufacturer, or due to inadequate sealing of the connection point. This research aimed to evaluate grouted pile pocket connections to assist the standardization process. Information was gathered through simulating different flow spaces (grout gaps) as well as varying grout consistencies and temperatures, while documenting the flow, final air voids, the temperature development during the hardening process, and final grout strength. For acceptance testing, contractors generally model the structural elements from plywood. Therefore, the pile head for the mockup specimens was made from plywood as well. However, to allow for grout flow observations, the pile pocket was constructed from acrylic glass. PVC pipes were installed on top of the pile-pocket model to aid the filling and ventilation process, simulating ducts used in field construction. Throughout the research, it was determined that the fresh grout temperature, the viscosity of the material and the thickness of the gap between the pile head and the bent cap does not significantly affect the quality of the grout flow and fillability. However, it was found that a tapered roof (7%) inside the pile pocket promotes proper ventilation for the displaced air and helps to avoid air entrapment above the pile head corners. Additionally, it was noted that the current construction tolerances may lead to critical hydration temperatures for massive (high volume-to-surface ratio) grout volumes under hot weather conditions. The research suggests more rigorous construction tolerances to achieve a desired maximum gap size opening of less than 4 in. (100 mm).

Contents

List of Figures	IV
List of Tables	VII
Acronyms	VIII
1 Overview	1
1.1 Introduction	3
1.2 Problem Statement	4
1.3 Research Objective	5
1.4 Research Scope	5
1.5 Report Organization	7
2 Background	8
2.1 Introduction	8
2.2 Grout Constituents	8
2.3 Hydration Process	12
2.4 Additional Ingredients	13
2.5 Properties – Fresh Grout Material	15
2.6 Properties – Hardened Grout Material	18
3 Experimental Program	21
3.1 Experimental Methodology	21
3.1.1 Mockup Specimen	22
3.1.2 Experimental Concept	23
3.1.3 Monitoring	25
3.2 Materials	26

3.2.1	Dry Grout Powder — MasterFlow 928 (BASF)	26
3.2.2	Water	28
3.2.3	Color Liquid	29
3.3	Devices and Equipment	29
3.3.1	Thermometer	30
3.3.2	Electric Mixer and Compressor	30
3.3.3	Flow Cone	32
3.3.4	Cube and Cylinder Molds	32
3.3.5	Digital Cameras	33
3.3.6	Thermocouples	33
3.3.7	Compressive Strength Test Machine	34
3.4	Test Procedures	36
3.4.1	Specimen Preparation	36
3.4.2	Mixture and Filling Process	40
3.4.3	Post Grouting Activities	43
4	Experimental Results	47
4.1	Fresh Grout Properties	47
4.1.1	Vertical Side Volumes	49
4.1.2	Horizontal Top Volumes	51
4.2	Temperature Development	53
4.2.1	Identical Gap Size Openings for all Vertical Volumes	53
4.2.2	Various Gap Size Openings for Vertical Volumes	56
4.2.3	Temperature Development Throughout Various Grout Batches	58
4.3	Air Void Formation	60
4.3.1	Vertical Side Surfaces	60
4.3.2	Horizontal Top Surface	62
4.4	Intermixing of Subsequent (Fresh-in-Fresh) Grout Batches	67
4.5	Compressive Strength	70
4.5.1	Compressive Strength Results for Cast Cubes	70
4.5.2	Compressive Strength Results for Extracted Cubes	74
4.5.3	Compressive Strength for Cast and Extracted cylinders	76

5	Analysis and Discussion	78
5.1	Significance of Study	78
5.2	Critical Analysis of Major Findings	79
5.3	Additional Findings	83
5.4	Limitations	85
5.5	Further and Future Directions	86
6	Conclusion	88

List of Figures

1.1	3D model - PBES system (Ebbing, 2016)	3
1.2	3D model - connection detail	3
1.3	Mockup specimen for connection type Level 1 20710 series	6
2.1	Basic ingredients of grout	9
2.2	Side view flow cone (ASTM-International, 2016b)	17
3.1	Comparison between on-site model and laboratory mockup specimen	22
3.2	Experimental Monitoring	25
3.3	BASF MasterFlow928	27
3.4	Thermometers	30
3.5	Mix and pumping system	31
3.6	Flow cone	32
3.7	Cube and cylinder molds	33
3.8	Video Cameras	34
3.9	Thermocouple system	35
3.10	Compressive strength test machine	36
3.11	Formwork for mockup specimen — disassembled	37
3.12	Formwork for mockup specimen — assembly of individual pieces	38
3.13	Thermocouple set up	39
3.14	Mockup specimen — formwork	40
3.15	Laboratory Setup	41
3.16	Mockup specimen MU9 — after grouting was completed	43
3.17	Cast 2 in. (50 mm) grout cubes — example based on MU8	44
3.18	Mockup specimen 48 h after grouting	45
3.19	Mockup specimen MU8 — tested samples	45

4.1	Filling sequence for MU7 — vertical side volume	50
4.2	Filling sequence for MU7 — horizontal top volume (with a slope of 3.5%)	52
4.3	Filling procedure MU9 — horizontal top volume	53
4.4	Temperature development after mixing grout for MU2	54
4.5	Temperature development after mixing grout for MU9	55
4.6	Temperature development after mixing grout for MU10	56
4.7	Temperature development after mixing grout for MU5	57
4.8	Temperature development after mixing grout for MU7	58
4.9	Temperature development after mixing grout for MU8	59
4.10	Temperature development after mixing grout for MU11	59
4.11	Outer vertical side surface monitoring	60
4.12	Inner vertical side surface for MU9 — maximum grout volume thickness of 2.0 in. (50 mm) Gap	61
4.13	Top Surface MU3 — representative for specimens with lower water-to-material ratio	62
4.14	Air void pattern indicate the grout flow (for mockup specimen MU3)	63
4.15	Top surface MU6 — representative for specimens with higher water-to-material ratio	64
4.16	Outer horizontal top surface of MU8 — minimum volume thickness 0.5 in. (12.5 mm), maximum volume thickness 1.0 in. (25 mm)	65
4.17	Outer horizontal top surface of MU11 — minimum volume thickness 1.0 in. (25 mm), maximum volume thickness 2.0 in. (50 mm)	65
4.18	Inner top surface for MU11 — maximum grout volume thickness of 1.0 in. (50 mm)	66
4.19	Air voids around shims — comparison between differently tapered top surfaces	67
4.20	Outer side surface MU1 — 2.0 in. (50 mm) gap	68
4.21	MU8 with color coded layers	69
4.22	Cast cube compressive strength after one (1) day — Task 2	70
4.23	Cast cube compressive strength after three (3) days — Task 2	71
4.24	Cast cube compressive strength after 28 days — Task 1	72
4.25	Cast cube compressive strength after 28 days — Task 2	72
4.26	Compressive strength development of each batch for MU7 (based on average of cast cubes)	73
4.27	Cube Compressive Strength Development MU8	73
4.28	Compared Cube Compressive Strength for MU7 after 28 days	74
4.29	Compared Cube Compressive Strength for MU9 after 28 days	75
4.30	Compared Cube Compressive Strength for MU10 after 28 days	76
4.31	Compared Cylinder Compressive Strength for MU7	76

4.32 Compared Cylinder Compressive Strength for MU8	77
---	----

List of Tables

2.1	Four (4) different clinker phases	10
2.2	Portland cement types — ratios	11
2.3	Chemical reactions during hydration process	12
2.4	Supplementary Cementitious Materials (SCM)	14
3.1	Test matrix	23
3.2	BASF MasterFlow 928 — Compressive Strength Requirements	27
3.3	Florida Department of Transportation (FDOT) — Compressive Strength Requirements	28
4.1	Fresh grout properties MU1 – MU6	48
4.2	Fresh grout properties MU7 — MU11	49

Acronyms

AASHTO	American Association of State Highway and Transportation Officials
ABC	Accelerated Bridge Construction
ASTM	American Society of the International Association for Testing and Materials
CRM	Cement Replacement Materials
CSF	Condensed Silica Fume
EDC	Every Day Count
FAMU	Florida A&M University
FDOT	Florida Department of Transportation
FHWA	Federal Highway Administration
FSU	Florida State University
GGBFS	Ground Granulated Blast Furnace Slag
MU	Mockup Specimen
PBES	Prefabricated Bridge Elements and Systems
PFA	Pulverised Fuel Ash or Fly Ash
PIBC	Precast Intermediate Bent Caps
SCM	Supplementary Cementitious Materials
SSDO	State Structure Design Office
USA	United States of America
US 90	US 90 over Little River/Hurricane Creek pilot ABC/PBES project

Chapter 1

Overview

The Federal Highway Administration (FHWA) financially supports the construction, maintenance and preservation of highways, bridges and tunnels in the United States of America (USA). The FHWA is divided into several state and local agencies, that initiate different research projects and offer technical assistance.¹ The Florida Department of Transportation (FDOT) is one of FHWA's partner organizations that is concerned with the state infrastructure in Florida (USA). The FDOT is responsible for about 122 000 highway miles and 3800 railway miles, as well as for different public transportation systems, to realize and improve a well designed infrastructure. Within these responsibilities, FDOT constructs and maintains structural projects that include approximately 6300 state owned bridges, several air ports, and spaceports or seaports. In addition, the FDOT provides assistance for approximately 6000 locally owned bridges. The major goal of each project targets safety, preservation, mobility, economy and environment safety. Every year, Florida welcomes the third biggest population within the USA with about 105 million visitors annually.² In 2009, FHWA initiated a collaboration with American Association of State Highway and Transportation Officials (AASHTO) to introduce an innovative program called Every Day Count (EDC). This initiative was designed to minimize traffic impairments and high costs, if any construction work is necessary within the transportation system. New construction projects under this initiative should target faster construction times, lower cost, and improved construction details and processes. The EDC program collects new developments from all over the country every two (2) years. After an efficient analysis of innovative projects, the best technologies are selected to distribute the concepts among participating agencies across the USA.³ Accelerated Bridge Construction (ABC) is one of the ideas within this initiative, to specifically improve the efficiency of bridges and bridge construc-

¹ Information retrieved on November 16, 2016
from: <https://www.fhwa.dot.gov/>

² Information retrieved on November 16, 2016
from: <http://www.fdot.gov/agencyresources/aboutFDOT.shtm>

³ Information retrieved on November 16, 2016
from: <https://www.fhwa.dot.gov/innovation/everydaycounts/about-edc.cfm>

tion, and to facility faster bridge replacements. The major goals are better site constructibility, reduced total project durations, and improved work-zone safety for the traveling public.⁴

Based on FHWA’s EDC initiative, the FDOT recently deployed design requirements for evaluating Prefabricated Bridge Elements and Systems (PBES) for state bridges. “PBES is defined as the structural elements of the bridge that are built in a prefabricated manner either off site or adjacent to the existing alignment (Anthony Rotondo, 2013)⁵“, and promises many benefits — especially for ABC projects. PBES projects results in time savings, cost savings, safety advantages and convenience for travelers. The on site time, especially for bridges built over water, becomes shorter, such that the environmental impact and safety risks from construction work can be reduced. Additionally, the work schedule on site can easily be adjusted, to minimize the seasonal impact on wildlife activity and native flora (Roddenberry and Servos, 2012). However, different and new challenges are inherent to modern construction developments because long-term analyses are unavailable and local experiences have to be collected, on the design level and in the field by contractors (fabrication and construction). While individual bridge elements (deck panels, girders, bent caps, etc.) may have been proposed for standardization, the connection details are still under refinement. It is emphasized that the connection details are more critical in ABC projects, not just because of the increased number of connections, but also because each individual connection contributes to the final unified structural behavior. PBES projects consist of separated elements, that have to be transported, assembled and connected on-site. Figure 1.1 schematically shows an example for a PBES structure, in which the bearing system is based on two (2) columns that support the prefabricated bent cap. Above the bent, individual beams are spanned along the traffic direction to support the individual transversely placed deck panels. Other components are necessary to complete an ABC project, but the shown elements suffice to exemplify the concept.

Each bridge project has to meet different site specific requirements — geometrical and aesthetic — so that no two (2) bridges are alike. The connection details between the prefabricated elements such as piles, bents, or deck panels, may differ to accommodate specific local requirements (i.e.; varying climate conditions). A recent demonstration PBES project in Florida included four (4) individual bridges that spanned over Little River and Hurricane Creek on US 90 over Little River/Hurricane Creek pilot ABC/PBES project (US 90) (between Tallahassee and Quincy). Certain issues related to individual connection details obstructed the construction process, which was the genesis for this research project.

⁴ Information retrieved on November 20, 2016
from: <http://www.fhwa.dot.gov/bridge/abc/>

⁵Past Bridge Program Manager for the Federal Highway Administration

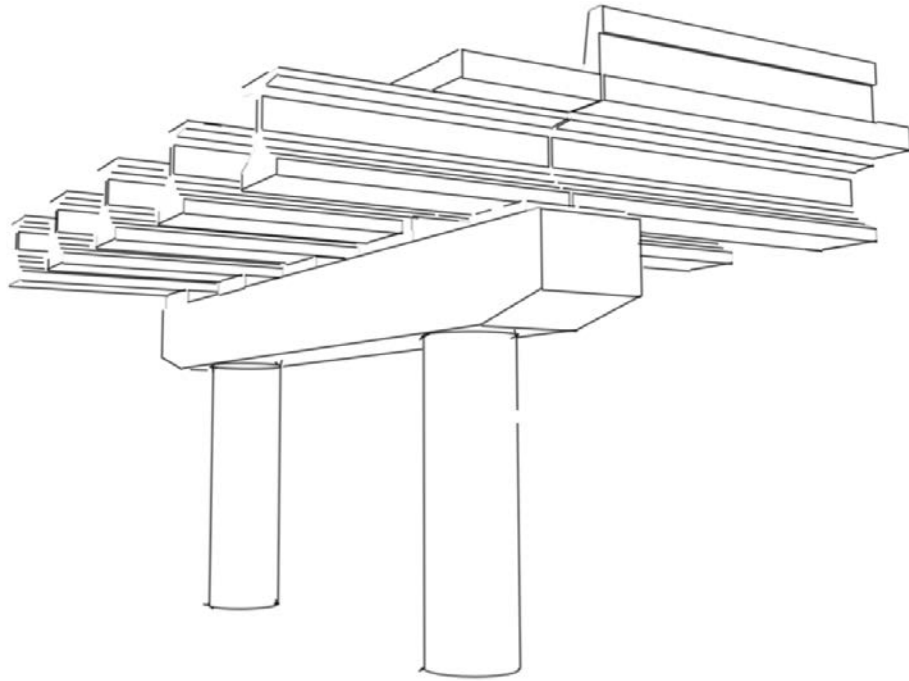


Figure 1.1: 3D model - PBES system (Ebbing, 2016)

1.1 Introduction

The State Structure Design Office (SSDO) currently develops standard details and specifications⁶ for different ABC elements and construction details. The general concept of PBES for a pile-to-bent cap interface may be addressed in different ways, and a grouted pile-pocket inside the bent cap appears to be a promising solution. Figure 1.2 illustrates such a concept for a pile with a square cross section. The lower portion of the bent

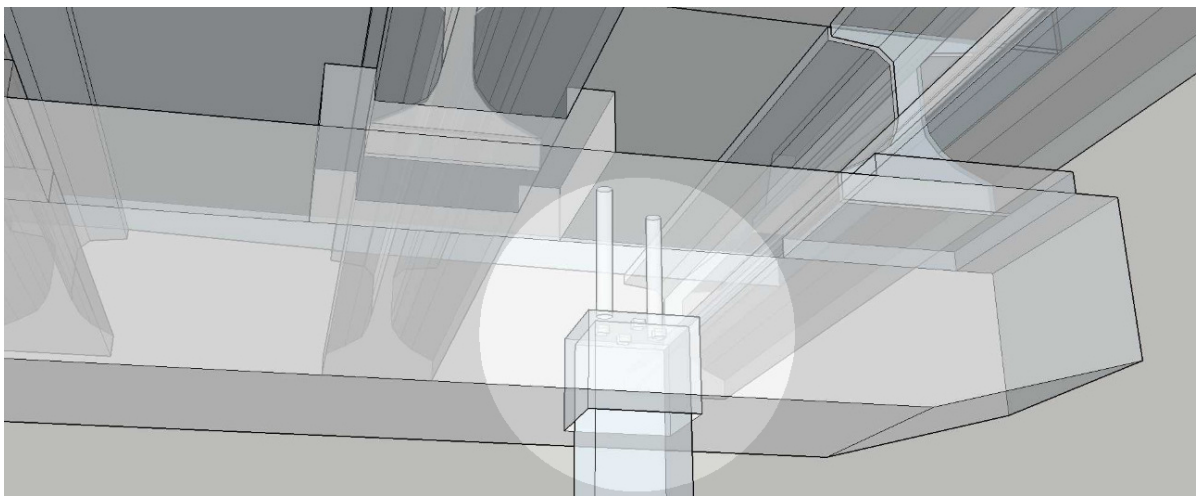


Figure 1.2: 3D model - connection detail

cap encases the pile head via a preformed pile-pocket, so that the bent cap can be placed over the pile head

⁶to expand the state-of-practice and design standards at <http://www.fdot.gov/roadway/DesignStandards/Standards.shtm>

(shims serve as spacers, or fiction collars can be used). The opening between the pile and the pocket have to be sealed with grout to guarantee a unified behavior of the composite structure. After sealing the bottom of the remaining openings under the pile-pocket via a formwork collar, the fresh grout can be filled into the open gaps through one (1) of the pipes that protrude to the top surface of the bent cap, as seen in Figure 1.2, while the other pipe serves a ventilation purpose and as visual inspection port.

1.2 Problem Statement

Recently, during the US 90 demonstration project, it was observed that grouted connections may be challenging for contractors in Florida due to the tight temperature range limitations set by grout manufacturers — depending on the actual product, the material temperature must range between 45 °F and 90 °F (7 °C and 32 °C) during pumping, placement, and initial curing. Due to imposition of even stricter “preferred” temperature ranges, a lot of freshly mixed grout material had to be wasted throughout the US 90 demonstration project, since the temperatures of the fresh grout significantly exceeded the manufacturers’s preferred temperature 70 °F to 80 °F (21 °C to 27 °C) temperature range (Steve Nolan, 2015). In consequence, it appeared beneficial to further/closer evaluate the temperature tolerances in the upper range that is not considered “preferred“ for use in local projects.

In addition, it was observed that the formwork collar on the bottom of the drilled shaft connection detail was not adequately caulked at times, so that additional material was lost during grout placement and an unknown amount of grout probably remained within the openings.

Although the construction workers responded quickly and sealed the formwork to continue the grouting process, it was uncertain how much residual material remained inside the open space and how that material was distributed. After the grouting process was finished, it was impossible to monitor the connection to confirm if the grout entirely filled all gaps with minimal air entrapment. The experienced set-backs on the construction site during the US 90 project suggested that the proposed pile head-to-bent cap connection detail should be studied in more detail to evaluate the flow and fillability of the grout material under varying geometric (gap sizes) and hot weather conditions.

While it is assumed that pile-pockets emulate cast in-place designs/behavior after grouting, it must be noted that such structural behavior can only be guaranteed if the grout material can flow freely to penetrate the entire pile pocket, without significant air voids. This does not only depend on the flowability of the grout, but also on the available openings between the surfaces of the pile and the surfaces of the pockets (flow-space), as well as on the surface friction during flow. Flow space is contingent on the precision of the pile installations and/or the accuracy of the bent cap placement — in practical applications, less than ideal conditions may be encountered. Consequently, properly defined placement tolerances (max/min gaps

around and over the pile) are an important consideration for the standardization process. It appears that no published research on the topic was available, and that constructibility of the proposed connection detail — at the marginal limits of the rheological properties of the grout material — should be evaluated. To ensure sound connections through adequate standards, the flowability and consolidation of grout during placement under various conditions must be observed and evaluated.

Finally, it is noted that local projects entailing such grout connections currently require contractors to perform mockup tests for material and procedure acceptance. Contractors generally model the mockup structural elements with different materials, other than concrete; plywood seems to be the material of choice due to its adaptability and cost efficiency. Although the surface properties of the structural elements clearly impact the flow of the grout, it is unknown how critical this effect may be for proper consolidation of grout in pile pockets for PBES projects. The flow over concrete surfaces (relatively smooth and less absorptive) may differ significantly from the flow over plywood surfaces (not as smooth and more absorptive). Hence, the commonly used plywood surfaces should be evaluated for grout flowability under representative conditions to determine if plywood models are suitable for proper representation during acceptance testing.

1.3 Research Objective

This research aims to evaluate grouted pile pocket connections to gather subsidiary information on limiting factors — anticipated throughout the construction process — to assist the SSDO in the standardization of Precast Intermediate Bent Caps (PIBC). It was the objective to identify or establish preliminary limits for the acceptability of grout properties and geometrical restrictions to ensure adequate consolidation of gravity fed grout for the proposed connection detail. The study intended to obtain such information through the simulation of different flow-spaces (gaps between pile and pocket surfaces) and varying grout flow rates and fresh temperatures throughout the placement process. Additionally, it was the goal of this project to qualitatively study and rate the residual air voids, construction joints between batches, and the suitability of plywood surfaces for mockup specimens.

1.4 Research Scope

Different connection types are currently under development for FDOT implementation. FDOT's proposed Index D20710 series — pile and bent cap with grouted pile pockets — as exemplified in Figure 1.2 is considered one of the most common connection types used for bridge constructions in Florida. Therefore, this research focused on this particular connection and does not discuss other types of connection details. However, most pile/column to bent connections follow a similar concept and the results are expected to be applicable to

many of these other systems as well. Figure 1.3 illustrates two (2) sections of FDOT’s Index D20710 series, that were obtained from a preliminary (08/03/2016) design, which has not been published by FDOT yet. The

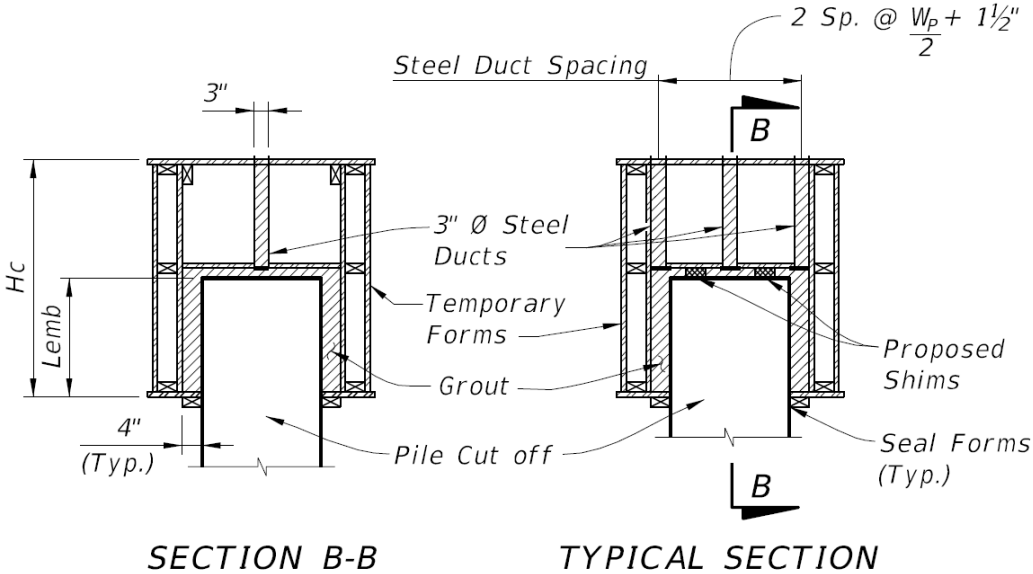


Figure 1.3: Mockup specimen for connection type Level 1 20710 series

drawing proposes a gap size opening of 4 in. (100 mm) for the vertical side volume (adjacent to the pile), and a 3 in. (75 mm) diameter for the three (3) ducts, which are needed to gravity feed the grout into the gaps (via one (1) of the ducts) and to simultaneously provide an escape route for the displaced air (through the other two (2) ducts). Additionally, the preliminary design suggests tolerances for the size of the bent cap pocket and for the pile head, as well as for the pile placement. According to FDOT Standard Specifications (Section 455), the position of the pile head may vary within ± 3 in. (± 75 mm) relative to the plan position. As a result, the gap size of the vertical volume may decrease to 1 in. (25 mm), or it may be as wide as 7 in. (178 mm). To provide flow space for the dropped in grout, the drawing shows two (2) shims on top of the pile head without specified minimal dimensions. Also, it should be noted that the roof of the pile-pocket is proposed with a level surface. The FDOT proposed connection detail in Figure 1.3 was evaluated in this research — all specimen dimensions and geometric details were based on this initial draft, and the experimental phase was designed to evaluate the limiting cases for various gap dimensions.

This project focused on the rheological properties of the grout material under varying placement temperatures, flow rates, and different flow-space geometries. Task 1 studied six (6) pile pocket mockup specimens with varying properties of fresh grout materials. Based on Task 1 findings, five (5) additional mockup specimens were prepared for Task 2, to further study the geometric properties of the grout spaces (gap width and slope of pile-pocket roof), and to evaluate the grout flow, temperature development, and hardened material properties under extreme conditions (minimum and maximum gap sizes, high grout temperatures, and high

viscosity). Due to the small number of specimens, the utilized grout material for the mockup specimens was limited to a single product; BASF MasterFlow 928. This grout material was chosen because previous SRC mockup bridge deck panel tests and the US 90 PBES demonstration project both employed BASF MasterFlow 928 for all grouted connections, and it was anticipated that the specific material would be used for similar projects in the future (Vikie Young and Dennis Golabek, 2016). A proper flow and void analysis was essential to this project, which was facilitated through transparent and translucent molds — the outer formwork for all mockup specimens was constructed from clear acrylic sheets. The pile heads were generally modeled from plywood — except for the control specimen (MU1) — as contractors would typically utilize plywood for preconstruction grouting demonstrations and acceptance tests. Furthermore, the temperature developments of the hardening grout and the compressive strengths at different maturity levels were measured to monitor the material properties of the placed grout.

1.5 Report Organization

This research report was organized and separated into six (6) chapters. Chapter 2 discusses the major aspects and properties of grout materials. A detailed overview of the individual grout constituents is provided and background information about the fresh and hardened properties are provided. In addition, literature that appears applicable to this research project is reviewed. Chapter 3 provides the research approach, the test matrix, the construction of the mockup specimens, the material properties, and the test procedures are detailed in the experimental program. All test results and findings are documented in Chapter 4, and a detailed discussion with future research recommendations is presented in Chapter 5. Chapter 6 concludes this report and provides quick access to the most essential interpretations of the findings.

Chapter 2

Background

2.1 Introduction

After placing the individual prefabricated bridge elements together, the gaps between the concrete elements have to be properly connected to guarantee a unified behavior of the bridge as a whole. The gaps between the pile head and the bent cap are generally grouted for those types of bridges. Therefore, this chapter details and discusses the principle aspects and key aspects of grout. Grout materials are mixtures that consist of different ingredients — cement, fine aggregates, admixtures, water — dependent on the individual project requirements. Throughout recent years, several different developments lead to many varying options for grouting and grout materials. Nevertheless, a few basic materials are essential to any grout mixture mixture. Section 2.2 provides information about the general material aspects and discusses the basic ingredients that are most common today. After mixing and placement, the grout needs time to become hard. The hydration process, that takes place during hardening, is described in Section 2.3. Modern developments and technologies allow engineers to specifically target certain fresh or hardened properties through the addition and adjustment of certain ingredients. These materials are discussed in Section 2.4, for both scenarios — during/after mixing, and during/after hardening. While Section 2.5 provides information about the main characteristics of fresh grout, Section 2.6 discusses the major properties of the hardened grout.

2.2 Grout Constituents

Fresh grout is a semi-liquid mixture of sand, water, and cementitious materials, which hardens through chemical reactions between the water and the cementitious powder (see Subsection 2.3). The basic constituents are illustrated in Figure 2.1. In general, only cement and water are necessary for the hardening process, that ultimately produces an artificial stone mass. However, sand is relatively cheap and used as a filler to produce

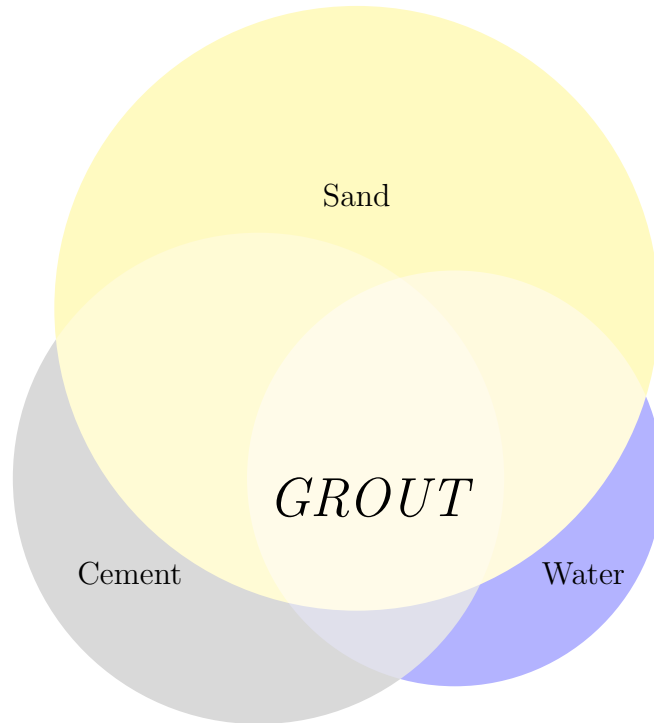


Figure 2.1: Basic ingredients of grout

a large volume more efficiently. Therefore, sand is presented in the biggest bubble due to its huge portion compared to the other constituents. All three (3) ingredients can be added in different ratios, and an endless number of grout materials with varying properties (see Section 2.5 and Section 2.6) can be produced. Even, if the individual ingredients have the same ratio, each single material — sand, cement and water — has multiple different variations, so that same grouts with identical properties are rarely seen. However, instead of self-mixed grout, nowadays factory prepackaged dry grout materials that contain all basic ingredients (and other additives) are common. Such material, was used for the drilled shaft column to bent cap interface for connecting the PBES of the US 90 demonstration project. These bags contained cement, sand, and other proprietary ingredients and admixtures. The exact composition and proportions of these materials are only known to the grout manufacturer. To obtain a suitable grout mixture, water (at specific quantities) must be added and well mixed into the grout powder to produce a coherent and flowable fresh grout that properly fills the gaps. The following paragraphs provide additional information about the individual grout ingredients, sorted according to their weight percentages of the mixture.

Sand Because sand is a filler material in grout, it makes up the biggest portion of the volume and weight of the grout material. Due to its amount and weight, it is uneconomical to transport sand over long distance and manufacturers for ready mixed grout bags as well as contractors on site, usually use regional sand materials, such that the final grout product is normally highly influenced by the locally available materials.

Portland Cements The grout material matrix contains cement as the second biggest constituent — by weight. Through the addition of water, a chemical reaction (hydration) is initiated that promotes the hardening process (see Subsection 2.3).

The history of cementitious materials goes back to the Phoenicians, Greeks and Romans, who burnt lime, mixed the result with different additives and developed the so-called “Opus Caementitium” — Roman concrete Bosold and Pickhardt (2014). The Pantheon in Rome, Italy, was constructed between 110 and 114 AD, it was made from “Opus Caementitium” and it is still standing strong today (Ballantyne, 2012). Many centuries later, in 1824, the Englishman J. Aspdin developed a cement that was similar to the Portland cement that we know and use today. He ground limestone and clay, to produce the raw materials that were burned (sintered) at 2650 °F (1450 °C). Because the final concrete product looked quite similar to the light gray stones around the area called Portland in England, this type of cement made from limestone as the major ingredient was termed Portland cement Bosold and Pickhardt (2014). Today, almost 200 years later, chalk and limestone (CaCO_3) are still the major ingredients in modern Portland cement production. Additionally, clay and shales with a basis of alumina, silicate oxide and iron oxide, that are necessary for chemical reactions in the later procedure, are used. All materials are mined separately or simultaneously for the first production step [1]. Because the quarried rocks are too big, they are crushed and broken into smaller pieces for further processing [2]. The raw materials are mixed together in a specific ratio for a certain type of cement [3]. The mixture passes through a grinding system, which ultimately outputs a fine dry powder — the raw meal [4]. The raw meal is first calcinated at 1550 °F (850 °C) and then passed thorough a long (usually up to 30 meter long) rotary kiln that is sloped at 3-4 % [5]. At the end (lowest point) of the kiln — in the sintering zone — the raw meal is heated up to 2650 °F (1450 °C), at which the material undergoes solid state chemistry [6]. Different chemical reactions take place during the burning process that ultimately lead to specific chemical phases in the new material called clinker. Table 2.1 presents the four (4) most common chemical phases that are present after the sintering process Bosold and Pickhardt (2014). The first column lists the cement

Table 2.1: Four (4) different clinker phases

Abridgment	Chemical Formula	Cement Chemist Notation
C_3S	$3 \text{CaO} \cdot \text{SiO}_2$	Tricalcium silicate
C_2S	$2 \text{CaO} \cdot \text{SiO}_2$	Dicalcium silicate
C_3A	$3 \text{CaO} \cdot \text{Al}_2\text{O}_3$	Tricalcium aluminate
$\text{C}_2(\text{A} \cdot \text{F})$	$2 \text{CaO} \cdot (\text{Al}_2\text{O}_3 \cdot \text{Fe}_2\text{O}_3)$	Tetracalcium aluminoferrite

chemist notation (or abbreviation) for the clinker phases. The corresponding chemical formula is shown in the second column and the last column presents the mineral name. When water is added, these phases react exothermically and become responsible for the hardening process of a cementitious mixture (see Section 2.3). The individual clinker phases have different properties, and therefore, they each have a different impact on

the final product. C_3S facilitates a fast hardening process with high temperatures in the grout material. Moreover, C_2S reacts slower and is responsible for longterm hardening at lower hydration heat. At high C_3A amounts, cement tend to react faster under higher temperatures, which simultaneously leads to a higher sensitivity against sulfates. Finally, $C_2(A \cdot F)$ produces more resistance against sulfates and causes a slower hardening process. These phases are a result of the solid state chemistry process in the kiln, which also fuses the material together to approximately 1.2 in. (30 mm) diameter “clinker nodules”. The Nodules are quickly cooled down to 175 °F (80 °C) and ground to a fine powder (45 μm on average) in roller mills [7]. Varying compositions with different relative phase proportions and additional ingredients like gypsum or gypsum anhydrite lead to different products. The resulting Portland cement is a hygroscopic product, which reacts quickly with water, so that a completely dry storage is mandatory. Besides a few specialized cements, five (5) basic Portland cements, called *Type 1 through 5* are available to address different aspects throughout the placement and hardening processes.

Table 2.2 shows the relative proportions of the clinker phases for the five (5) most comment cement types according to Domone and Jefferis (1994a). Each column represents the percentage amount of an individual

Table 2.2: Portland cement types — ratios

Type	C_3S %	C_2S %	C_3A %	$C_2(A \cdot F)$ %	Others %
Type 1	50	25	12	8	5
Type 2	45	30	7	12	6
Type 3	60	15	10	8	7
Type 4	25	50	5	12	8
Type 5	40	40	4	10	6

clinker phase per cement type. Besides the main five (5) phases, other byproducts are produced during sintering, and the quantity of those other chemical phases are shown in the last column. As the table shows, Tricalcium and Diacalcium silicates always make up the major portion of the clinker, ranging between 40 and 60%. All other phases are less than 24%. Different literature sources vary slightly, but the values shown in Table 2.2 are an average representation of these five (5) cement types.

Water The hardening process of fresh grout material is initiated through chemical reactions due to the addition of water. Regular potable water from the faucet is commonly used at the constructions site or in the laboratory. Sometimes, there are temperature requirements for fresh grout material, so that is could be necessary to add a certain amount of ice to the mixture instead of liquid water.

2.3 Hydration Process

After all ingredients are blended together, the liquid grout begins to harden through chemical reactions. The hydration process is highly complicated, because each of the five (5) primary phases — C_3S , C_2S , C_3A , C_4AF and gypsum — react with the mixing water (Mehta and Monteiro, 2005). “As a consequence the chemistry of cement hydration is still not completely understood, despite the enormous worldwide research over many years [...]” (Domone and Jefferis, 1994a). For each clinker phase, table 2.3 shows the major chemical reactions that are part of the hydration process (Mehta and Monteiro, 2005). The left side of the

Table 2.3: Chemical reactions during hydration process

Fresh grout mixture Chemical components (before mixing)				→	Hardened grout material Chemical components (after hydration)	
$2(3CaO \cdot SiO_2)$ Tricalcium silicate	$[C_3S]$	+	$6H_2O$ Water	→	$3CaO \cdot 2SiO_2 \cdot 3H_2O$ Calcium silicate hydrates	+ $3Ca(OH)_2$ Calcium hydroxide
$2(2CaO \cdot SiO_2)$ Dicalcium silicate	$[C_2S]$	+	$4H_2O$ Water	→	$3CaO \cdot 2SiO_2 \cdot 3H_2O$ Calcium silicate hydrates	+ $Ca(OH)_2$ Calcium hydroxide
$3CaO \cdot Al_2O_3$ Tricalcium aluminate	$[C_3A]$	+	$12H_2O$ Water	+	$Ca(OH)_2$ Calcium hydroxide	→ $3CaO \cdot Al_2O_3 \cdot Ca(OH)_2 \cdot 12H_2O$ Calcium aluminate hydrates
$4CaO \cdot Al_2O_3 \cdot FeO_3$ Tetracalcium aluminoferrite	$[C_4AF]$	+	$10H_2O$ Water	+	$2Ca(OH)_2$ Calcium hydroxide	→ $6CaO \cdot Al_2O_3 \cdot Fe_2O_3 \cdot 12H_2O$ Calcium aluminoferrite hydrates
$3CaO \cdot Al_2O_3$ Tricalcium aluminate	$[C_3A]$	+	$10H_2O$ Water	+	$CaSO_4 \cdot 2H_2O$ Gypsum	→ $3CaO \cdot Al_2O_3 \cdot CaSO_4 \cdot 12H_2O$ Calcium monosulfoaluminate hydrates

table lists the individual clinker phase and the amount of water it reacts with. The resulting components for the hardened grout material are represented on the right side of the table. The early hydration process within the strength development is dominated by the chemical reactions of C_3S , the alite phase. This leads to the final product calcium silicate hydrates, which is one of the major compounds during hydration called C-S-H — and calcium hydroxide (Bullard et al., 2011). C_2S reacts similarly and produces the C-S-H as well, but with a smaller amount of calcium hydroxide (at a comparatively slower rate). C_3A by itself would react very quickly (exothermically), so that gypsum is added to the clinker powder to slow down reactive C_3A . Without gypsum, the freshly mixed grout would stiffen up very early. The leftover C_3A , that does not react due to missing amount of gypsum, hydrates with calcium hydroxide as a by-product from the chemical reaction of C_3S and C_2S . Lastly, C_4AF reacts slowly with water and calcium hydroxide to calcium aluminoferrite hydrates Domone and Jefferis (1994a). In general, the chemical reactions are highly dependent on each other. As shown in the Table 2.3, the C_3S produces calcium hydroxide as a by-product that is necessary for the reactions of C_3AF and C_4AF .

The relative proportions of water and cement for the mixture is called water-to-cement ratio. Usually, the so-called w/c ratio ranges around 40 % (Biscopig and Richter, 2013) for cementitious materials without chemical admixtures. More water leads to more pores in the hardened grout material, because the excess water

that does not react with the cement evaporates and eventually leaves empty pore space behind. If, on the other hand, not enough water is available, the cement cannot fully hydrate, and it therefore, does not develop its full strength. However, there is no generally defined w/c ratio, because different compositions have varying needs (due to varying properties of all influencing ingredients — fine aggregates, cementitious products, admixtures, etc.). There are a number of manufacturers for prepacked grout bags — i.e.; BASF <https://www.basf.com/>, Laticrete International <https://www.laticrete.com/>. Each manufacturer provides different grout compositions, that vary in their fresh grout or hardened grout properties, which are described Section 2.5 and 2.6.

2.4 Additional Ingredients

Throughout recent years, grout materials have been extensively studied (Shannag, 2002; Toumbakari et al., 1999; Tan et al., 2005) and material advancements have been implemented in various commercially available products. Thanks to the recent developments and modern research, it is possible to use different supplementary cementitious material to replace the most costly constituent — Portland cement. At the same time, chemicals and admixtures can be added to enhance specific properties. The text below provides more insight on the most common additives and supplementary materials that are used in modern grouts to produce more economical mixtures. Because the dry grout powder, that was used in this research, was a proprietary product made by BASF, the specifics of that product cannot be discussed. However, a general overview and the most important properties of specific grout constituents are listed below.

Supplementary Cementitious Materials (SCM) Different industry branches (steel manufacturing, generation of electricity through coal burning, etc.) produce various waste materials which are useful for cementitious materials. Most of them are used as mineral admixtures for cement replacement or as an additional ingredient for grout mixtures. These materials are sometimes called Pozzolans, but the term Supplementary Cementitious Materials (SCM) provides a better and more precise description. More than 2000 years ago, Romans were the first to use volcanic ash from Italian’s city Pozzuoli, as a natural mineral admixture for their early concrete products (Mehta and Monteiro, 2005; Wilson and Kosmatka, 2011). For this reason (name of the city), SCM are also known as Pozzolans. However, it is more precise to call SCM from natural origin Pozzolana. The Romans noticed that certain properties of the material improved when volcanic ash was present as a supplementary ingredient. Because of modern science, it is now known that the general benefit behind SCMs, stems from its ability to consume calcium hydroxide — $\text{Ca}(\text{OH})_2$. Usually $\text{Ca}(\text{OH})_2$ is a byproduct of the cement hydration process that offers no additional strength to the cement matrix. In fact, it is the component that weakens the material and weakens the durability of cementitious

materials. However, up to 25 % of the final grout material may be made from $\text{Ca}(\text{OH})_2$, if no SCM is used. On the other hand, if a SCM is effectively used, the calcium hydroxide is consumed as times goes on, and converted to calcium silicate hydrate, C-S-H — the component that is responsible for the strength of the hardened grout material.. Through this process, SCM increase the strength and density, which leads to decreased efflorescence and propensity for an alkali-silica reaction.

The three (3) major SCM that are most commonly used in the concrete and grout industry are listed in Table 2.4 to exemplify their compositions (Domone and Jefferis, 1994a) — similar ratios are also provided by Khayat et al. (2008). It can be seen that four (4) major constituents describe the chemical composition

Table 2.4: Supplementary Cementitious Materials (SCM)

Name	Abbreviation	SiO ₂ %	Al ₂ O ₃ %	Fe ₂ O ₃ %	CaO %	Others %
Pulverised Fuel Ash or Fly Ash	PFA	50.0	31.1	8.1	1.9	8.9
Ground-Granulated Blast Furnace Slag	GGBFS	36.5	11.3	0.9	39.6	11.7
Condensed Silica Fume	CSF	96.6	1.7	0.1	0.0	1.6

of these SCMs (and "Others" to account for the minor chemical phases).

Fly ash due to ASTM C618 (ASTM-International, 2015b) is a by-product from the electric power industry. Coal-fired power plants burn finely powdered fuel to produce steam that drives the turbines and generators. Due to modern environmental laws, the small airborne residuals are not allowed to be released into the atmosphere, so electrostatic filters are needed to retain the particles. These particles are collected and stored as Pulverised Fuel Ash or Fly Ash (PFA). As shown in the table, the major components in PFA are about 50 % of SiO₂ and 30 % of Al₂O₃. Generally, the PFA are spherical because they solidify in an airborne state. In addition, the particles are also smaller than the ground cement particles (Domone and Jefferis, 1994a).

Another waste material that is a useful SCM is called Ground Granulated Blast Furnace Slag (GGBFS), a by-product of the iron-producing industry. During the smelting process, iron ore is reduced to iron and other side products that float on top, the slag has the lowest density and makes up the upper most material layer at the bottom of the furnace. This slag classified in ASTM C989 (ASTM-International, 2014b) is separated from iron and rapidly cooled down, before it is ground into a fine powder that is called GGBFS (Mehta and Monteiro, 2005). GGBFS consists of about 36.5 % of SiO₂ and 40 % of CaO.

During the production of ferrosilicon as well as throughout the extraction of silicon, silica fumes are produced. The fume particles, that must meet the ASTM C1240 (ASTM-International, 2015a) requirements, are collected through a filter system similar to the filtration approach described for PFA. Therefore, these particles are also spherical. However, Condensed Silica Fume (CSF) particles are comparatively the smallest particles within the grout/concrete mixture (Domone and Jefferis, 1994a).

Besides mineral admixtures (SCM), other chemicals can be added to the grout mixture to adjust certain

properties. These chemical admixtures are explained next.

Chemical Admixtures The following four (4) chemical admixtures according to Domone and Jefferis (1994a) are the most commonly used admixtures for grouts and concretes. The adjustment of the hydration process is often needed to accelerate or to delay the setting time. Chemicals for accelerating or retarding can be added to the grout mixture to change the kinetics of the chemical reactions. In certain situations, it may be advantageous to extend the handling time to address delays on the construction side. Likewise, it may be necessary to speed up the hydration process if an high early strength is need — for example for early formwork release. Retarders are effective because they latch on to the C_3S and C_3A phases of the cementitious products, while accelerators add more calcium chloride, calcium formate and/or sodium chloride to speed up the hydration process of C_3S .

To improve the workability of the fresh grout materials, the water content could be increased (water of convenience), such that excess water — beyond the amount that is needed for the hydration process — is available to the mixture. However, the consequences of increased water amounts can be drastic, because it leads to weaker concrete with increased permeability, and therefore, reduced durability. To avoid these drastic consequences, water reducing admixtures can be added to obtain a grout mixture with increased workability at low water contents. Similar to retarders, water reducers latch on to the surfaces of the cement particles and add surface charge so that the individual particles repeal each other for an improved and more uniform particle distribution. Water reducer also have a retarding effects. However, water reducers with different ranges (low, mid and high) are available, and even superplasticizers exist, which are basically high range water reducers.

Other chemical admixtures are available, but they are not discussed here, because they are rarely used for commercially available grout products (like the product used throughout this project). However, additional information about individual chemical admixture was discussed by Rixom and Mailvaganam (1999), to provide additional details about individual admixture types and their specific functions. Chemical admixtures are regulated by ASTM C494 (ASTM-International, 2016a).

2.5 Properties – Fresh Grout Material

After all ingredients (see above) are well mixed, the fresh grout material should look highly homogeneous so that it appears as a liquid uniform mass. As mentioned before, grout is a highly complex system that is dependent on many factors. Different compositions of grout obtain different types and amounts of sand, cement, water and additional admixtures, which leads to a high variability in grout properties. The text below lists the most important grout properties (fresh and hardened) and the influencing factors.

Three-Phase System The complex grout system consisting of three (3) different phases — solid, liquid and gas (Domone and Jefferis, 1994b). Entrapped air during the mixing process is responsible for the gas phase. Water and dissolved components makeup the liquid phase, while the solid phase is described by the components that remain in the initial form (i.e.; sand). When the grout is poured into the formwork, these individual phases separate from one another, because of the different densities. Different admixtures can be added to improve certain fresh properties of the three-phase system — for example air entrainer can produce a more homogeneous mix by distributing the air inside the mixture more evenly (Domone and Jefferis, 1994b). This can lead to a more coherent mix with an improved interaction between the three (3) phases.

Bleeding Under certain circumstance, the excess water in the grout mixture can rise to the top surface and form a layer of clear water — this occurrence is called bleeding. Because of sedimentation and consolidation, solid particles in a fresh grout mixture tend to move downwards, while the lighter phases (the liquids) tend to move upwards. The separation of bleeding water influences the total volume of the grout mass, such that the density of the fresh grout is much higher than the density of the hardened material. The true water loss is difficult to specify due to potential re-absorption of the hardened grout material (Domone and Jefferis, 1994b). However, if the proper amount of water (that is needed for the hydration process) is used, bleeding can be avoided (Draganović and Stille, 2012).

Hydration heat The so-called hydrations process is an exothermic reaction that produces hydration heat throughout the hardening phase. Generally, for more massive elements (higher volume-to-surface ratio), the hydration heat increases due to impeded heat dissipation. The internal temperature of large grout elements with a water-to-cement ratio of 0.40 may reach up to 250 °F (120 °C). For example, a not so recent research project from 1988 showed that the grout temperature inside a pipeline support reached 230 °F (110 °C) at 1.6 in. (40 mm) below the surface (Domone and Jefferis, 1994b). This specific temperature was reached 5 hours after mixing and maintained for about 3 hours, before the temperature of the grout started to decrease. Such high temperature levels are problematic, because the grout volume dilates under increasing temperatures (it then starts to harden), and then cracks due to material contraction during the cooling phase. Consequently, Domone and Jefferis (1994b) recommends that the grout temperature should be carefully controlled.

Grout rheology Depending on the material compositions, freshly mixed grout may be very flowable or not. The relative proportions of cement, sand, water and admixtures (as well as the dosage) determine if the mixture is highly fluid or extremely stiff. The two (2) most common methods for adjusting the flowability are i) through the addition of plasticizers (chemical admixture) or ii) through increased water amounts (water of convenience). In the USA, there are two (2) standardized methods to characterize the rheology of freshly

mixed grout materials. These methods include the flow table according to ASTM C 230 (ASTM-International, 2014a) and the flow cone per ASTM C 939 (ASTM-International, 2016b). The later one is detailed below, because the flow cone method according to ASTM C 939 was used to measure the rheology properties of the grout material for this study. Further details related to the flow table method can be found in ASTM C 230 (ASTM-International, 2014a).

The following Figure 2.2 illustrates the flow cone, which is suitable for use in the field or in the laboratory. The cone in the picture is made from cast iron that holds a stainless steel orifice on the bottom. The cone

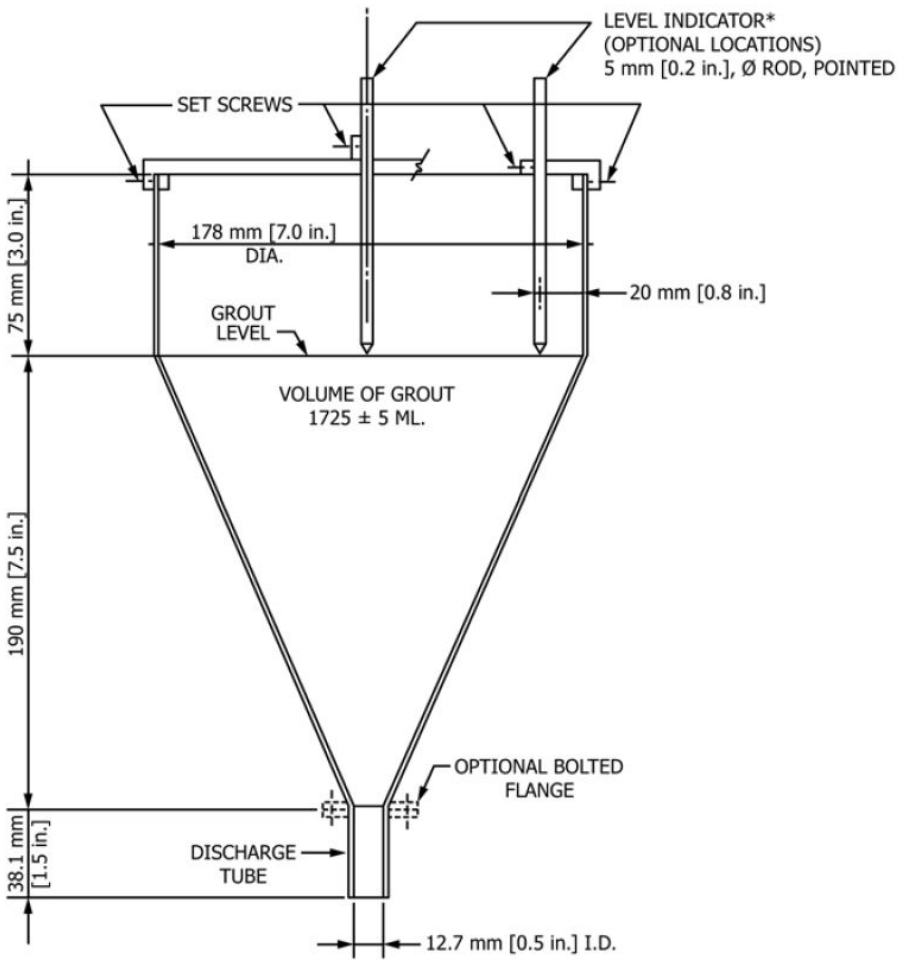


Figure 2.2: Side view flow cone (ASTM-International, 2016b)

itself has two (2) different sections. The top section has vertical side walls with a height of 3.0 in. (75 mm), while the lower section is conical shaped with a slope of about 45% over a height of 7.5 in. (190 mm) The orifice has a diameter of 0.5 in. (12.7 mm). For grout testing, the orifice is closed and the material is filled into the cone such that it resides only within the conical portion of the test device. According to ASTM C 230 (ASTM-International, 2016b), the total volume of cone has to be large enough to accommodate 1725±5 mL of grout. To guarantee proper filling of the device (with the correct grout volume), two (2) long threaded

rods are mounted inside of the cone and 0.8 in. (20 mm) or 3.5 in. (89 mm) from the outside wall. Before filling the cone, it has to be leveled and moistened at all inner surfaces. Then the orifice is closed and the cone can be filled with grout material so that it reaches up to the lower tips of the threaded rods. After a short resting period, the orifice is opened and the time measurement begins. The time measurement is stopped at the moment light passes through the bottom orifice. To guarantee proper equipment conditions, a trial run with water — 1725 ± 5 mL — is performed before actual grout testing. The equipment is acceptable for ASTM testing, if the water discharges from the cone within 7.8 s to 8.2 s. Afterwards the actual test procedure is conducted twice for two (2) different grout samples and the efflux time of each test run is recorded (ASTM-International, 2016b).

Hot Weather Grouting (or) Concreting Due to hot weather during mixing and placement of the grout material in certain states of America (e.g. Florida), the grout material may have different fresh and hardened properties compared to colder construction conditions. Fresh grout material solidifies faster than in moderate weather conditions, so that placement times become shorter, which is one of the main undesirable effects on the construction site (Soroka and Ravina, 1998).

2.6 Properties – Hardened Grout Material

Throughout the hydration process, the liquid grout system hardens into a solid mass. Although cementitious materials continue to gain strength throughout their lifespan, the strength after 28 days is generally accepted as full strength or 100 % strength.

Shrinkage Even after initial setting and hardening, the water content of the grout matrix changes, and due to vaporization it usually decreases over time. Because the water that is not consumed by the hydration process dries out, the material shrinks. Two (2) kinds of shrinkage exist; i) inward shrinkage is the process in which internal voids dry out, or new air voids form and ii) outward shrinkage is the contraction of the entire material, which leads to decreasing outer dimensions (Lea, 1970).

If the grout has to fill a certain volume as shown by the examined connection bridge detail in this research project, shrinkage can be highly critical. A loss of volume leads to increased air voids between the prefabricated elements and the grout material. Different “non-shrinkage grouts” are available on the market. One of them is called MasterFlow 928 — product by BASF — and it was used for the US 90 demonstration project and evaluated in this research. Further information according to this specific grout material are represented in Chapter 3 (see Subsection 3.2.1).

Creep After a concrete element is exposed to permanent loading, it might experience creep, such that the element contracts under sustained compression or extends under sustained tension. Creep is a complex phenomenon that has been studied by others (Do et al., 2016; Padevet and Bittnar, 2015). Attempts have been made to explain creep via the sponge analogy, in which water is pressed out of the grout/concrete volume under sustained load conditions — decreasing the apparent volume (Lea, 1970). Creep can be reversible, irreversible, or both. When unloading an element, it may initially recover elastically to a certain extent. The shape recovery, then, slows down and it is possible that the apparent volume never returns to its original shape (irreversible creep) Creep is also affected by temperature (Lea, 1970) as it impacts the moisture movement throughout the system.

Strength The compressive strength is the most important strength and characterizing property of grout materials. The tensile strength, for example, measures only 10% of the compressive strength (Domone and Jefferis, 1994c). The compressive strength can be measured on different sample types and sizes, but the most common sample types are cylinders and cubes. There seems to be an agreement, that the surface friction at the compression interface has a significant impact on the strength measurements Roddenberry et al. (2011); Kampmann et al. (2013); Kampmann (2012); Yazici and Sezer (2007); Blanks and McNamara (1935); Gonnerman (1925); Indelicato and Paggi (2008), but it has been hypothesized that cylinders with a diameter-to-length ratio of 1-to-2, measure the most realistic material strength (Malhotra, 1976). Comparatively, such cylinders usually measure 80% to 90% of the compressive strength that cubical specimens measure (Domone and Jefferis, 1994c).

It is known that many different factors impact the compressive strength and the strength development, such as age, water-to-cement ratio, curing conditions, cement properties, aggregates admixtures, and others. The early days after casting and the curing conditions throughout the early period are most important for the proper strength development of the grout material. To prevent premature drying at the outer surfaces, cementitious materials require moisture to accommodate the complete hydration process and to avoid early shrinkage that usually leads to cracking.

Deformation Mechanical stresses on a grout mass lead to deformations in shape. In general, higher stresses cause more deformation. These stresses result from self-weights, the construction process, as well as external influences, e.g. weather conditions. When two (2) concrete elements are connected via grout (as it is the case in this research for the connection between the bent cap and the pile head), the dead load of one element must be transmitted into the other one (for example, via shims) before the gaps between the elements can be filled with grout. Therefore, the loads initially are carried by small supporting elements (i.e.; shims). However, the a non-shrinkage grout should fill the remaining space such that the loads are mostly carried by the grout.

In addition, non load bearing volumes that are exposed only to thermal and mechanical deformations might have to be grouted, to guarantee a solid bond between different elements. In those case, it is important that the grout structure is not just able to withstand high stresses, but also offers a durable grout matrix that guarantees an extended lifetime.

Durability While strength is one of the most important characteristics for cementitious materials, its chemical resistance and response to non-mechanical attacks may be more critical thought the service life. Sulphates, sea water, acids and alkali-silica reactions are chemical attacks that are harmful to grout materials because they ultimately impact the physical performance of the material. In addition, frost and fire are thermal effects that tend to damage the grout structure with negative effects on the physical properties. In general, there are three (3) major transport mechanism for decreasing the durability of grout material — permeation (pressure difference), diffusion (movement under concentration gradient) and absorption (capillary attraction). The grout material, used to fill the gaps in this research project, was covered by the pile head from one side and the bent cap from the other side, so that the connection can only be controlled by taking great effort. However, non-shrinking grout material can provide a high level of complete filled caps, which avoids environmental influences of decreasing durability of the grout. If the grout volume contains reinforcing steel, the durability of the structure also depends on the steel (Domone and Jefferis, 1994c) and how the steel is protected from the environment (grout density, cover, etc.), which is not evaluated in this research project.

Chapter 3

Experimental Program

This study evaluates a specific connection point to provide additional information for standardizing the geometrical and material requirements for PBES projects in Florida. Throughout the experimental program, various grout properties and the dimensions of the pile head to bent connection were varied to determine limiting factors. This chapter explains the experimental program and details all associated aspects and constrains — for the experimental approach, materials, equipment, and procedures.

3.1 Experimental Methodology

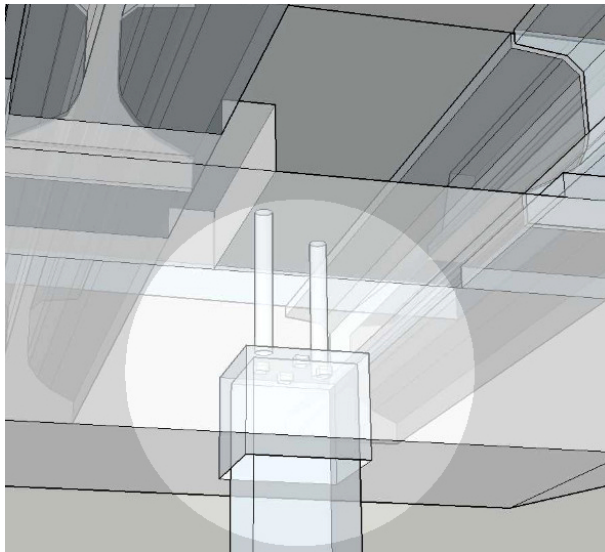
Different types of pile/column to bent connection types exist. The specific connection type addressed in this research program is proposed for FDOT's Index D20710 series — unreinforced grouted connection between a square pile and the bent cap. This research aims to evaluate this type of connection from the materials point of view, to expand the current requirements, such that both aspects — structural, and material — can be adequately addressed in future projects.

A high quality grout connection relies on three (3) important factors. i) any gap between the connecting pieces must be filled completely with grout material. ii) the hardened grout material has to have a high density and minimal air voids. iii) the compressive strength of the grout has to meet the structural requirements, as well as the minimum requirements set by the manufacturer and/or the FDOT. Only if all of these conditions are satisfactorily met, the grout connection can serve its strength and durability purpose. Although field and laboratory conditions may vary slightly, an effort was made throughout this research project to closely simulate the field conditions in the laboratory via mockup specimens and similar equipment choices, to address the real challenges on the construction site during an ABC projects. The following subsections explain how the experiments were conceptualized and how the simulations closely resemble the problems and situations of a real world project.

3.1.1 Mockup Specimen

The presented research evaluated limiting conditions for grout materials used for precast bent cap pile pockets in ABC projects. While the temperature developments of the hardening grout and the compressive strengths at different maturity levels were measured, the experimental program mainly focused on the flow and fillability of the chosen grout material. To verify that contractors have the ability to produce high-quality products, they are required to build and fill connection details, similar to the ones found at the construction site. The samples used for verification purposes are called mockup specimens (MU). Eleven mockup specimens for a bent cap-to-pile head connection detail with different boundary conditions were produced for this research project to determine the fresh grout requirements for a high quality pile-pocket connection. The mockup specimens for the experimental program were constructed and tested in the two different research phases — Task 1 and Task 2. After completion of Task 1 (MU1 through MU6), the results were analyzed, before the details and test variables for the remaining specimens in Task 2 were determined. Specimens MU1 through MU6 were part of Task 1 and tested mainly to evaluate different fresh grout properties including temperature and flowability, while specimens MU7 through MU11 were geometrically adjusted throughout Task 2.

Figure 3.1 compares the on-site bent cap-to-pile head connection to the laboratory formwork that was constructed for each mockup specimen. On the left, Figure 3.1(a) shows a wire model rendering of the actual



(a) Wire model (of actual connection)



(b) Mockup specimen

Figure 3.1: Comparison between on-site model and laboratory mockup specimen

connection on the construction site. On the right, the formwork of a (non-grouted) mockup specimen can be seen in Figure 3.1(b). On the top of the specimen, three (3) ventilation pipes are visible. The grout was filled into the mockup specimen through one (1) of the outer pipes and the air vented through the other two (2)

pipes. The formwork for all specimens consisted of two (2) parts — the inner and the outer formwork. The inner box (plywood surface) simulated the concrete pile head and the outer formwork (acrylic glass surface) represented the pile-pocket inside the bent cap.

The smallest plywood box — MU7 — had a width of 20 by 20 in. (500 by 500 mm) and a height of 19 in. (475 mm). Mockup specimen MU11 was produced with the biggest inner box by volume with a width of 26 by 26 in. (650 by 650 mm) and a height of 20 in. (500 mm).

The outer formwork was made from acrylic glass to guarantee that the filling process and the flowability of the grout could be observed and monitored. The outer formwork had cross-sectional dimensions of 28 by 28 in. (700 mm) with a minimum height of 23 in. (575 mm). The height of the inner formwork (pile head) ranged from 20 in. (700 mm) to 21.5 in. (700 mm). The roof of the outer formwork for Task 1 specimens was completely leveled, mockup specimens from Task 2 were built with tapered top surfaces to evaluate the air void formation — especially under the roof — for different pile-pocket conditions. The pitch of the roof of the mockup specimen show in Figure 3.1(b) measured 1.0 in. (25 mm) over a length of 14 in. (350 mm) for a slope of 7%. However, some mockup specimens were produced with a shallower slope — 0.5 in. (12.5 mm) over a length of 14 in. (350 mm) for a slope of 3.5%. Other specimens were produced without any slope, and therefore, with a leveled top surface that simulated the roof of the pile-pocket in the bent cap.

3.1.2 Experimental Concept

All test variables and the specific material and geometric properties are listed in Table 3.1 for each mockup specimen (MU1 through MU11). The table lists six (6) specimens that were tested for Task 1 and the five

Table 3.1: Test matrix

	Specimen	Pile Surface	Vertical Side Thickness		Taper	Horizontal Top Thickness		Temp. Range		Efflux Range ^a				
			minimum in.	maximum mm		in.	mm	°F	°C		s			
Task 1	MU1	Concrete	2	50	2	50	No	2	50	2	50	70-75	21-24	35-45
	MU2													
	MU3	Plywood	0.5	12.5	3.5	87.5	No	0.5	12.5	0.5	12.5	85-90	29-32	20-30
	MU4													
	MU5													
	MU6													
Task 2 ^b	MU7	Plywood	0.5	12.5	7.5	190	Yes	2	50	2.5	62.5	85-90	29-32	max. 48
	MU8 ^c							0.5	12.5	1	25			
	MU9							2	50	2	50			
	MU10							0.5	12.5	1.5	37.5			
	MU11 ^d							1	25	1	25			

a Flowability was measured by the cone discharge time of a 0.456 gallon (1.725 L) sample of fresh grout through a 0.5 in. (12.7 mm) tube orifice at the bottom of the cone.

b The outer top surface from all specimens of Task 2 were tapered (towards the center). Additionally, shims were placed on top of the pile head.

c Every other layer was produced with different color pigments to study the mixing between the batches.

d Layers were poured 90 min apart.

(5) specimens that were evaluated for Task 2. As explained above, all mockup specimens were made from two (2) different parts, the inner and the outer formwork. The inner formwork — plywood box — for all specimens, besides MU1 that simulated a real concrete pile surface, were made from plywood to guarantee that the mockup specimens for this research were representative of the mockup specimens that a contractor would generally produce. The gap sizes between these plywood boxes — simulated pile head — and the outer acrylic glass formwork — simulated bent cap — were varied to analyze the grout flowability and its temperature development under different conditions (more and less massive elements). Comparatively, MU7 and MU8 had the biggest and smallest vertical gaps with 7.5 in. (187.5 mm) at two adjacent sides and 0.5 in. (12.5 mm) at the other two adjacent sides. To evaluate the air void formation depending on differently tapered top surfaces, it was decided to taper the top surface (roof) of the bent-cap model (outer box) for some specimens in Task 2, as it promotes ventilation of the grout material. The top surface was tapered such that the minimum gap size was guaranteed along two opposing edges (of the square cross-section) and sloped upwards towards the ventilation pipes. Therefore, the minimum gap size only existed at the very edge of the specimen on top of two opposing vertical gap volumes, and everywhere else the vertical gap was larger than the minimum but smaller than the maximum gap at the center line, right under the PVC pipes (see test matrix). To analyze the worst case scenario in Task 2, the grout for MU5 through MU11 was prepared to reach a temperature range from 85 °F to 90 °F (29.4 °C to 32.2 °C). The specimens with the highest efflux time (according to ASTM C 939) of max. 48 s were MU7 through MU11. On the construction site, the bent cap does not rest directly on top of the pile head, nor does it float above it. Under actual conditions on the construction site, the bent cap must rest on some support surface before the grout can flow into all gaps. However, because the grout has to flow and fill the horizontal opening, the bent cap cannot directly rest on top of the pile head, and therefore, shims (or spacers) are used in construction. To evaluate if such shims have a potential impact on the grout flow and fillability, two 4 by 4 in. (100 by 100 mm) shims were placed on top of the pile-head for each specimen in Task 2. The shims were modeled such that they were thick enough to span the vertical distance from the pile head to the tapered roof of the bent cap. Additionally, MU8 was produced with color pigments to study the intermixing of layers due to small sized batches. While the first and third layer were not altered for color, the second and fourth layer were mixed with red color liquid. Normally, the different batches were filled into the mockup specimen with a 15 to 20 min time difference, because the fresh material had to be prepared as well as checked for temperature and efflux time. In addition, 2 in. (50 mm) grout cubes and 3 in. (75 mm) by 6 in. (150 mm) cylinders had to be produced for quality control of the grout, and pumping the material into the mockup specimen required additional time. However, to evaluate the grout material under extreme conditions, the grouting interval for the last specimen (MU11) were altered to simulate equipment failure on the construction site. The individual grout layers for MU11 were filled into the

formwork with 90 min interruptions (between the 15 to 20 min filling period), such that the entire specimen was produced within three (3) hours.

3.1.3 Monitoring

To facilitate the analysis process for proper conclusions, the results and test parameters for each specimen had to be properly measured, monitored, and recorded. Consequently, numerous data points were documented for each test phase (pre-testing, testing, post-testing), and Figure 3.2 illustrates the monitoring approach. While the diagram illustrates all conceptual aspects, the exact details for each test procedures are discussed in Section 3.4 (Test Procedures). In the laboratory, the date for each individual sample was collected in

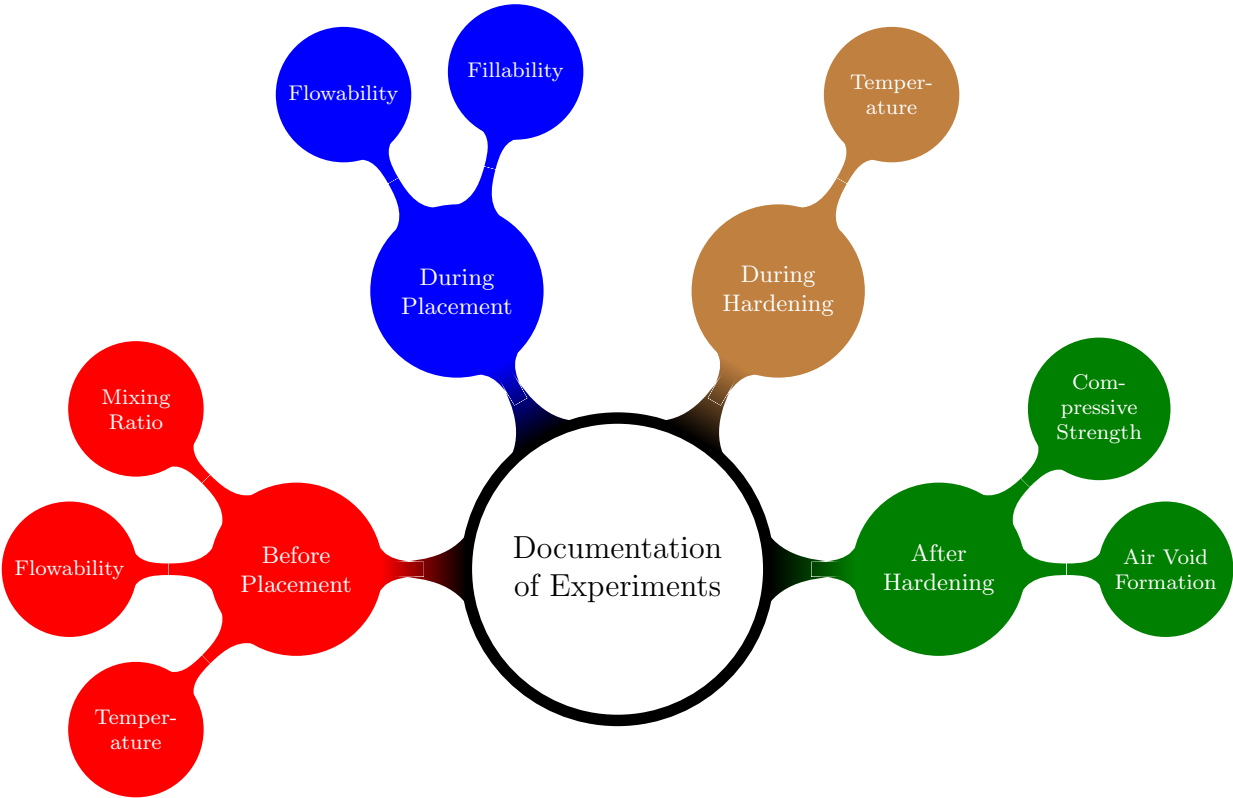


Figure 3.2: Experimental Monitoring

four (4) consecutive phases, from grout batching to hardened grout testing. Figure 3.2 presents the different phases, centered around the middle circle, in chronological order (clockwise from left to the right). Each phase consisted of different parameters that were recorded, the individual parameters are listed along the outer-most perimeter (smallest bubbles). The first monitoring period Phase 1 started with the preparation of the grout mixture. Due to small differences between individual grout bags and because specific test requirements had to be met, the water-to-material ratio was adjusted and recorded. For each individual sample, different fresh grout properties — temperature and flowability (efflux time) — were targeted to meet

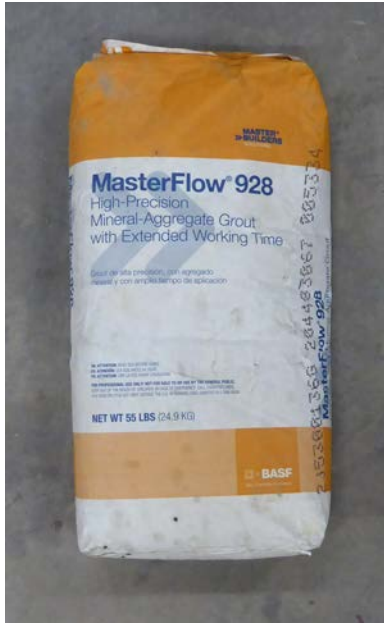
the test conditions presented in the test matrix. After the fresh grout was well blended, the material was pumped into the formwork. During the placement (Phase 2), the flow and fillability of the grout was visually observed through video cameras at different vantage positions. Phase 3 focused on the hardening process of the grout material. The temperature development and evolution at the centers of each grout volume (gap) were measured and recorded for a certain time interval, until the temperature differences between the specimen and the ambient air temperature was insignificant. Finally, the air voids and the compressive strength of the grout material were measured and recorded during Phase 4. Therefore, the formwork was removed, after the temperature measurements were completed, and the surfaces were inspected for air voids. In addition, the grout volume of some specimens were cut open to check for air pockets and to evaluate the internal density of the grout. While the actual specimens were cast, companion grout cubes (for all mockup specimens) and cylinders (only Task 2 mockup specimens) were cast for compression testing at various maturity levels. In addition, for specific mockup specimens in Task 2, cubes and cores were extracted from the actual mockup specimen to measure the strengths of placed grout.

3.2 Materials

The following subsections provide all information and specific properties for the individual materials, that were needed to produce the fresh grout. The described materials are: i) the dry grout powder from BASF (Subsection 3.2.1), ii) water (Subsection 3.2.2), and iii) color liquid (Subsection 3.2.3) — which was only used once, for MU8, to identify and evaluate the intermixing of individual grout layers.

3.2.1 Dry Grout Powder — MasterFlow 928 (BASF)

For this research project, the same dry grout powder that was used on the construction site for the US 90 demonstration project was used, because that material appeared sensitive during the hot weather grouting in Florida. The specific material is produced by BASF and is termed “MasterFlow 928”. The material was obtained through Coastal Construction Products in Jacksonville (Florida, USA), and it was delivered in prepacked 55 lbs. (24.9 kg) bags. Figure 3.3 shows a closed grout bag as it was delivered (a) and the actual content of the bag — the dry grout powder (b). Detailed information and precise material proportions of the grout powder are proprietary and therefore unknown — specifics cannot be listed here. However, MasterFlow 928 is known as a hydraulic cement-based grout with mineral aggregates. From the material data sheets and manufacturers specifications, it is known that this specific product is designed for an extended working period during installation, and reduced shrinking during hardening (BASF Corporation Construction Systems, 2016). According to the manufacturer, the allowable temperatures for the fresh grout material



(a) Grout powder bag



(b) Loose grout powder

Figure 3.3: BASF MasterFlow928

during placement range between 45 °F and 90 °F (7 °C and 32 °C).

During bridge construction and throughout this research project, different grout requirements had to be met to guarantee a high quality connection. As explained before, the grout material must i) completely fill the gaps, ii) be dense without large air voids, and iii) provide an adequate compressive strength. Table 3.2 lists the different compressive strength requirements that are provided by the grout manufacturer (BASF Corporation Construction Systems, 2016). BASF does not guarantee their MasterFlow product, if any of these values cannot be met. The table categorizes four (4) different maturity levels for the grout material.

Table 3.2: BASF MasterFlow 928 — Compressive Strength Requirements

Consistency	1 day		3 days		7 days		28 days	
	psi	MPa	psi	MPa	psi	MPa	psi	MPa
Plastic ^a	4500	31	6000	41	7500	52	9000	62
Flowable ^b	4000	28	5000	34	6700	46	8000	55
Fluid ^c	3500	24	4500	31	6500	45	7500	52

^a 100-125 % flow on flow table according to ASTM C 230

^b 125-145 % flow on flow table according to ASTM C 230

^c 25-30 s through flow cone according to ASTM C 939

Additionally, the values are separated in three (3) different consistency classes that relate to the flowability of the fresh grout, and therefore, they depend on the water-to-dry grout powder ratio. These consistency

classes can be evaluated through two (2) different methods that determine if the material is plastic, flowable or fluid. The plastic and flowable consistencies must be measured by the flow table method according to ASTM C 230, while the fluid consistency has to be measured via the ASTM C 939 flow cone method. Due to the laboratory setup, only the flow cone method, that is described in the previous chapter, was used to measure the flowability of the fresh grout material. As expected, Table 3.2 shows that a higher compressive strength (for all consistency classes) is to be achieved for a higher maturity level. Likewise, the strength requirements increase for decreasing water-to-dry grout powder ratio (the final product can only become more flowable through the addition of more water).

Besides manufacturer requirements, a non-shrink grout product (like MasterFlow) used for Florida infrastructure projects has to meet the FDOT article 934-4.1 specifications for non-shrink grout materials (Florida Department of Transportation, 2013). The following Table 3.3 reprints the requirements listed in FDOT article 934-4.1. Unlike the grout manufacturer, FDOT does not provide and specific values for one (1) day or for

Table 3.3: FDOT — Compressive Strength Requirements

Material	1 day		3 days		7 days		28 days	
	psi	MPa	psi	MPa	psi	MPa	psi	MPa
Non-Shrink-Grout	N/A	N/A	4000	28	N/A	N/A	6750	47

seven (7) days compressive strength testing. However, FDOT clearly specifies minimum strength values for non-shrinkage grout at three (3) and 28 day after mixing and placement. In general, the FDOT requirements are less restrictive than the minimum requirements according to the grout manufacturer.

3.2.2 Water

The water, used for quality grout mixtures, has to be clean and without contaminants. Clean tap water (city supply) from the laboratory faucets was used for all grout mixtures. The following paragraph describes how the water quantity was calculated for all specimens to target the properties listed in the test matrix .

Since MasterFlow 928 is a proprietary product, specific details about the material composition were unknown. Consequently, it was impossible to precisely define a water-to-cement ratio, but a water-to-material ratio (dry grout powder) was determined. According to the manufacturer, most efflux times listed in the test matrix (see Table 3.1) range over the fluid consistency, which means a time between 25 and 30 s. The lowest amount of water for this fluid consistency is suggested by the manufacturer as 9.9 lbs. (4.5 kg) per 55 lbs. (25 kg) of dry grout powder, which relates to a water-to-material ratio of 0.18 for the first material iteration (BASF Construction Chemicals UAE LLC, 2014). The highest amount of water for a fluid consistency fluid is provided with 11 lbs. (5.0 kg) per 55 lbs. (25 kg) of dry grout powder — water-to-material ratio = 0.20. To

reach a stiffer consistency the water-to-material ratio should be reduced. MU4 through MU6 were produced with a water-to-material within these borders — between 0.185 and 0.195 — to meet the requirements for the fluid consistency. However, MU8 and MU9 were produced with a water-to-material ratio of about 0.18 to evaluate the precise manufacturer specifications for a fluid consistency, which would be the most commonly expected case at a bridge construction site. MU1 through MU3 as well as MU7, MU10 and MU11 were produced with a lower amount of water, to evaluate the next viscosity level (flowable). These mixtures were initiated with a water-to-material ratio of 0.16 — based on a theoretical value for the prepackaged MasterFlow928 powder with a precise weight of 55 lbs. (25 kg) per bag. Additional water was added, if the material was too stiff, to adjust for the desired efflux time. The adjustment of water was limited to no more than two (2) iterations (after all ingredients were mixed for the first time), to prevent material inconsistencies throughout the experimental phase.

3.2.3 Color Liquid

To evaluate the intermixing between individual grout layers, every second batch for MU8 was mixed with color pigments. The liquid color agent was "QUIKRETE Cement Color (#1317-4) — Terra Cotta", a product of The QUIKRETE Companies. Each bottle contained 10 oz. (296 mL) color liquid, and can be used to color up to 80 lbs. (36.3 kg) of prepackaged powder material. Accordingly, two (2) bottles of liquid color were used for the second and fourth batch of MU8, with five (5) and four (4) bags of dry grout powder with 275 lbs. (125 kg) and 220 lbs. (100 kg), respectively. The maximum quantity of one (1) bottle for 60 lbs. (27.2 kg) was not exceeded. The liquid coloring agent (The QUIKRETE Companies, 2016) met the for standard specifications for pigments for integrally colored concrete according to ASTM C 979 (ASTM-International, 2014b). For the mixtures that contained the pigments, the water volume was reduced by the volume of color liquid, to keep the water-to-material ratio consistent between the different layers.

3.3 Devices and Equipment

This section describes all major devices and equipment, that were necessary to prepare and complete the experiments. The following subsections, are chronologically ordered according to the work flow. The subsection describes the thermometer (3.3.1), the mixer and compressor (3.3.2), the flow cone (3.3.3), the cube and cylinder molds (3.3.4), the digital cameras (3.3.5), the thermocouple system (3.3.6), as well as the compressive strength test machine (3.3.7). In general, all equipment was either brand new or thoroughly cleaned before it was used for the intended purpose. This section describes the devices and the specific requirements for the equipment. The usage of the devices and the individual test procedures are explained below in Section 3.4.

3.3.1 Thermometer

Two (2) different types of thermometers were used throughout the experimental phase of this research. Figure 3.4 illustrates both thermometer types in three (3) different photos. Figure 3.4(a) shows a side view

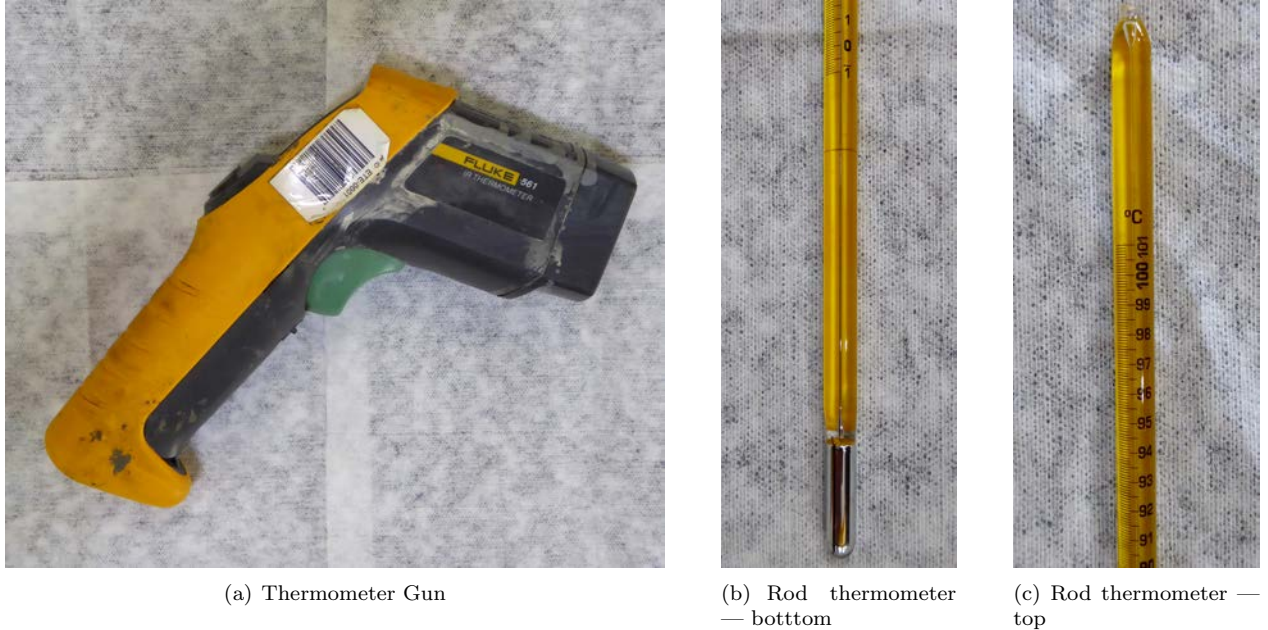


Figure 3.4: Thermometers

of the thermometer gun — the "Fluke IR Thermometer 561". It was used to measure the temperatures of the MasterFlow 928 (BASF) bags before they were introduced into the mixer, as well as the temperatures of the fresh grout material. The thermometer can be used for non-contact temperature measurements with a reading accuracy of 0.18°F (0.1°C). The measurements are based on the amount of infrared energy that a surfaces returns. Temperatures between -40°F to 1022°F (-40°C to 555°C) can be measured, and the accuracy above 32°F (0°C) is about 1% or 2°F (1.1°C) depending on which value is higher (Fluke Corporation, 2010).

Figures 3.4(b) and (c) illustrate the mercury rod thermometer that was used to measure the water temperature (before the water was added to the mixer). Part (b) demonstrates the bottom and picture (c) illustrates the top. The analog scale measured Celsius in a range from -1°C to 101°C (55.8°F to 213.8°F). The reading accuracy is 0.18°F (0.1°C).

3.3.2 Electric Mixer and Compressor

A few devices were needed to batch, mix, and place the grout. Figure 3.5 shows four (4) different photos that illustrate the major components that were necessary to mix and place the material. The two photos



(a) Mixer — Front view



(b) Mixer — Side view



(c) Compressor



(d) Exhaust valve

Figure 3.5: Mix and pumping system

on the top (Figures 3.5 (a) and (b)) show the body of the electric mixer, which was made from steel. The mixer in the laboratory was not the same mixer as the contractors used on the construction site for the US 90 demonstration project. However, the mixer used for this research project had similar properties, e.g. a comparable grout mixing volume. Part (a) shows the front of the mixer and picture (b) illustrates a sideview. The FDOT Structures Research Center owns this mixer and provided the equipment for this study, ChemGrout manufactured this mixer. The drum of the mixer had a limited volume capacity, so that no more than five (5) bags of dry grout powder could be mixed together with water. After the mixture was well blended, the fresh grout flowed out of the mixing drum into the cone below the drum. From there on, the grout was pushed through a rubber hose to the exhaust valve shown in Figure 3.5(d) via a pump that is located below the drum in the gray box shown in Figure 3.5(b). The pump was driven by the compressor shown Figure 3.5(c) The compressor was rented from United Rentals in Tallahassee, Florida, and the model was specified as “Atlas Copco XAS 185 JDHH”.

3.3.3 Flow Cone

The procedure idea behind the flow cone method according to ASTM C 939 (ASTM-International, 2016b) is described in the previous chapter. Figure 3.6 shows the equipment, that was used twice — directly after each batch was mixed — to quality control the targeted fresh grout properties. As shown in Figure 3.6(a),



(a) Overview



(b) Detailed view

Figure 3.6: Flow cone

the device consisted of a ringstand, the flow cone, and a measuring cup. The flow cone was made from stainless steel and produced by Humboldt MFG CO. Figure 3.6(b) details the inside of the flow cone and shows the transition zone between the vertical surface and the sloped cone, it also shows the threaded rod that provides a reference point during filling. Before the flow tests were conducted, the ringstand and the flow cone were leveled for accuracy during testing. Furthermore, the internal cone surfaces were moistened with water before each grout flow test. To measure the flow duration — the amount of time that was necessary for the grout to completely flow through the effluent on the bottom — a stop watch with a reading accuracy of 0.1 s was used.

3.3.4 Cube and Cylinder Molds

To evaluate the compressive strength of the grout material at different maturity levels, grout subspecimens — cubes and cylinders — were produced. Figure 3.7 shows two (2) different types of molds, that were used

for this research. Figure 3.7(a) illustrates the 2 in. (50 mm) cube molds. Each brass mold system (Humboldt



Figure 3.7: Cube and cylinder molds

Mfg. Co) was used to cast three (3) individual cube. In general, the system consist of three different components — two (2) sides plates and one (1) bottom plate. As shown in Figure 3.7(a), two (2) screws were used to connect the side walls on both ends, and two (2) additional screws were used to fix the side walls to the bottom. Wax was used to caulk the outside edges, such that the liquid grout was properly contained within the molds. The reusable molds were repeatedly used throughout this research project, and they were thoroughly cleaned after the grout cubes were removed — one (1) day after grouting.

Figure 3.7(b) shows the single molds made from plastic that were used for the cast cylindrical specimens with a 3 in. (75 mm) diameter and a length of 6.0 in. (150 mm). After the molds were filled, the caps were closed. One (1) day after pouring, the plastic molds were cut open to extract the grout cylinders.

3.3.5 Digital Cameras

After the fresh grout was well blended and ready to be pumped into the formwork, video cameras were used to capture and document the flow and fillability of the grout material during placement. Figure 3.8 shows the camera that was used to record the grout flow from two (2) different angles. Two (2) Canon EOS REBEL T4i — reflex camera — were used to observe the experiments from two (2) distinct vantage points. The cameras were attached to tripods and adjusted to the same height and placed around the mockup specimen, so that two (2) opposite corners (with two vertical grout volumes) were captured.

3.3.6 Thermocouples

To monitor the temperature throughout the hardening process of the grout material, thermocouples were used. The thermocouple system consisted of thermocouple wires, plugs, and a data logger, that managed and stored the temperature data. Figure 3.9 shows all necessary components of the system. Different types of



(a) Back view



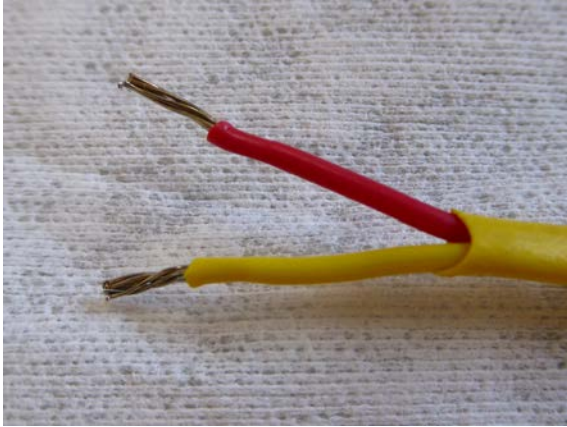
(b) Front view

Figure 3.8: Video Cameras

thermocouple systems are available, they differ in accuracy and temperature range. Type K thermocouples were used in this research. Figure 3.9(a) shows a thermocouple wire that has two (2) separated leads. On one end, these individual leads had to be correctly installed into the plug shown in Figure 3.9(b). That plug was then inserted into the eight-channel-logger shown in Figure 3.9(c), that ensured proper recording of the temperature data. The measuring end of the thermocouple wired is illustrated in Figure 3.9(d). The individual leads were vigorously twisted together, to guarantee accurate measurements. The end at which both leads were connected, was fed into the center of the grout volume that was monitored for temperature. After all thermocouple wires were installed in their proper locations, and before any grout was pumped into the mockup specimen formwork, the thermocouple system was tested and checked for full functionality.

3.3.7 Compressive Strength Test Machine

As explained above in Subsection 3.2.1, the hardened grout material has to reach a minimum strength to be acceptable for FDOT projects. Accordingly the companion subspecimens that were produced throughout this research study had to be tested for compressive strength. Figure 3.10 shows two (2) photos of the machine that was used to test the grout cubes and cylinders — an overview is presented in Figure 3.10(a), while a more detailed view is shown in Figure 3.10(b). The Test Mark load frame and test system was provided by the FDOT Structures Research Center. This machine meets the requirement of ASTM 109 (ASTM-International, 2016d) for grout strength evaluations. Both photos show the set up that was used to test the 2 in. (50 mm) cubes, which required an additional stand — black cylinder — to reach the appropriate distance between the top and bottom compression interface. To test the cylindrical specimens with a 3 in.



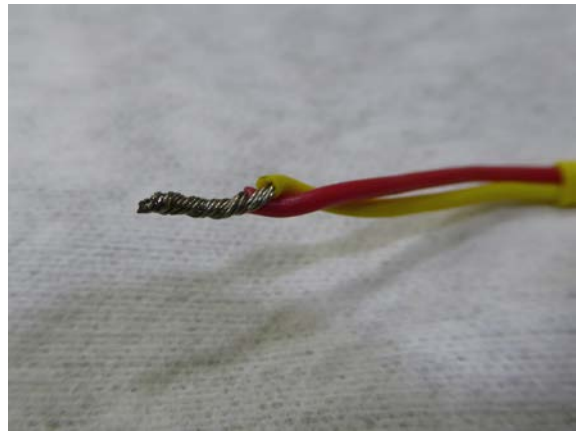
(a) Thermocouple wire — separated



(b) Thermocouple wire & plug



(c) Thermocouple box



(d) Thermocouple wire — twisted

Figure 3.9: Thermocouple system

(75 mm) diameter and a length of 6.0 in. (150 mm), the black steel cylinder was replaced by a smaller stand. For all tested samples — cubes and cylinders —, the load rate for these compressive strength tests was set up to 300 lbs./s. The machine was thoroughly cleaned after each cube or cylinder test, to prevent stress concentrations at the compression interfaces.



(a) Front view



(b) Detailed view

Figure 3.10: Compressive strength test machine

3.4 Test Procedures

The section outlines and details the preparation steps that were necessary to build the mockup specimens, describes the test procedures, and explains how the research work was carried out in the laboratory. Subsection 3.4.1 discusses the preparation of the individual specimens. Afterwards, the grout batching, mixing, and placement processes are described in Subsection 3.4.2. Finally, Subsection 3.4.3 explains which monitoring and test procedures were conducted after the grout was pumped into the mockup specimen formwork.

3.4.1 Specimen Preparation

First, the formwork for the mockup specimen, that is introduced in Subsection 3.1.1, was built. In total eleven (11) different mockup specimens were produced and tested. The major materials used for the formwork were plywood, solid wood and acrylic glass. Each individual specimen consisted of an outer and an inner formwork to simulate the targeted gap size openings listed in the test matrix. Figure 3.11 separately exemplifies the bent cap pile-pocket model and the pile head model, that ultimately were pieced together to form the mockup specimen. The outer formwork was made from four (4) vertical side walls and one (1) bottom plywood sheet as shown in Figure 3.11(a). Two (2) parallel vertical side walls were as wide as the inner dimensions of the grout body, while the other two (2) parallel side walls as wide as the outer dimensions of the formwork, such that all four (4) elements were structurally sound while meeting the dimensional requirements. The frame



(a) Outer formwork — bent cap pile-pocket

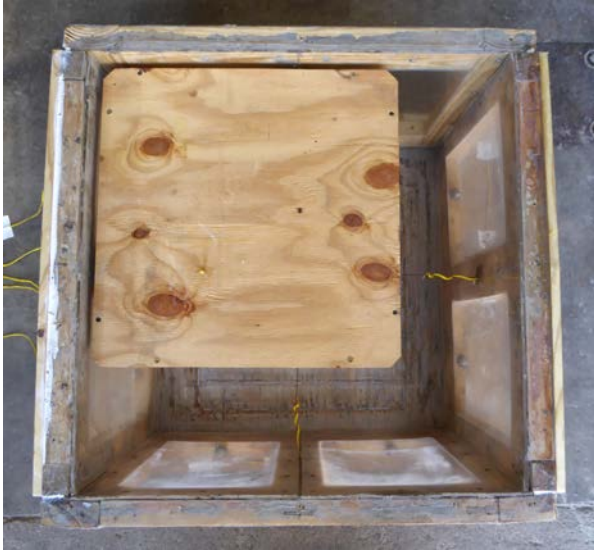


(b) Inner formwork — pile head

Figure 3.11: Formwork for mockup specimen — disassembled

work for the individual vertical side walls were made from five (5) pieces of construction wood — two (2) horizontal elements at the top and bottom and three (3) vertical elements; one (1) at each side and one (1) at the center. Acrylic glass was used for the side walls to seal the outer surfaces and to allow for visual observations during the filling process. The outer formwork measured dimensions of 28 by 28 in. (700 mm) with a minimum height of 23 in. (575 mm) — some specimens had a tapered roof with a total height of 24 in. (610 mm) at the center line. All four (4) vertical side walls were screwed together and connected to the bottom sheet with two (2) bolts per side wall. As shown in Figure 3.11(a), the west (right) and east (left) side walls also accommodated additional wood wedges for a few specimens — specimens MU7 through MU11 — to simulate a tapered roof for the pile-pocket model. The roof was sloped from two (2) opposite sides — North and South side in Figure 3.11(a) — towards the elevated centerline. The taper measured either 0.5 in. (12.5 mm) over a length of 14 in. (350 mm) with a slope of 3.5% for MU7 and MU8 or 1.0 in. (25 mm) over a length of 14 in. (350 mm) with a slope of 7% for MU9 to MU11. All other specimens were produced with a leveled roof in the pile-pocket model. To accommodate a later process, an opening was cut into the bottom plywood sheet to easily feed the thermocouple wires into position. Figure 3.11(b) presents the inner formwork, which simulated the pile head, and consisted of plywood for all mockup specimens, except for MU1. To target the required gap sizes stated in the test matrix, the dimensions for some pile head models (MU7, MU8, and MU11) were altered. All four (4) vertical edges were chamfered by 45° over the thickness of the plywood sheet with 0.75 in. (19 mm) to simulate the pile head on the construction side. The photo in Figure 3.11(b) also demonstrates that surface imperfections in the plywood were alleviated via putty, as shown for the vertical side surface on the right.

Figure 3.12 illustrates the assembly process and shows how the elements were pieced together. The



(a) Mockup specimen MU7



(b) Mockup specimen MU11

Figure 3.12: Formwork for mockup specimen — assembly of individual pieces

plywood pile head (inner box) was placed inside outer formwork and precisely placed to accommodate the targeted gap size openings. Figure 3.12(a) exemplifies the extreme case for MU7, with two (2) gaps that measured 0.5 in. (12.5 mm) and two (2) gaps that measured 7.5 in. (187.5 mm). Besides MU7 and MU8, MU5 and MU6 also had at two (2) sides with such narrow grout volumes. On the right side, Figure 3.12(b) shows the formwork for MU11. The gab size was 1.0 in. (25 mm) for all vertical side volumes. All inner boxes were screwed down to the base plywood sheet to avoid buoying or floating of the pile head model. Additionally, Figure 3.12(b) includes 4.0 in. by 4.0 in. (100 mm) shims on top of the plywood pile head that were used to simulate the spacers used in the field during placement of the bent cap. All specimens in Task 2 were produced with these shims, they were made from rubber, isolation foam, and secured with silicon to properly adjust for the height, so that the shims remained in place during grout placement and so that no grout flows between the shims and the acrylic glass. If used, the shims were placed at a 4.0 in. (100 mm) distance from the vertical side surface of the inner plywood box. Both shims were placed along along the center line that was perpendicular to the ridge line of the tapered top surface (roof of pile pocket).

After the pile head plywood box was placed inside the pile-pocket and attached to the bottom plywood sheet, the thermocouples were installed. Figure 3.13 illustrates the thermocouple set up for the vertical side volumes as well as for the horizontal top volume. The measuring end of each thermocouple was placed at the center of each grout volume. Figure 3.13(a) shows the location of thermocouple and how it was held in place for the vertical side volume. As seen in the photo, a wire was used to hold the thermocouple in position during the grouting process. Because the thermocouple had to span a shorter distance for the smaller gaps with 0.5 in. (12.5 mm), supporting wires were not used in these vertical side volumes. The

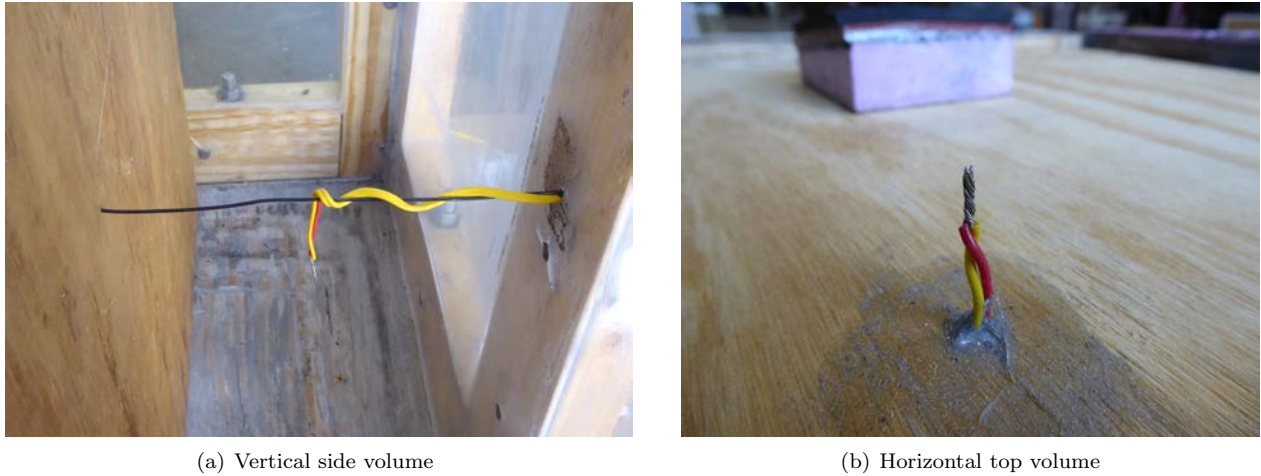


Figure 3.13: Thermocouple set up

thermocouples for the side volumes were installed from the outside of the formwork. For MU11, it was decided to measure the temperature development for each individual batch — because each batch was placed with a 90 min delay, relative to the previous batch — so that the thermocouples for this specimen were differently arranged. Accordingly, the temperatures were measured at three (3) different elevations — 4 in. (10 mm), 12 in. (300 mm) and 20 in. (500 mm), based on the theoretical volumetric center of each batch — on two (2) perpendicular sides of the mockup specimen. Figure 3.13(b) shows a photo of the thermocouple setup at the top surface of the pile head — inner formwork. The measuring end of the thermocouple wire was installed at the center of the top volume, exactly between two (2) fill/ventilation tubes. The thermocouple wire was installed from the bottom and fed through the hole in the bottom plywood sheet (described above) and through the top plywood piece that formed the top of the pile head model. After installation, the open space between the drilled holes and the wire were caulked to properly seal the formwork.

The completely assembled formwork for the mockup specimen is shown in Figure 3.14, to exemplify the entire setup via MU8 through two (2) distinct side views. After the inner formwork and the thermocouples were installed, silicon was applied to the top of the shims to guarantee a proper fit and to prevent grout material from seeping between the shims and the formwork lid. As Figure 3.14(b) shows, the formwork lid (pile-pocket roof) consisted of two (2) individual pieces, that were jointed at the centerline below the fill/ventilation pipes, to accommodate a tapered top volume — for the specimens in Task 2. Both parts were screwed down to the side walls to securely and tightly connect the lid to the outer formwork. For proper ventilation and to facilitate the filling process, three (3) PVC pipes with an diameter of 3 in. (75 mm) were installed along the centerline. Then, the thermocouple wire were carefully routed around the formwork and secured to the formwork via adhesive tape, as it can be seen in Figures 3.14(a) and(b). Finally, all joints were caulked with silicon to avoid leakage and to prevent unnecessary waste of fresh grout.



(a) South side



(b) East side

Figure 3.14: Mockup specimen — formwork

3.4.2 Mixture and Filling Process

After the formwork for an individual mockup specimen was prepared and set up, the laboratory was readied for the grouting process. For consistency purposes, the laboratory was identically arranged and prepared for each mockup specimen. Figure 3.15 illustrates the floor plan for the experimental setup and shows all relevant materials and devices, that were needed throughout the batching, mixing, and filling process. The cardinal directions — in reference to the FDOT Structures Research Center — are shown along the four (4) sides of the figure. The dry grout powder, BASF MasterFlow 928, was stored at the Northeast corner ①. The temperature of the dry grout powder was very important to target the test temperatures of the fresh grout material. Relative to the mixing water, the dry grout powder has much more mass and a higher heat capacity. Depending on the target temperatures of the fresh grout, the grout powder (inside the sealed bags) was preconditioned to reach uniform temperatures. Depending on the time of the year and ambient temperatures in the laboratory, the grout powder was either preheated in an oven, or exposed to the surrounding ambient temperature for more than 24 hours. The required grout powder temperature was experimentally determined via small size batches, which were evaluated for temperature and efflux time via the flow cone. For example, for Task 2 throughout August and September, it was found that the grout powder had to be at 85 °F (29.5 °C) for the fresh grout to reach 85 °F to 90 °F (29.4 °C to 32.2 °C) as it was targeted by test matrix. Sometimes, up to 6 lbs. (2.72 kg) ice had to be substituted for parts of the mixing water to stay within the desired fresh grout temperature range. A hose provide a continuous water source for mixing and equipment cleaning ②. The water-hose was connected to a faucet outside of the laboratory ③,

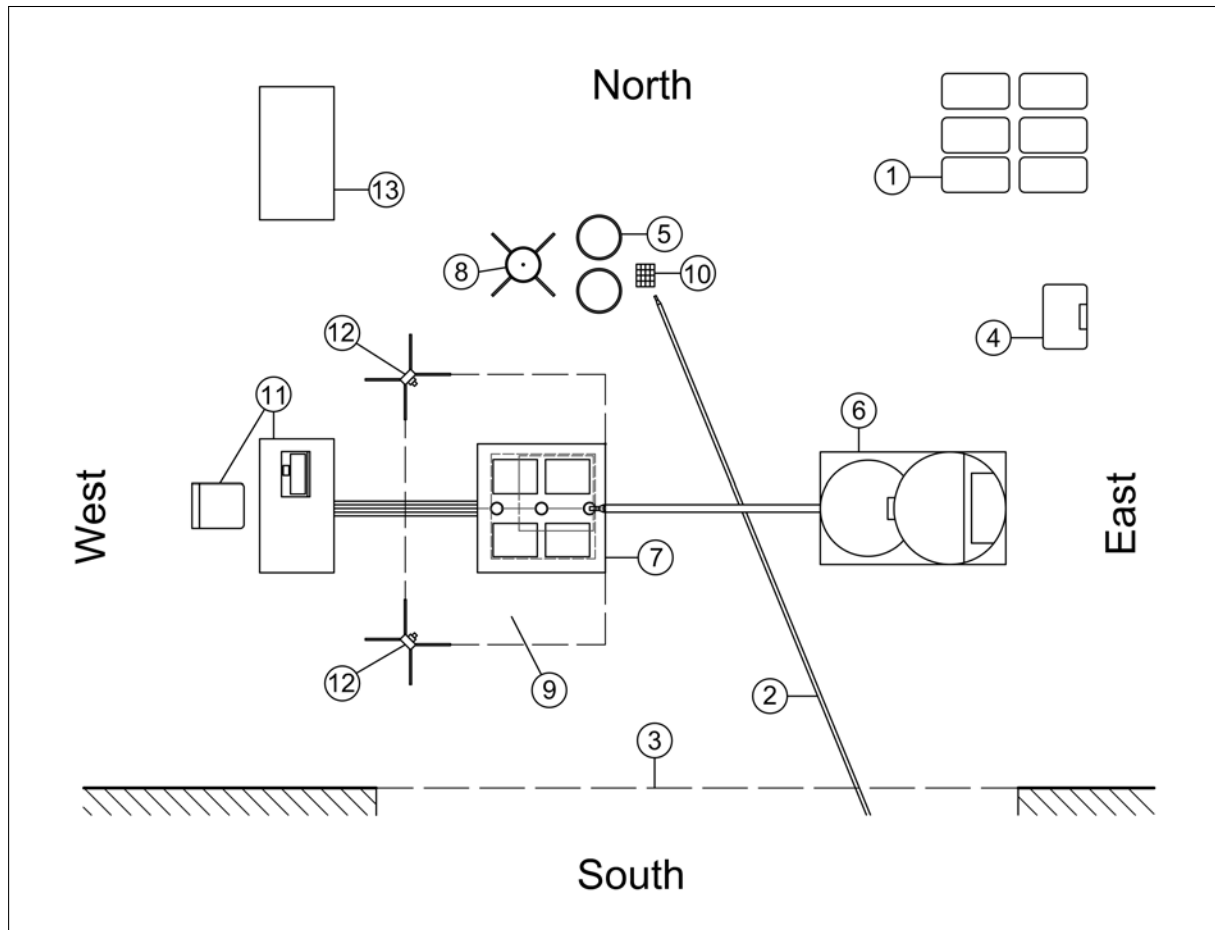


Figure 3.15: Laboratory Setup

which provided city water. To guarantee stable water temperatures throughout the research, the hose was not exposed to direct sunlight and the water flowed continuously through the hose, such that the mixing water did not come from water that reside too long inside the hose. A scale (4) with an accuracy of 0.01 lbs. (0.2 kg) was used to measure and proportion the grout, water, and color liquid. Additionally, buckets (5) were needed to measure and transport the water, as well as for cleaning and pre-wetting the equipment. The electric mixer (6) was placed at the East side of the laboratory so that the pump was directed towards the specimen (7). The flow cone test equipment (8) was located close to the actual test area (9) and next to a grade (10) to avoid long distances for the water during the cleaning process of the flow cone. To control the temperature logger for the thermocouple measurement and to provide a designated space for data documentation, a laboratory desk and a chair (11) was set up at the West side next to the specimen. Two (2) digital cameras (12) were installed at the Southwest and Northwest corner — at the edge of the test area — to monitor the flow and fillability. A table was placed at Northwest (13) corner of the working area, to provide.

Before the mixing procedure was initiated, the water was allowed to flow through the hose for at least two (2) minutes to dispose the water that resided inside the hose — due to the high ambient temperatures in

Florida, the resting water inside the hose was significantly warmer than the water after a two (2) minute flow period. The water flowed throughout the whole experimental process (batching, mixing, and grout placing) to ensure similar water temperatures at all times. All mockup specimen had to be filled with multiple batches, due to a limited capacity of the mixing drum. While each batch was prepared similarly, the required material amount was altered based on the geometric properties of the mockup specimen — three (3), four (4) or five (5) bags of dry grout powder were used per batch/layer. First, the water for the fresh grout mixture was weight out and its temperature was measured. To accommodate temperature differences, the water amount described in Subsection 3.2.2 was first reduced by 10%, and then ice (by weight) was added instead of liquid water, if necessary. After the water temperature was properly targeted, the temperature of the preconditioned grout was verified — if the grout powder temperature was not within $\pm 5^{\circ}\text{F}$ ($\pm 5^{\circ}\text{C}$) of the required temperature range (see test matrix), the grout powder was not used for the mixture. Then, the water (and in some cases ice) was introduced into the mixing drum. To account for slight weight differences in the prepackaged grout powder, the grout powder bags were weighed before and after they were opened and the grout powder was poured into the mixer. The grout powder was slowly fed into the mixing drum while the mixing paddles were rotating. Then the mixer blended the grout powder and the water for at least four (4) minutes. The temperature during mixing was measured and monitored, and either the remaining water or remaining ice was added to the mixing drum and mixing was continued for another two (2) minutes. After mixing was completed, 2 L (0.53 gal.) of the fresh grout material were poured into a vessel for the flow cone test procedure. To guarantee that the desired efflux time was targeted, the flow cone procedure was completed twice, with two distinct fresh grout samples. If the fresh grout was too viscous, water or ice was added to the mixing drum to adjust the flowability for the first time. The mixing then continued for another two (2) minutes. Afterwards, the cone efflux time was measured for another two (2) times, and the temperature was recorded. If necessary, the water content was adjusted for a second time, and the procedural steps were repeated accordingly. However, in case the grout did not have the desired flowability (within acceptable tolerances) after the second adjustment, the material had to be discarded. If the fresh material met the temperature and the flowability requirements listed in the test matrix, the material was pumped into the formwork for the mockup specimen through one (1) of the three (3) tubes. At that time, the video cameras were turned on to record the flow and fillability. Simultaneously, companion grout cubes and cylinders — cylinders only for Task 2 (MU7 through MU11) — were prepared according to ASTM C1019 (ASTM-International, 2016c). For each batch, nine (9) 2 in. (50 mm) cubes and two (2) cylindrical specimens with a 3 in. (75 mm) diameter and a length of 6.0 in. (150 mm) were cast. After a batch was completely pumped into the formwork, the following batch was immediately prepared, according to procedure outlined above. For the last layer/batch, grout was pumped into the formwork from one (1) PVC pipe, until the grout

clearly over flowed into the other two (2) PVC pipes. Figure 3.16 shows two photos that were taken directly after the filling process was completed. After the formwork was completely filled as shown in Figure 3.16(a),

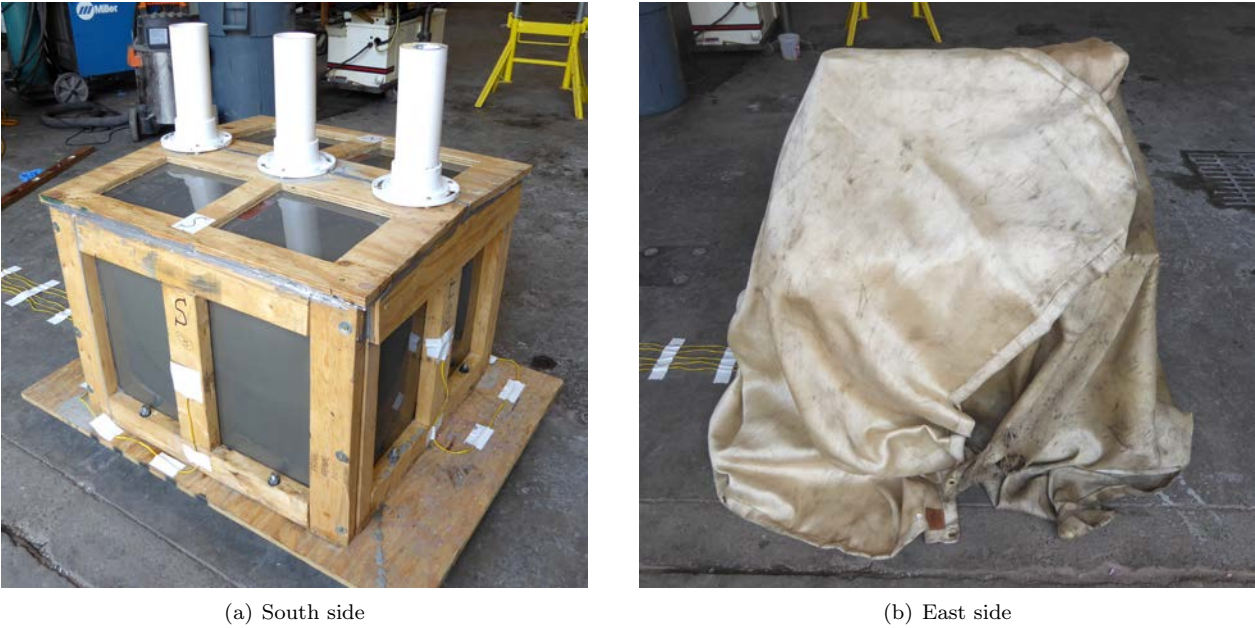


Figure 3.16: Mockup specimen MU9 — after grouting was completed

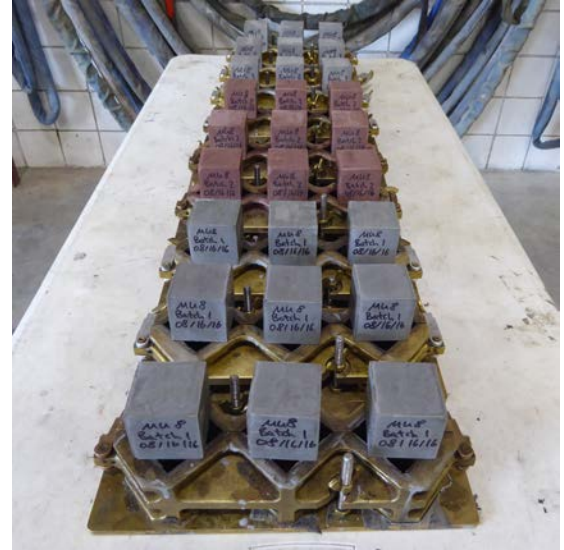
the data logging for the thermocouples was initiated to record the temperature once every minute (1/60 Hz). For Task 1 specimens, the temperature was recorded throughout a 24 h period. However, during data analysis of Task 1 data, it was noted that the temperature of the grout did not reach full equilibrium with the ambient temperature, and it was decided to record the temperature development over a time period of 48 h for all Task 2 specimens. The same procedure was followed for all mockup specimens, except for MU11; because this specimen was filled with 90 min pauses between each batch/layer (simulating equipment failure), the temperature logging was initiated after the first batch was placed into the specimen. Additionally, insulating blankets were used to cover all exposed surfaces of the mockup specimen — see Figure 3.16(b) — to simulate the on site conditions by entrapping the hydration heat. Finally, after the mockup specimen was completely prepared, all equipment was thoroughly cleaned to guarantee identical conditions for the following mockup specimen.

3.4.3 Post Grouting Activities

After the grouting process, all specimens in Task 1 rested untouched for 24 h and all specimens in Task 2 rested for 48 h in the formwork. At a maturity level of one (1) day, the casted cubes and cylinders were demolded. Figure 3.17 shows two (2) photos that exemplify the cast 2 in. (50 mm) grout cubes taken from mockup specimen MU8. The picture in Figure 3.17(a) shows the grout material immediately after the cubes



(a) Fresh grout in cube molds



(b) Cubes removed from molds

Figure 3.17: Cast 2 in. (50 mm) grout cubes — example based on MU8

for the third batch were cast. After one (1) day of hardening, all specimens were removed from the molds and carefully labeled as shown in Figure 3.17(b), the cubes as well as the cylinders were then placed into a lime batch — at a concentration of 3% of lime and 97% of water (by mass).

Figure 3.18 shows mockup specimen MU8 at 48 h after grouting — inside the formwork and after the formwork was removed. Photo (a) demonstrates the specimen with formwork, while part (b) illustrates the specimen after the formwork was completely removed. After the individual pieces of the pile-pocket model were carefully removed, the formwork was thoroughly cleaned for reuse. Afterwards the vertical and horizontal surfaces of the grout body were carefully examined and evaluated for surface air voids and air pockets.

As explained above in Subsection 3.2.1, the compressive strength of the grout material has meet certain manufacturer and FDOT requirements. Accordingly, the cast cubes and cylinders were tested at specific maturity levels. After one (1), three (3) and 28 days, three individual companion cubes were tested according to ASTM C109 (ASTM-International, 2016d) for each batch. In addition, the two (2) cast companion cylinders that were produced for each grout batch in Task 2 were tested for compressive strength 28 days after grouting. Also, cubes and cores were extracted from selected mockup specimens in Task 2, to evaluate the difference between the material in the small scale molds and the material that was actually used to build the mockup specimen. The cubes were cut out with a diamond blade and the cores were drilled out with a coring bit. The subspecimens were extracted 27 days after grouting was completed, to minimize interruptions during the hardening process. Mockup specimens MU7, MU9 and MU10 were used to cut out additional 2 in. (50 mm) cubes. The cores with a 3 in. (75 mm) diameter and a length of 6.0 in. (150 mm) were extracted from



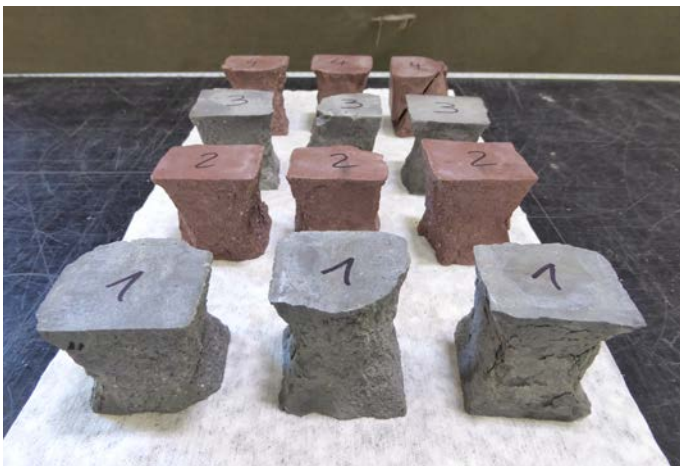
(a) MU8 — before demolding



(b) MU8 — after demolding

Figure 3.18: Mockup specimen 48 h after grouting

MU7 and MU8, because these mockup specimens provide a gap size that was large enough to accommodate the cylinder length. In total three (3) cubes per batch were extracted from two (2) different vertical side volumes for MU9 & MU10 and from one (1) vertical side volumen for MU7. Two (2) cores from each batch from two (2) different — perpendicular to each other — vertical side volumes were drilled out of MU7 and MU8. All extracted samples were tested 28 days after grouting was completed. Figure 3.19 illustrates two (2) photos of the compression tested cubes and cores — these particular companion samples were tested for MU8. On the left side, Figure 3.19(a) shows all MU8 cubes that were cast for 28 day compressive



(a) Tested cubes



(b) Tested cores

Figure 3.19: Mockup specimen MU8 — tested samples

strength testing, after they were taken to failure. Figure 3.19(b) shows an extracted core that failed after it

reached its compressive strength. The same test procedure was identical for all specimens that were tested in compression, such that the stress was applied without shock, at a rate of 300 lbs./s.

Chapter 4

Experimental Results

All tests were performed in compliance with the procedures outlined in the previous chapter, using the described materials and equipment. The test data was captured and recorded according to the applicable ASTM test protocols and according to the described methodologies. The recorded test data was reduced to concisely present the most significant findings in this chapter. While the results are presented and elucidated here, they are further processed and analyzed (using statistics and other mathematical methods) in following chapter for proper engineering interpretation and clarification.

Section 4.1 details the fresh grout properties — per mockup specimen and per batch. The flowability observations are presented in Sections 4.1.1 and 4.1.2 to provide information about the filling procedure based on photo and video material that was captured for every mockup specimen. To evaluate the temperature development dependent on the different geometric conditions (gap size openings) and to obtain additional data throughout the hardening process, Section 4.2 illustrates the recorded temperature developments during the initial hydration phase. The following Section 4.3 presents and details the visual properties of the side and top surfaces of the grout to discuss the air void formation. Because the mockup specimens were produced from multiple batches (due to mixer capacity), the different grout layers from MU8 were color tinted to evaluate the intermixing of the material. The interaction of fresh grout layers is shown in Section 4.4 The chapter concludes with the presentation of the compressive strength results for cube specimens and cylinders as well as a comparison between cast and cut out samples in Section 4.5.

4.1 Fresh Grout Properties

The fresh grout property variables shown in the test matrix in Subsection 3.1.2, were measured and recorded according to the applicable ASTM requirements. Directly after mixing, the fresh grout temperatures as well as the efflux times according to ASTM C 939 (ASTM-International, 2016b) were measured. Each of these

properties were measured twice — consecutively, directly after the fresh grout material was homogeneously mixed. To confirm the test matrix and to study the temperature impact of the individual components, the temperature of the grout powder, of the mixing water, and of the ambient air were monitored. To account for slight weight differences in the packaged grout powder, the bags were weighed before and after they were emptied into the mixer. Based on the actual material added to the mixer, the water content for each batch was adjusted.

Table 4.1 represents the mixing ratios, temperatures (ingredients and mixture) as well as the efflux times measured for each batch and specimen for MU1 through MU6 (Task 1). All specimens were made from three

Table 4.1: Fresh grout properties MU1 – MU6

Specimen	Batch	Mixing Ratio	Temperature				Efflux Time	
			Water °F	Grout °F	Ambient °F	Mix °F	I s	II s
MU1	#1	0.184	55	68	61	72	36	40
	#2	0.176	59	68	64	74	35	36
	#3	0.177	60	68	65	75	35	38
MU2	#1	0.182	60	68	68	73	36	40
	#2	0.182	55	69	68	74	35	36
	#3	0.184	59	68	68	73	35	38
MU3	#1	0.180	61	85	58	80	35	35
	#2	0.182	61	84	57	83	35	35
	#3	0.182	61	84	58	81	35	35
MU4	#1	0.189	71	100	69	90	24	25
	#2	0.188	66	98	70	89	26	27
	#3	0.188	66	97	74	88	23	23
MU5	#1	0.189	69	86	74	88	21	21
	#2	0.188	66	87	76	87	27	29
	#3	0.190	66	87	77	87	26	27
MU6	#1	0.187	65	94	74	88	28	28
	#2	0.188	72	94	74	90	22	24
	#3	0.189	55	85	77	87	21	22

(3) batches. The ingredient temperature was measured directly before mixing, the mixture temperature was determined during the efflux time measurements. The efflux time was measured twice with the flow cone method — directly after mixing and 30 minutes after mixing. As seen in the table, if both values differ from each other, the second measured efflux time was slightly higher than the first one. MU1 through MU3 were prepared with a lower water-to-material ratios, while MU4 through MU6 were mixed with more relative water. In general, the efflux times of all specimens met the requirements provided by the test matrix in the previous chapter.

These measurements are presented in Table 4.2 for all mockup specimens in Task 2. Because of the highly different gap size opening during Task 2, various amounts of grout volume were necessary to completely

Table 4.2: Fresh grout properties MU7 — MU11

Specimen	Batch	Mixing Ratio	Temperature				Efflux Time	
			Water °F	Grout °F	Ambient °F	Mix °F	I s	II s
MU7	#1	0.165	81.5	87.2	89.6	88.3	41.2	41.2
	#2	0.163	81.1	88.3	89.6	89.4	44.8	47.8
	#3	0.167	81.9	87.3	89.6	86.6	46.0	50.0
	#4	0.167	81.3	86.5	89.6	86.4	31.0	38.4
MU8 ^a	#1	0.179	86.0	88.6	87.3	89.1	27.3	26.1
	#2	0.178	87.0	89.5	87.3	89.3	42.6	46.9
	#3	0.178	85.7	89.6	87.3	89.8	38.8	41.0
	#4	0.177	86.2	89.9	87.3	90.0	47.0	50.0
MU9	#1	0.183	82.4	89.9	87.4	89.2	35.3	35.0
	#2	0.179	83.7	90.1	87.4	88.2	30.0	29.0
	#3	0.179	83.3	90.3	87.4	87.6	24.0	27.8
MU10	#1	0.167	82.4	86.8	86.9	87.0	41.0	45.8
	#2	0.171	82.4	87.6	86.9	89.0	38.6	37.0
	#3	0.169	82.8	88.3	86.9	87.2	37.0	36.8
MU11	#1	0.169	80.6	83.9	81.9	85.4	29.0	36.2
	#2	0.165	81.5	88.0	81.9	86.9	47.2	44.2
	#3	0.164	81.5	86.9	81.9	89.0	45.7	45.4

^a Batches were produced with color pigments. The volume of water was substituted by the identical volume of color liquid.

fill the mockup specimens. Therefore some specimens required four (4) batches while three (3) batches sufficed to fill the specimens with smaller gaps. It can be seen that the initial temperatures of the dry grout powder, the water, and the ambient air did not vary significantly throughout the entire experimental phase for Task 2. According to the experimental design (see test matrix), MU7 through MU11 aimed to target fresh grout temperatures of 85 °F to 90 °F (29 °C to 32 °C) — right after the mixing sequence was completed. Additionally, the average efflux time (based on two (2) consecutive measurements directly after mixing) remained at or below 48 s at all times.

4.1.1 Vertical Side Volumes

Figure 4.1 illustrates the filling sequence for the vertical side volumes of MU7. Three (3) pictures, that were taken from the same position, are chronologically ordered to illustrate the grout flow inside the formwork at different times. For this particular specimen, two (2) vertical gaps measured 0.5 in. (12.5 mm) at two (2) adjacent sides, the other two (2) adjacent vertical side gaps had a thickness of 7.5 in. (187.5 mm). The presented view shows the corner with the two (2) adjacent 0.5 in. (12.5 mm) thick vertical volumes, which was chosen because this was the minimum thickness throughout Task 2 (MU7 through MU11), and therefore,



(a) 2 min 37 s after pumping was initiated (Batch 1)



(b) 3 min 40 s after pumping was initiated (Batch 2)



(c) 4 min 10 s after pumping was initiated (Batch 2)

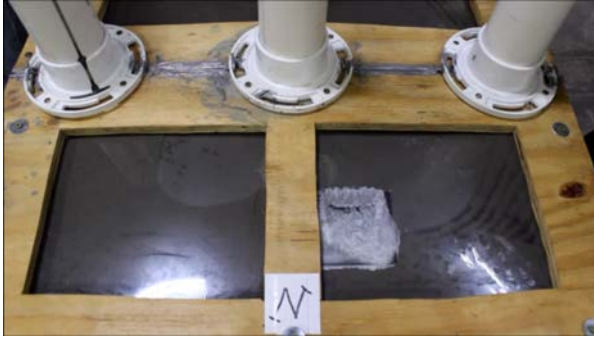
Figure 4.1: Filling sequence for MU7 — vertical side volume

the worst case scenario. The grout was filled into the formwork through the pipe on the left side in the pictures. The grout for this specimen was dropped into the formwork from the side with the bigger gap size of 7.5 in. (187.5 mm). Due to the two (2) large vertical volumes (not seen in the pictures, in the back of the specimen), four (4) batches/layers were needed to completely fill MU7. In total, it took 9 min 12 s to complete the grouting process — pure grout pumping duration.

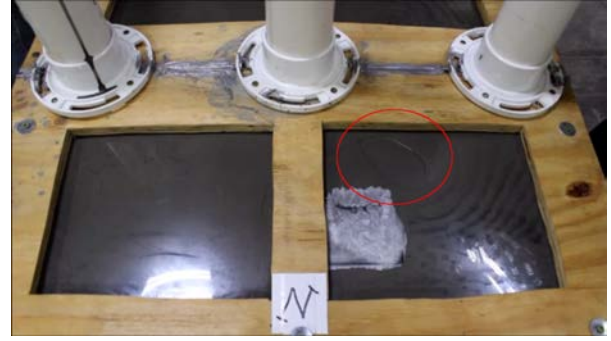
Figure 4.1(a) shows the grouting at the completion of Batch 1. The first batch was pumped from 0 min 0 s to 2 min 40 s and the photo at 2 min 37 s exemplifies the fillability of grout near the end of the pumping process for Batch 1. It can be seen, that the fresh grout flowed well around the corners and that it was almost level within the two (2) smaller gaps. Although the grout material was slightly higher where the material was poured into the mockup specimen, the grout filled all four (4) side volumes with a similar speed. Batch 2 was pumped into the formwork between 2 min 40 s and 5 min 50 s. Figure 4.1(b) shows a photo that was taken shortly after pumping for Batch 2 began (3 min 40 s). As seen in the figure, the grout material sloped from the larger gap sizes (where the specimen was filled) towards the corner of the two (2) adjacent gaps with a thickness of 0.5 in. (12.5 mm). Finally, the third picture (c) shows the grout state after 4 min 10 s during Batch 2. As seen in these subfigures, the grout filled the gaps well without any entrapped air voids and with nearly self leveling abilities. Nevertheless, at the beginning of grout placement, the material was so viscous that it initially accumulated under the inlet pipe, so that the material flowed under an angle of approximately 10° around the simulated pile head as soon as enough material was pumped into the form. It took up to 60 s after pumping was initialized (MU7), for the grout to completely level out and to continue to fill the formwork with uniform and even height increments — for each layer. In general, the grouting process and the filling behavior was similar for all specimens in Task 2. However, with a 60 s leveling transition period from the thick to the thin gap volume, MU7 needed the longest time to achieve a level flow. In comparison, MU8, that was produced with the same vertical side gaps of 0.5 in. (12.5 mm) and 7.5 in. (187.5 mm), but was filled through the pipe over the smaller gap size opening, had a leveling transition period of only approximately 30 s from the thin to the thick gap volume, which simulated the opposite set up as seen with the results for MU7 (from thick to thin gap volume, but in general with same vertical gap dimensions). MU9 through MU11, that were produced with the same vertical gap sizes on all four (4) sides, had leveling transition periods of about 20 to 25 s.

4.1.2 Horizontal Top Volumes

Figure 4.2 illustrates two (2) photos that were captured while grouting the last batch for MU7. This particular specimen was produced with a taper of 0.5 in. (12.5 mm) over a length of 14.0 in. (300 mm) — 3.5 % slope. The left picture presents the grouting stage 9 min 12 s after pumping was initiated (Figure 4.2(a)). The



(a) 9 min 12 s after pumping was initiated (Batch 4)



(b) 9 min 20 s after pumping was initiated (Batch 4)

Figure 4.2: Filling sequence for MU7 — horizontal top volume (with a slope of 3.5%)

specimen was filled through the left pipe that is seen in the picture. The shim can be identified through the silver colored silicon that was applied above the shim to avoid any grout overflow for improved observation. The top volume was mostly filled and no significant air void formation was noted. Black wavy marks were visible on the right bottom of the photo. These marks were discolorations without any concerns for the quality of the connection detail. However, the discolorations follow the direction of grout flow from the pipes towards the corner opposite to the pipe used for filling. The photo on the right shows the grout status 8 s later, as the grouting job was finished, and when the formwork was completely filled (Figure 4.2(b)). While most of the top surface area was free of air voids, one (1) larger air bubble with a maximum diameter of 4 in. (100 mm) was trapped — visible on the right site above of the shim. Similar observations were made for M8, the specimen that was almost identical to MU7, but produced with a lower minimum horizontal top gap size of 0.5 in. (12.5 mm), instead of 2 in. (50 mm). However, the slope of the pile pocket roof also measured 3.5% for MU8.

To compare these findings to the second type of tapered top volume, Figure 4.3 illustrates the observed fillability of the grout material under a 7% sloped roof, as MU9 was produced with an increased taper of 1 in. (25 mm) over a length of 14.0 in. (300 mm). Due to a smaller total volume of MU9, just three (3) batches were needed to completely fill the mockup specimen, so that the grouting was completed after 6 min 0 s. Figure 4.3(a) presents the surface of the horizontal top volume with a minimum gap size of 2 in. (50 mm) after 5 min 54 s, while Figure 4.3(b) shows the grout state after the pumping was completed. Both photos show that the grout cleanly filled the top volume and that virtually no air was trapped. Figure 4.3(a) exemplifies that the grout evenly filled the formwork, and Figure 4.3(b) shows that no significant macroscopic air voids formed under the acrylic glass roof. The observed flow and fillability for MU9 are similar to the observations made for MU10 and MU11.



(a) 5 min 54 s — Batch 3



(b) 6 min 0 s — Batch 3

Figure 4.3: Filling procedure MU9 — horizontal top volume

4.2 Temperature Development

To study the hydration process during curing in response to changing grout volumes, the temperature developments were recorded for all grout gaps (four (4) vertical volumes and one (1) horizontal volume). Welding blankets, made from glass fibers with special coating, were used to cover all outer surfaces of the mockup specimen. These blankets were immediately wrapped around the formwork after the grout placement was finished to contain the hydration heat — similar to the situation expected in the field due to more massive material around the pile pocket (bent cap). The gap sizes varied between 0.5 in. (12.5 mm) and 7.5 in. (187.5 mm). Because the curing grout did not reach ambient temperature after 24 h during Task 1, it was decided to extend the data acquisition period to monitor all temperatures throughout the first 48 h for all Task 2 mockup specimens. Data points were taken every minute (1 Hz) at the center of each volume. Additionally, the ambient temperature was measured alongside each specimen. Because some specimens had identical gap openings, and others had differently sized gap openings, the two (2) scenarios are outlined separately in Subsections 4.2.1 and 4.2.2. While most specimens (MU1 through MU10) were cast consecutively, MU11 was cast with 90 min time delays between each grout layer. Subsection 4.2.3 focuses on the temperature development within individual batches, based on a unique thermocouple probe arrangement (see Subsection 3.4.1).

4.2.1 Identical Gap Size Openings for all Vertical Volumes

Ideally the pile bent is centered in the pile pocket opening. To reflect such a scenario, MU1, MU2, MU3, and MU4 (Task 1) as well as MU9 and MU10 (Task 2) were modeled with identical vertical gap sizes all around the pile. Usually, the gap openings vary due to inherent problems related to the pile driving process — the gaps may possibly be as large as 7 in. (177 mm); however, to conserve resources and use less grout, a smaller gap size was chosen when possible.

MU1 through MU4 were produced with identical dimensions, but instead of using concrete, plywood was

used to model the pile head for specimen MU2. MU1 is not shown here, because the data acquisition system malfunctioned throughout the temperature monitoring phase. However, the following Figure 4.4 graphs the temperature developments for specimen MU2, which measured the same gap size openings as MU1. Furthermore, the temperature trends shown in the figure, are representative for specimens MU2 through MU4.

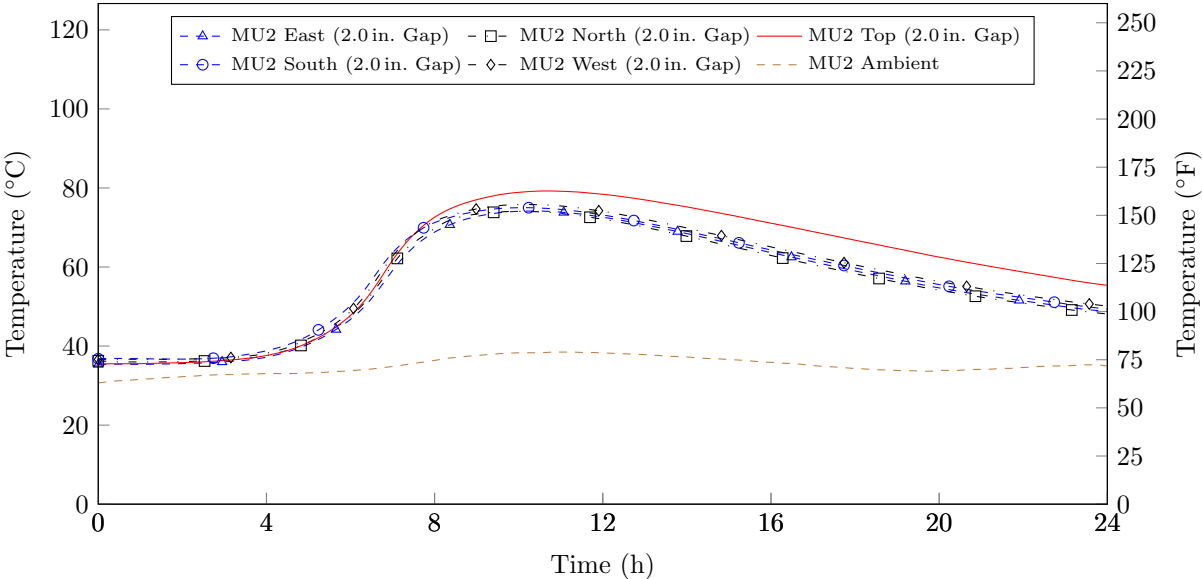


Figure 4.4: Temperature development after mixing grout for MU2

Temperatures at the side surfaces (vertical gaps) showed a very comparable development with almost identical values throughout. However, the top surface temperature deviated from the side surface temperatures with slightly higher values (hotter surface) after about 7 hours. The ambient temperature remained between 65 °F (18 °C) and 75 °F (24 °C). Furthermore, all grout test temperatures started increasing after about 4 to 6 hours, reached the highest value after 10 to 11 hours, and cooled down afterwards. The side surfaces reached about 150 °F (65 °C) and cooled down slowly to about 100 °F (38 °C) 24 hours after the grouting was completed. Compared to those, the top surface reached 10 °F (5.5 °C) higher temperatures (almost 160 °F (71 °C)) and cooled down to about 115 °F (46 °C).

All specimens from Task 2 — MU7 through MU11 — were made from grout with an efflux time from about 48 s and a temperature range between 85 to 90 °F (29 to 32 °C), so that the fresh grout material had the highest temperature and the highest efflux time, which was evaluate in this research project. Figure 4.5 illustrates the temperature development that was recorded for MU9, which was produced with a minimum horizontal (top) gap size of 2.0 in. (50 mm). Due to the tapered surface at the roof of the bent cap the top gap increased to a maximum thickness of 3.0 in. (75 mm). The graph plots time, in hours, on the horizontal axis and the temperatures, in °F and °C, on each vertical axis. The data shows that all four (4) vertical volumes responded identically with the same temperature development due to the hydration heat.

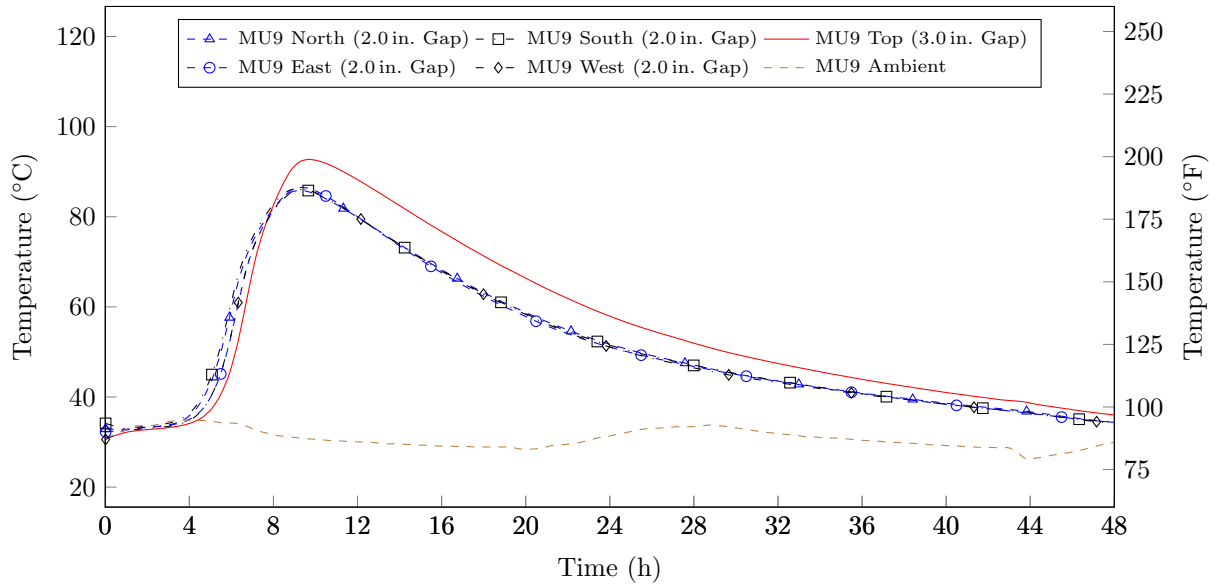


Figure 4.5: Temperature development after mixing grout for MU9

After the initial dormant period of four (4) hours, the temperatures increased rapidly and peaked at about 185 °F (85 °C), approximately 10 hours after the grout was poured. The thicker 3.0 in. (75 mm) top gap reached higher temperatures and peaked at about 205 °F (95 °C), after an additional 30 minutes. Initially the temperature of the top volume increased at the same rate as the temperature in the vertical volumes, but after approximately 6 hours, the temperature increased at a slower rate for the vertical surfaces, while the temperature of the horizontal volume kept rising. After reaching the peak temperatures, all volumes cooled down at an equivalent rate — rapidly until the 26th hour to reach temperatures below 120 °F (50 °C) and more slowly thereafter to equilibrate with the ambient temperature after 48 hours. While the heat development changed drastically in the grout, the ambient temperature remained relatively constant with slight variations between night and day time.

Figure 4.6 illustrates the temperature measurements for MU10 which was geometrically identical to MU9, except for the horizontal volume at the top of the specimen — it was less massive with a maximum thickness of 1.5 in. (37.5 mm). Similar to MU9 (Figure 4.5), all 2 in. (50 mm) vertical volumes responded identically to the hydration process, with a rapid temperature increase between hour four (4) and eight (8), and a cool down period thereafter — relatively fast until the 24th hour, and then less rapidly to eventually reach equilibrium with the ambient temperature after approximately 48 hours. The maximum temperature of the vertical volumes was 185 °F (85 °C) after approximately eight (8) to nine (9) hours. However, compared to MU9 (Figure 4.5), it is clear that the top volume in Figure 4.6 (MU10) did not reach such high temperatures — but instead peaked at 185 °F (85 °C), which remained well below all other temperatures measured for that specimen.

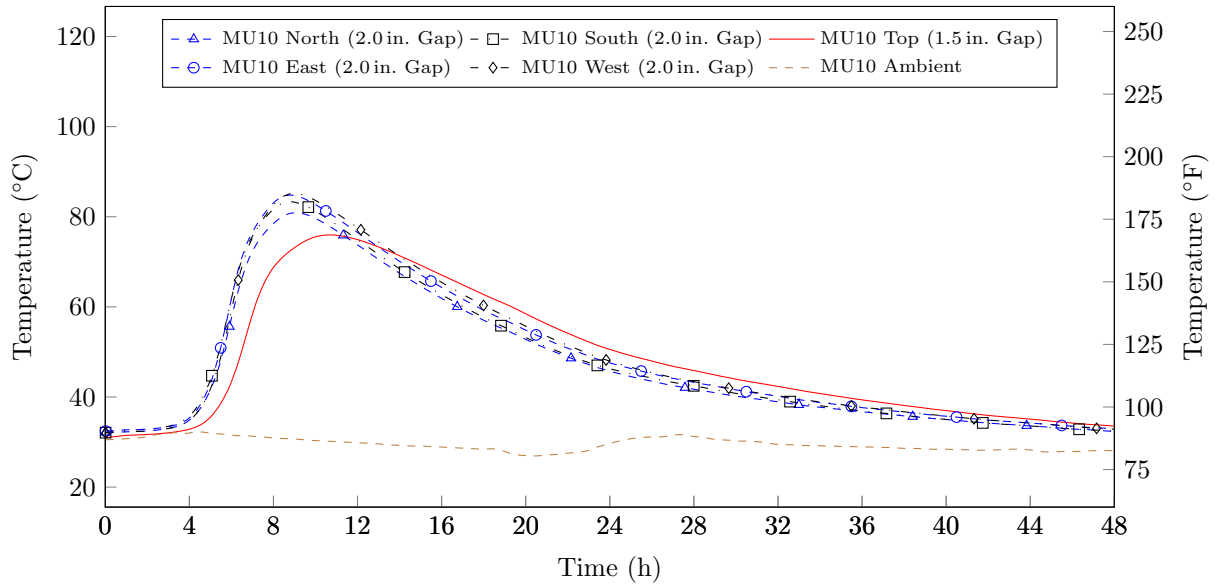


Figure 4.6: Temperature development after mixing grout for MU10

4.2.2 Various Gap Size Openings for Vertical Volumes

While the construction plans for a bridge project aim for a symmetric arrangement of the bent cap-to-pile head connection, construction tolerances account for imperfections due to fabrication and construction processes. It is very common for a construction project to take full advantage of geometric tolerances when placing the bent cap on top of the pile head. It is even possible, that the bent cap cannot be placed on the pile without violating the usual tolerances. To accommodate such limiting cases in this research project, MU5, MU6, MU7, and MU8 were produced with varying gap sizes. As shown and explained in Section 3.1.2, two (2) adjacent vertical side volumes had a thickness of 7.5 in. (187.5 mm) and the other two (2) adjacent ones were measured with 0.5 in. (12.5 mm).

The measured temperature development for specimens MU5 and MU6 were nearly identical, so that Figure 4.7 is representative for specimens with a higher initial grout temperature between 85 to 90 °F (29 to 32 °C) and a lower efflux time (20-30 seconds). Temperatures started out at 87 °F, increased up to 180 °F in the first eight (8) hours and then fell down slowly to less than 115 °F. The sensor for one (1) vertical side volume malfunctioned, so that results are not available for the south side for this specimen. Compared to the temperature development of MU2, mockup specimen MU5 reached higher maximum temperatures. In addition, the ambient temperature was slightly higher.

Figure 4.8 plots the temperature data of MU7 on the y-axis against the maturity along the x-axis. For this particular specimen, the top horizontal volume was built with a a minimum vertical gap size of 2.0 in. (50 mm) and a taper of 0.5 in. (12.5 mm) over a length of 14.0 in. (300 mm) — leading to a slope of 3.5%. Consequently, its thickest dimension at the center line (under the ventilation pipes) measured 2.5 in.

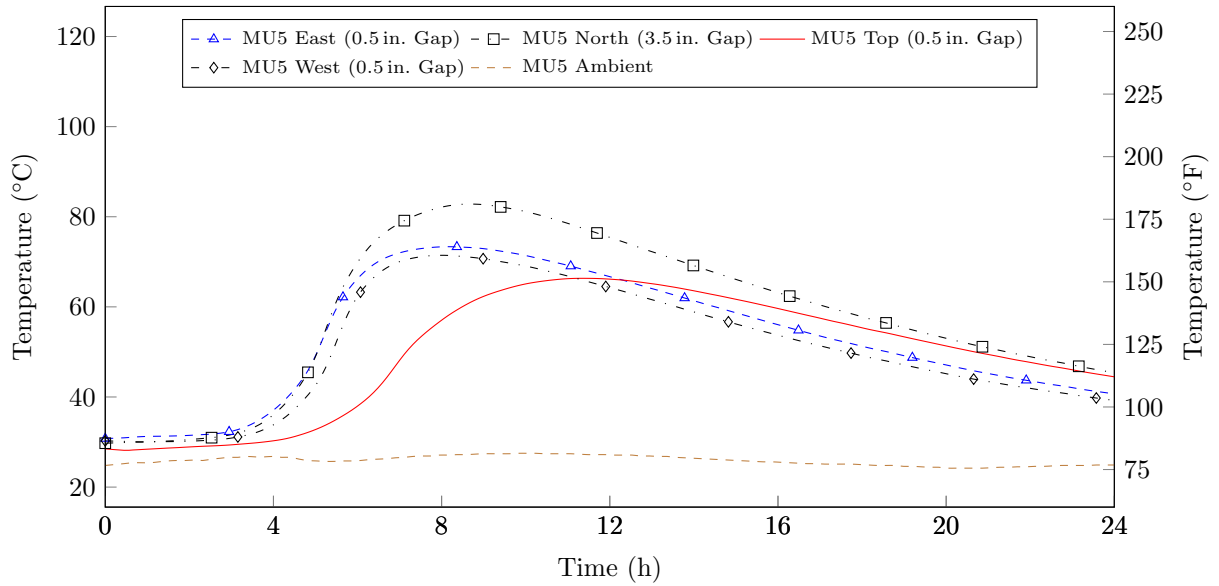


Figure 4.7: Temperature development after mixing grout for MU5

(62.5 mm). The temperatures in all four (4) vertical volumes began rising approximately four (4) hours after the grout was poured. The thicker 7.5 in. (187.5 mm) gaps reached a maximum temperature of about 220 °F (105 °C), after 10 hours, while the temperature in the thinner gaps peaked two (2) hours later with a value of about 160 °F (70 °C) for the vertical side volumes, and a value of 195 °F (90 °C) for the horizontal top volume. Similar to the previously described temperature development (MU9 and MU10), the temperatures dropped more rapidly throughout the next 10 to 12 hours, than throughout the last 24 hours to approach the ambient temperature. However, as seen before, the curing grout did not reach full equilibrium with the ambient temperature within the monitored duration of 48 hours — a trend that was noticed for all specimens within Task 2.

The temperature development plot for MU8 is provided in Figure 4.9. MU8 was built very similarly to MU7, but with a lower minimum gap size of the top volume of 0.5 in. (12.5 mm), such that the maximum thickness of the horizontal grout volume at the centerline under the ventilation pipes measured 1.0 in. (25 mm) instead of 2.5 in. (62.5 mm). The only significant difference between Figures 4.8 and 4.9 are the recorded temperatures for the horizontal top volume. The thinner top volume for MU7 peaked at 170 °F (75 °C), whereas the previously graphed thicker top volume for MU8 measured a maximum temperature of 195 °F (90 °C). Furthermore, the ambient temperatures varied slightly between 75 °F to 85 °F (25 °C to 30 °C) reflecting the differences between night and day temperatures.

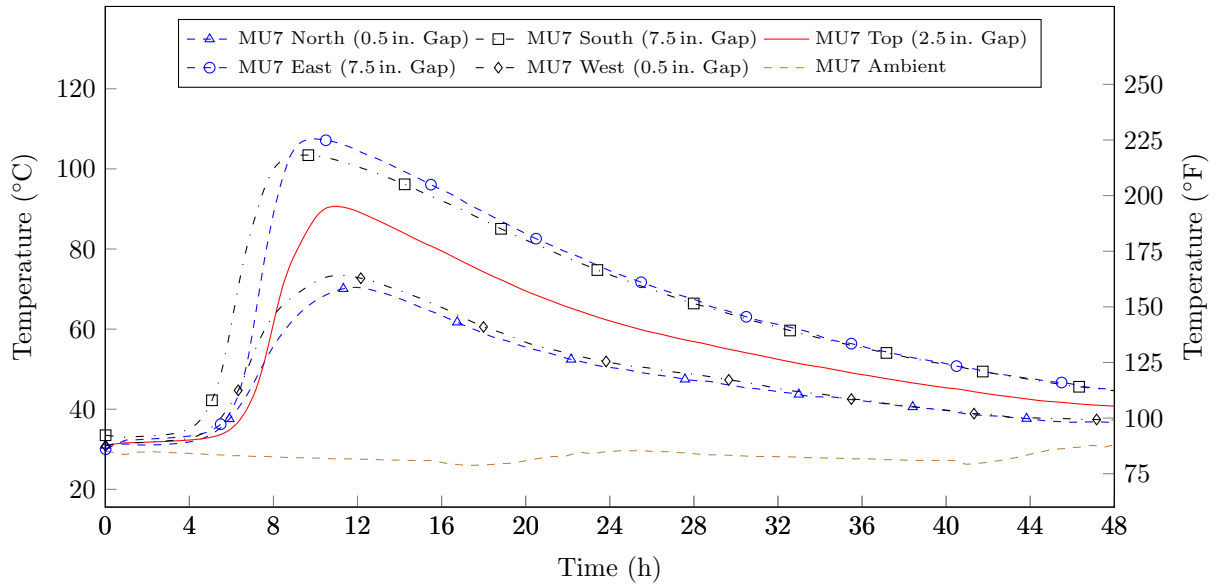


Figure 4.8: Temperature development after mixing grout for MU7

4.2.3 Temperature Development Throughout Various Grout Batches

The previous subsections detailed the temperature development for the five (5) individual grout volumes. These temperature values were measured precisely at the center of the volume, and therefore, represent an average of all three (3) or four (4) grout batches within that volume. Because MU11 was cast with 90 minutes time delays between individual batches, the thermocouples were arranged differently to measure the temperature of each individual batch (subsequently). However, the temperature recordings were started for all thermocouples at the same time and not for each thermocouple individually.

Besides the ambient temperature and the temperature within the top grout volume, Figure 4.10 plots the temperature development for the three (3) different batches that were necessary to fill MU11. Because all four (4) vertical volumes measured an identical gap size opening of 1.0 in. (25 mm), the presented data are the averaged results from two (2) thermocouples at the center of each batch at two adjacent sites (e.g.: North and East side). The top gap measured a maximum thickness of 2.0 in. (50 mm). As seen in Figure 4.10, the first batch reached the lowest maximum temperature of all three (3) batches with approximately 140 °F (60 °C). It was followed by Batch 2, and then by Batch 3 (top batch) with more than 160 °F (70 °C) The highest maximum temperature was measured for the 2.0 in. (50 mm) — most massive — horizontal grout volume. A similar dormant period of seven (7) hours was measured for all batches, but the temperatures rose rapidly thereafter. As Figure 4.10 shows, MU11 batches reached their peak temperature about 14 hours after the first batch was poured. After 48 hours, all grout volumes reached equilibrium with the ambient temperature, which did not change significantly throughout the monitoring period.

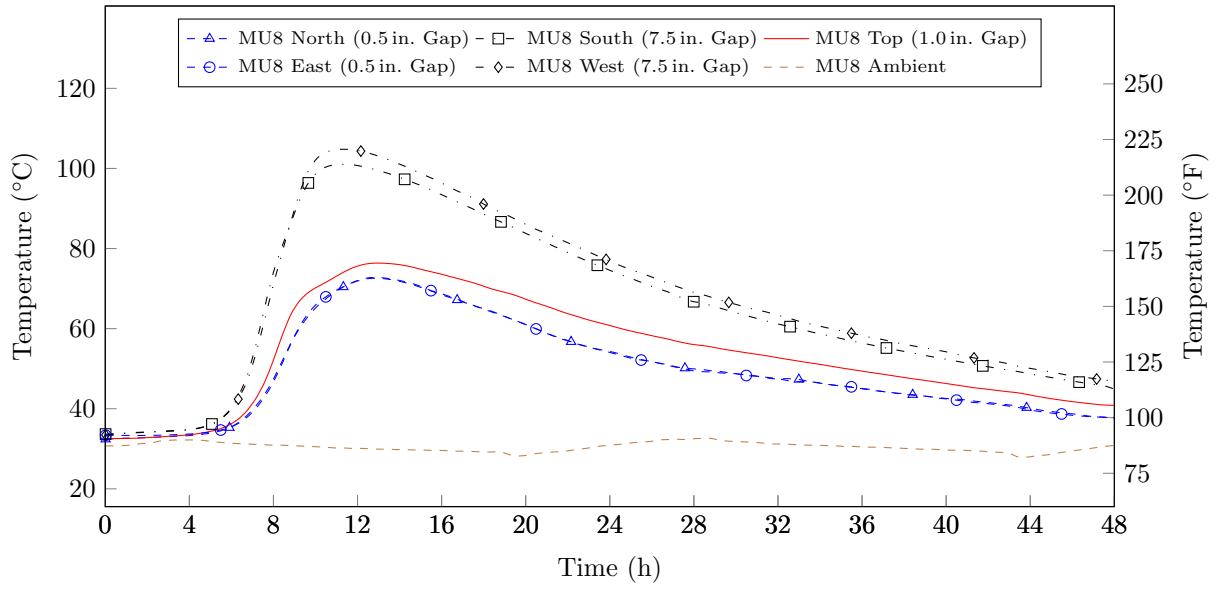


Figure 4.9: Temperature development after mixing grout for MU8

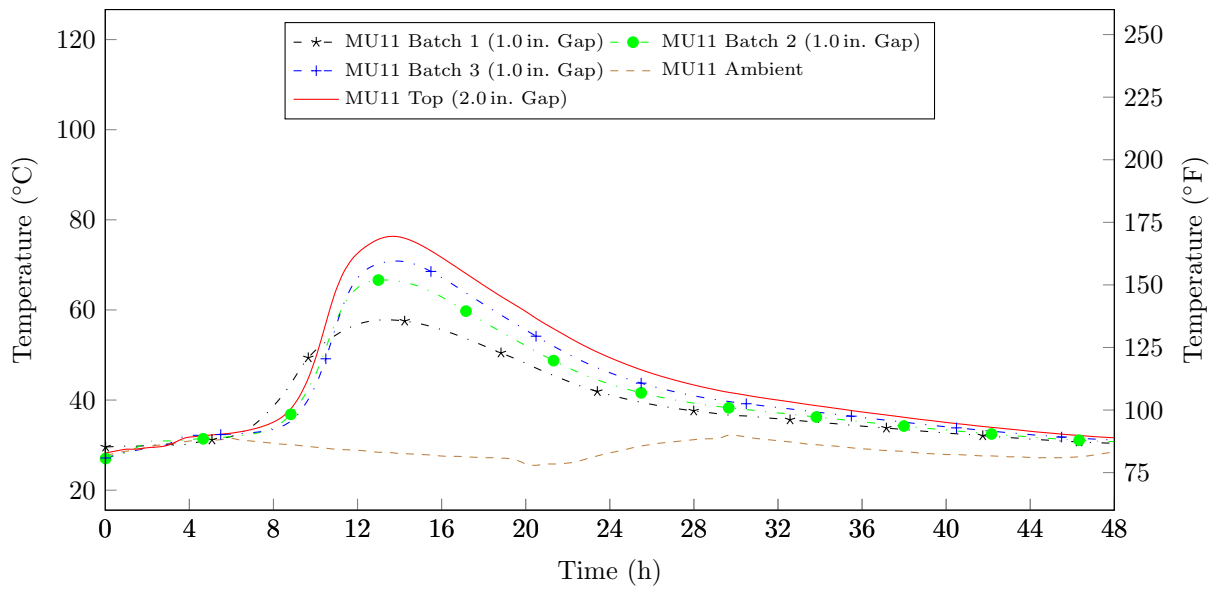


Figure 4.10: Temperature development after mixing grout for MU11

4.3 Air Void Formation

Flow and fillability are directly related to the potential formation of air voids within the grout volume and on the outer surface. A viscous mixture is more likely to trap air voids than a more liquid mixture. Likewise, a mixing, pumping, and filling process that induces additional air must be accommodated through a sufficiently liquid grout mixture that allows the entrapped air to vent out, when the grout is in place. However, (too much) entrapped air in the grout mixture may be problematic, regardless of the viscosity of the grout mixture or its ability to deair, because the air might rise through the grout volume (in its fresh state), it might be trapped inside the formwork (for example, if the only escape options are relatively small pipes at the center of a grout volume). To evaluate the overall connection detail quality, the grout materials for air entrapment, and the related surface properties, all side surfaces (Subsection 4.3.1) and top surfaces (Subsection 4.3.2) for each specimen were visually inspected and analyzed in detail after the formwork was removed (48 h after casting).

4.3.1 Vertical Side Surfaces

All four (4) side surfaces from MU1 through MU11 (Task 1 and Task 2) were examined and checked for air voids at the surface. The photos in Figure 4.11 present the vertical surfaces of MU7 and MU11. Both photos



(a) Vertical Surface MU7 — 0.5 in. (12.5 mm) Gap



(b) Vertical Surface MU11 — 1.0 in. (25 mm) Gap

Figure 4.11: Outer vertical side surface monitoring

show the North Face of the mockup specimens. While MU7 with a gap size of 0.5 in. (12.5 mm) is displayed in Figure 4.11 (a), Figure 4.11 (b) depicts MU11 with a 1.0 in. (25 mm) gap. The pictures demonstrate that the surfaces were very smooth with no significant air voids. While Figure Figure 4.11 (a) shows pattern and dark spots at the middle and bottom of the vertical surface, it must be noted that these imperfections resulted

from the formwork (screws) and not from the material or its flowability. A few insignificant surface air voids in Figure 4.11 (b) were not bigger than 1/8 in. (3.1 mm). The two (2) presented pictures are representative of the vertical surfaces for all specimens tested in Task 2, and generally, all specimens were found to have a similar outer surface quality. It is emphasized that the outer formwork was made from acrylic glass to facilitate the grout flow observations, which may have led to an improved grout surface, as compared to the surface at the plywood formwork used for the inner pile head model. Therefore, some vertical grout volumes were randomly dismantled and removed/separated from the inner plywood to gain access to the inner grout surface for quality control.

Figure 4.12 shows the inner vertical side surface of MU9, that was produced with a gap size of 2.0 in. (50 mm). The surface appeared very smooth and tight (dense grout), and the grout material was fine enough

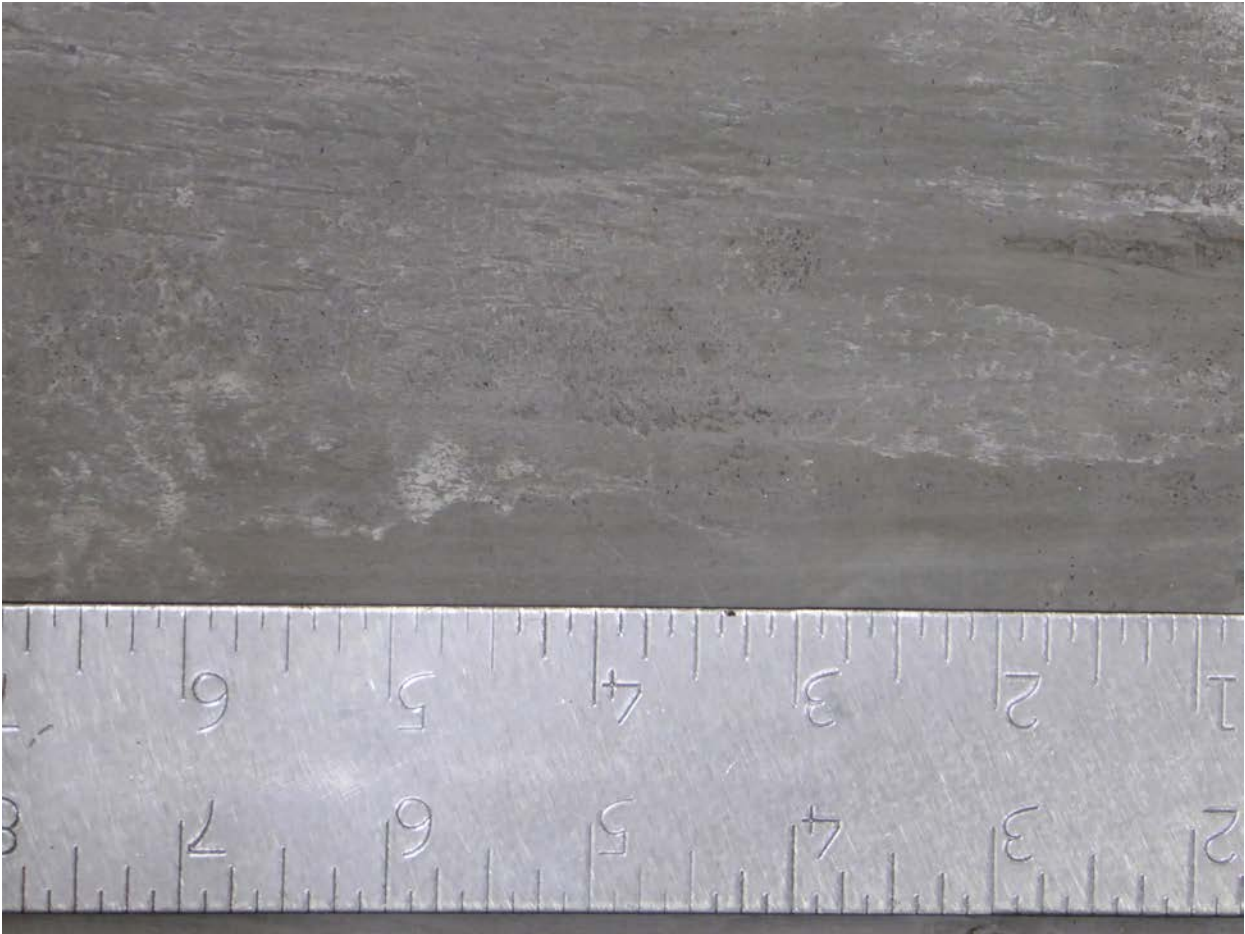


Figure 4.12: Inner vertical side surface for MU9 — maximum grout volume thickness of 2.0 in. (50 mm) Gap to mirror the minute surface imperfections of the plywood texture. No significant air voids were visible.

4.3.2 Horizontal Top Surface

Generally, the top surface of a grouted volume is most susceptible to air voids, because entrapped air that does not vent out during grout placement has a tendency to rise and float to the top surface, if the viscosity of the placed grout is low enough. The following described figures exemplify the properties of the top surface from all mockup specimens from Task 1 — MU1 through MU6 — which were produced with a completely leveled top surface. The following Figure 4.13 is representative for the top surface of the first three (3) mockup specimens (MU1 through MU3). While the photo shows the top surface of specimen MU3, it displays the

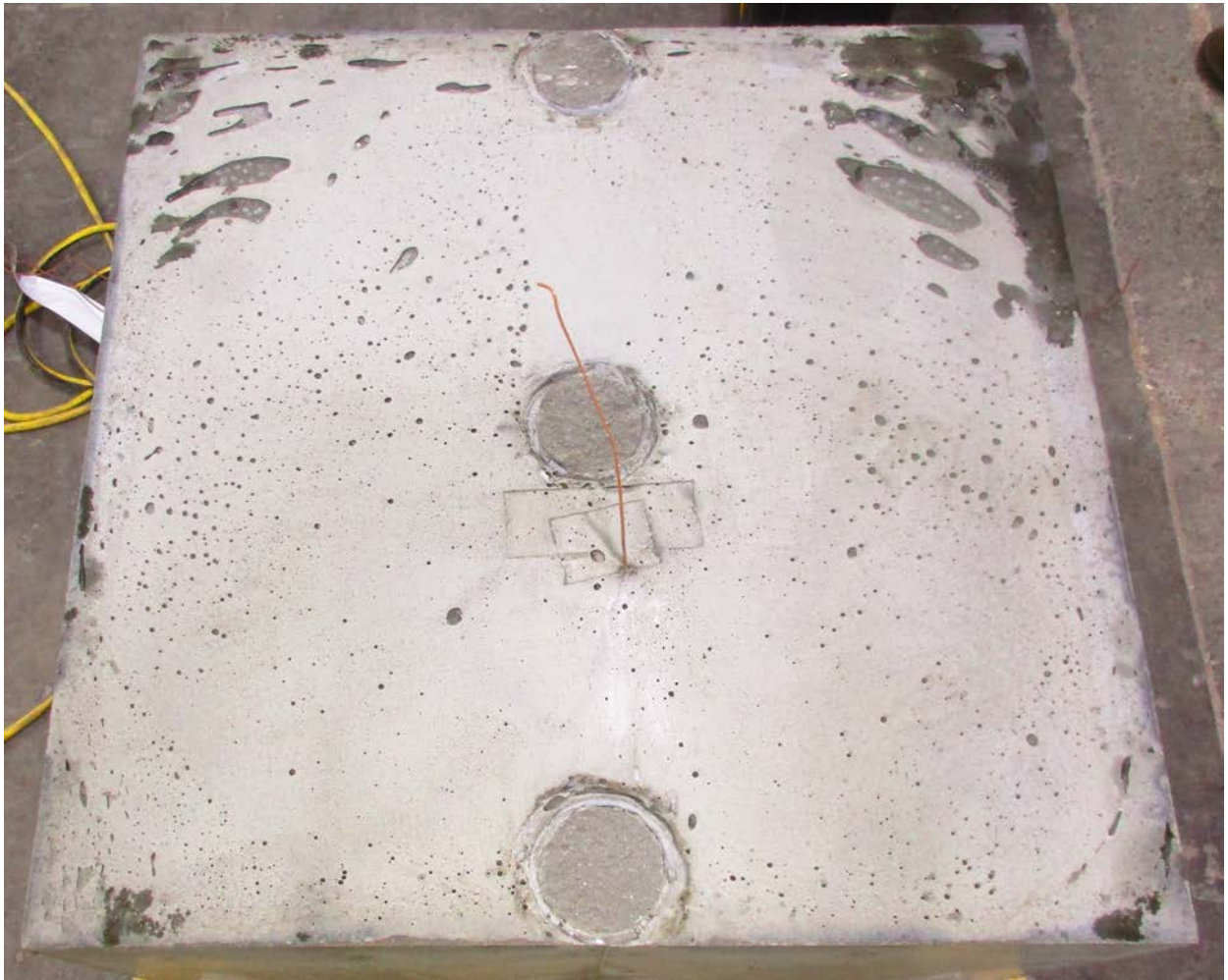


Figure 4.13: Top Surface MU3 — representative for specimens with lower water-to-material ratio

general pattern that was noted for the specimens that were made from the lower water-to-material ratio. The circular imprints along the center line of the top surface mark the positions of the filling and venting tubes. For the first three (3) specimens — MU1 through MU3 — air was entrapped under the top surface and pushed away from the filling tube into the corners. Besides these bigger air distribution, smaller air voids were presented (air void diameter smaller than 0.3 in. (7.5 mm)). The small air voids were irregularly

distributed over the entire surface, but mostly far distanced from the filling tube. Figure 4.14 shows a closeup of the big voids and schematically displays the distribution pattern of the grout. The larger air voids in the



Figure 4.14: Air void pattern indicate the grout flow (for mockup specimen MU3)

corners indicate the direction of the grout flow. Generally, these air voids had a diameter of less than 2 in. (25 mm) and were no deeper than 0.3 in. (7.5 mm)

The remaining three (3) specimens (MU4 through MU6) targeted a shorter funnel efflux time (between 20 and 30 seconds), and therefore, the fresh grout mixtures were less viscous. However, also the initial grout temperature was higher compared to MU1 through MU3. As a representative example, the top surface of specimen MU6 is displayed in Figure 4.15. Specimens MU4 through MU6 still had some air voids, but not as a concentrated at the corners as described for the first three (3) specimens. The air voids were randomly distributed throughout the entire surface with less large voids; most measured a diameter less than 0.3 in. (7.5 mm). While a limited number of air voids had a larger diameter, they were infrequent and less deep compared to specimens MU1 through MU3.

After a level horizontal roof inside the pile pocket (in the bent cap) was found to have a high potential for air entrapment (especially at the corners), it was decided to evaluate two (2) different pitches for a sloped roof in the pile pocket. MU7 and MU8 were tapered with 0.5 in. (12.5 mm) over a length of 14 in. (350 mm) or with a slope of 3.5%, and MU9 through MU11 measured a steeper slope of 7% with 1.0 in. (25 mm) over the same 14 in. (350 mm) length. In addition, the minimum top gap size varied between 0.5 in. (12.5 mm) for MU8 through MU10 and 2.0 in. (50 mm) for MU7 and MU9. Furthermore, MU11 was produced with a minimum top gap size of 1.0 in. (25 mm). Shims were added between the box and the roof of the pile pocket model for all specimens in Task 2 to collect information about the grout fillability around these obstacles.

Figure 4.16 presents two (2) different views on the top surface of MU8, which are also representative of MU7 with the same top surface taper. The entire top surfaces is shown on the left in Figure 4.16(a), and Figure 4.16(b) on the right shows a closeup of parts of the surface, which was produced with a 0.5 in. (12.5 mm) taper over a length of 14 in. (350 mm) with a slope of 3.5%. Figure 4.16(b) illustrates little air voids as well as some bigger bubbles up to a diameter of 1.5 in. (37.5 mm). Compared to Figure 4.16(a), it



Figure 4.15: Top surface MU6 — representative for specimens with higher water-to-material ratio

can be seen that these spots were noticeable throughout the entire horizontal top surface. Both photos show a partially colored mockup specimen. As described in Chapter 3, MU8 was produced to also examine the intermixing of different batches/layer within one mockup specimen. Therefore, the second and fourth batch of MU8 were produced with red color pigments. The findings based on the color tinted batches are discussed in Section 4.4.

For comparison, Figure 4.17 illustrates the 1.0 in. (25 mm) surface of MU11. Like the previously shown Figure 4.16, Figure 4.17 offers a complete overview of the top surface (a), and a closeup view of the Northwest corner (b). Figure 4.17 demonstrates findings, that were representative for all mockup specimens with a slope of 7% (MU9 through MU11). More air voids as noticed on the sides could be seen, but in total, the surfaces was very tight and almost non-porous. As seen in the North West corner, numerous 1.0 in. (25 mm) dark



(a) Overview



(b) Detail — Closeup of North West corner

Figure 4.16: Outer horizontal top surface of MU8 — minimum volume thickness 0.5 in. (12.5 mm), maximum volume thickness 1.0 in. (25 mm)



(a) Overview



(b) Detail — Closeup of North West

Figure 4.17: Outer horizontal top surface of MU11 — minimum volume thickness 1.0 in. (25 mm), maximum volume thickness 2.0 in. (50 mm)

spots appeared on that surface, which was similar to MU9 and MU10. However, overall the surfaces were very smooth with insignificant air voids. Compared to the previous Figure 4.16, and therefore compared to a lesser slope for the top surfaces, there are significantly less air voids.

The three (3) circular patterns at the centerline of the top surface (shown in Figures 4.16 (a) and 4.17 (a)), were reflective of the ventilation pipes and not a concern for the quality of the connection. Because it was necessary to completely fill the flow space with grout and to overfill the formwork into the ventilation pipes, these patterns occurred for all specimens in Task 2. It was noted that small air voids occurred for all Task 2 specimens within the close vicinity of the ventilation pipes. While these air voids (dark spots) appeared consistently along the ridge, they were considered insignificant because they were very small and traced back

to the construction methods used for building the formwork.

For quality control at the interface at the top of the pile head, the grout was dismantled and visually inspected. Figure 4.18 shows the bottom surface of the horizontal grout volume of MU11, which was produced with a minimum top gab size of 1.0 in. (25 mm) and a taper of 1.0 in. (25 mm) over 14 in. (350 mm) length. The surface appeared well consolidated with virtually no air voids. No significant differences between the



Figure 4.18: Inner top surface for MU11 — maximum grout volume thickness of 1.0 in. (50 mm)

inner horizontal top surfaces and the previously presented inner vertical side surfaces (exemplified by MU9 in Figure 4.12) were noted. The tiny voids shown on the left in Figure 4.12 were insignificant and showed up randomly at very isolated spots.

As explained previously, all Task 2 specimens were produced with two (2) shims with dimensions of 4.0 by 4.0 in. (100 by 100 mm) in each top volume. Figure 4.19 shows the grout surface conditions around the rubber shims 48 hours after grouting. Figure 4.19 (a) illustrates the shim detail for MU8 (0.5 in. (12.5 mm)) taper with a slope of 3.5%, while Figure 4.19 (b) shows the area around the shim for MU9 (1.0 in. (50 mm)) taper with a slope of 7.0%. The surface of MU8 (a) showed light air void accumulation around the entire shim and besides such small air bubbles, isolated air voids with a diameter of up to 2.0 in. (50 mm) occurred, as seen on the right side above the shim. In contrast, these larger air voids did not appear for MU9 in Figure 4.19 (b). The air void size was no larger than 1/8 in. (3.0 mm), and the voids were evenly distributed around the shim.



(a) Shim in specimen MU8 — 0.5 in. (12.5 mm) Taper



(b) Shim in specimen MU9 — 1.0 in. (25 mm) Taper

Figure 4.19: Air voids around shims — comparison between differently tapered top surfaces

The edge around the shim appears not perfectly clean (on the top left corner), because the shim was held in place and secured to the (very light) formwork lid with silicon. Due to the construction process and the assembly of the formwork for the mockup specimen, the silicon was squeezed randomly out of the interface between the bottom surface of the top acrylic glass sheet and the top surface of the shim.

4.4 Intermixing of Subsequent (Fresh-in-Fresh) Grout Batches

Depending on the equipment on the job site, it may not be possible to fill the grout connection with one lift. The grout mixer used in this study was not the same as the one used during the US 90 demonstration project. However, the used mixer had a similar capacity as the one used in the field, and due to that limited capacity, the mockup specimens had to be filled with three (3) or four (4) individual batches.

Figure 4.20 shows the vertical surface of one (1) randomly chosen specimens — MU1 — that was representative for all other specimens. According to the discolorations as shown on this vertical side volume with a gap thickness of 2.0 in. (50 mm), the four (4) different layers — marked in the picture — seem to be visible. If the this layering effect is truly noticed, the batches are critical isolated from each other. The imprint at the center of the surface resulted from the thermocouple installation and is of no further interest for the research.

However, because the following mixture was always pumped into the previously placed one with minimal time delays (fresh-in-fresh), it was decided to color code every other batch of MU8 with red pigments to study the intermixing of consecutively poured grout layers. Figure 4.21 shows two (2) photos that relate

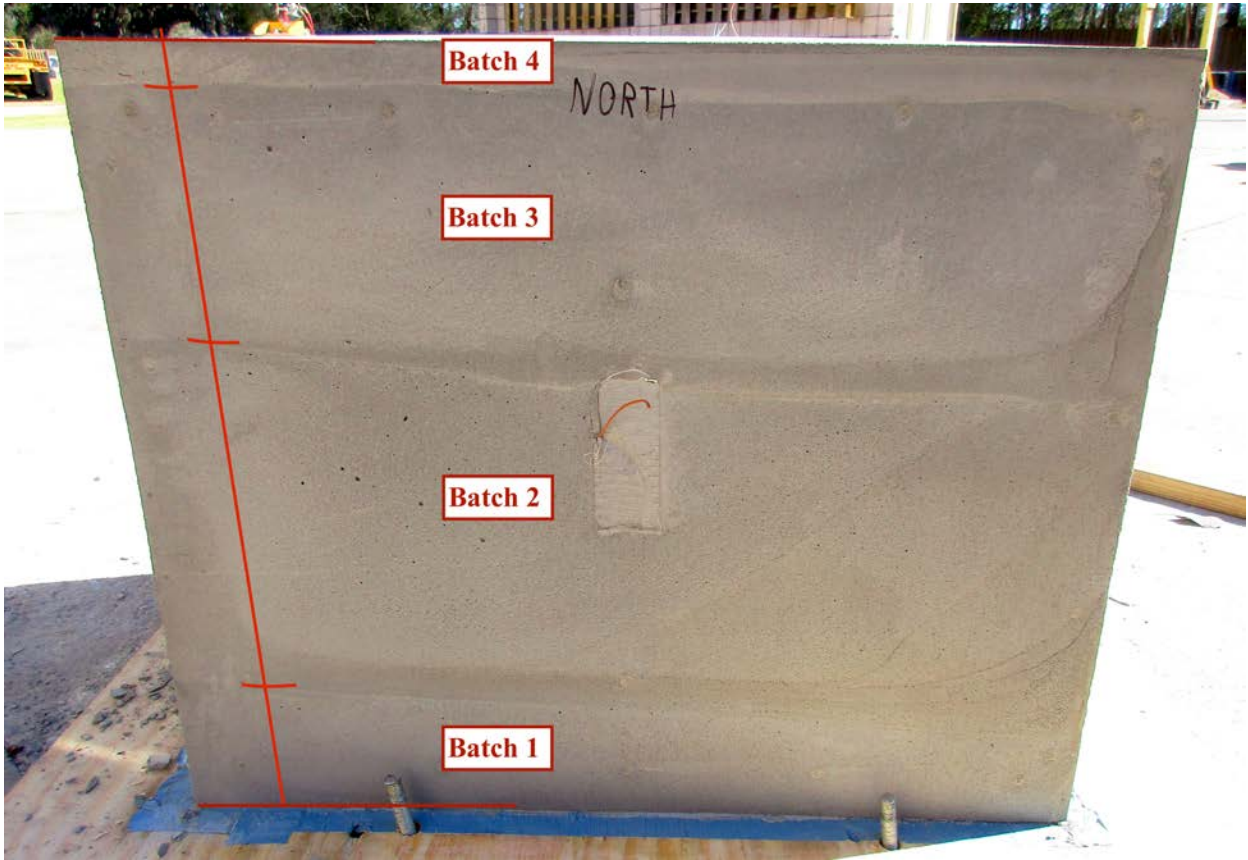


Figure 4.20: Outer side surface MU1 — 2.0 in. (50 mm) gap

to MU8 and the blending of different grout batches/layers. This particular specimen, MU8, was made from four (4) consecutive grout batches. While the colored grout material in Figure 4.21(a) can be assigned to an individual batch, it can clearly be seen that the pumped material mixed very well with the placed material, such that no horizontal layering occurred. Instead, the materials mixed so well that random color patterns developed and that transition zones with various red-gray shades appeared.

To gain further insight about the properties of the inner volume of the grout, horizontal cores were taken from those mockup specimens, that provided enough sidewall thickness for 6 in. (152.4 mm) long cylinders. A minimum of two cores per batch were extracted from MU7 and MU8, each with a diameter of 3 in. (75 mm) and a length of 7.5 in. (187.5 mm). The failed cylinder from MU8 in Figure 4.21(b), demonstrates that the transition zone between consecutive grout layers appeared randomized throughout the third dimension (length of cylinder = thickness of grout volume) as well, and therefore, that the material did not transition — between placed and flowing grout — at the same elevation. Furthermore, randomized little colored spots were found in some cylindrical cores, as seen on the right side of the core shown in Figure 4.21 (b)

After the cores were taken from the mockup specimens, they were tested for compressive strength. Strength results are detailed in Subsection 4.5.3. However, it is noted here that the tested cores did not



(a) Isometric view on Northeast surfaces



(b) Cylindrical cored from horizontal volume (West face) after compression failure

Figure 4.21: MU8 with color coded layers

fail directly at the layer interface.

4.5 Compressive Strength

While fillability and flowability are important characteristics, for a proper connection detail, the grout must also meet minimum strength requirements to guarantee adequate load transfer. Therefore, different sub-specimens for compressive strength testing were created to evaluate various specimen types. Companion 2.0 in. (50 mm) cubes and 3 by 6.0 in. (75 by 150 mm) cylinders were created from each grout batch (before the rest of that batch was used to fill the mockup specimen). In addition, the mockup specimens with the thicker 7.5 in. (187.5 mm) gaps for the vertical side volumes (MU7 and MU8), were cored to produce 3.0 in. (75 mm) diameter cylinders to test the strength properties of the actually cast grout. Additionally, 2.0 in. (50 mm) cubes were cut out of MU7, MU9 and MU10, because it was desirable to evaluate the difference between the cast cubes and the actually utilized material. The grout manufacturer and the FDOT set minimum requirements for the strength, depending on the grout consistency and the application type. To use a grouted connections for ABC projects in Florida, these minimum requirements must be met or exceeded. The following Subsection 4.5.1 describes the compressive strength results for the cast 2.0 in. (50 mm) cubes, Subsection 4.5.2 details the strength results for the cut out cubes, Subsection 4.5.3 presents the measured compressive strengths of the cast cylinders and the drilled cores. When applicable, the minimum manufacturer (BASF) and FDOT requirements are presented.

4.5.1 Compressive Strength Results for Cast Cubes

Before the mockup specimens were filled, the first grout material was poured into 2.0 in. (50 mm) cubes. Throughout the entire research project, the compressive strength was measured for up to three (3) samples per batch at different maturity levels (1,3, and 28 days). MU7 and MU8 required four (4) batches, while three (3) batches were sufficient to fill specimens MU1 through MU6 and MU9 through MU11.

Figure 4.22 presents the compressive strength for all specimens and batches at one (1) day of curing. The Graph shows individual bars, that represent the (individual) cube strength. Moreover, batches are

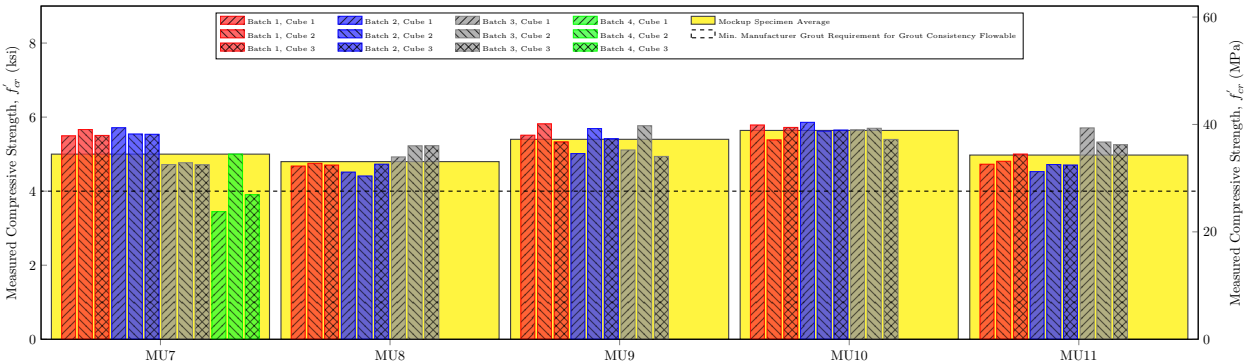


Figure 4.22: Cast cube compressive strength after one (1) day — Task 2

identified by same colors and the averages of the entire mockup specimens are the surrounding (yellow) bars. These large bars represent the average mockup specimen strength. Therefore, the figure presents five (5) groups with individual results for each specimen in Task 2. Two (2) cubes from MU7 (Batch 3) did not meet the minimum manufacturer (BASF) requirements of 4.0ksi (27.6MPa). A minimum value for one (1) day compressive strength from the FDOT does not exist. On average, MU10 measured the highest compressive strength with 5.64ksi (38.9MPa). The lowest average compressive strength was measured with 4.80ksi (33.1MPa). Due to limited test equipment (not enough molds), no cubes were produced for 1 day compressive strength testing of MU8 Batch 4.

Because the three (3) day cube compressive strength may be used for benchmark testing or for verifying early formwork release, each batch was also tested with three (3) cubes at that maturity level, these results are illustrated in Figure 4.23. All values were higher than the requirements provided by FDOT specifications

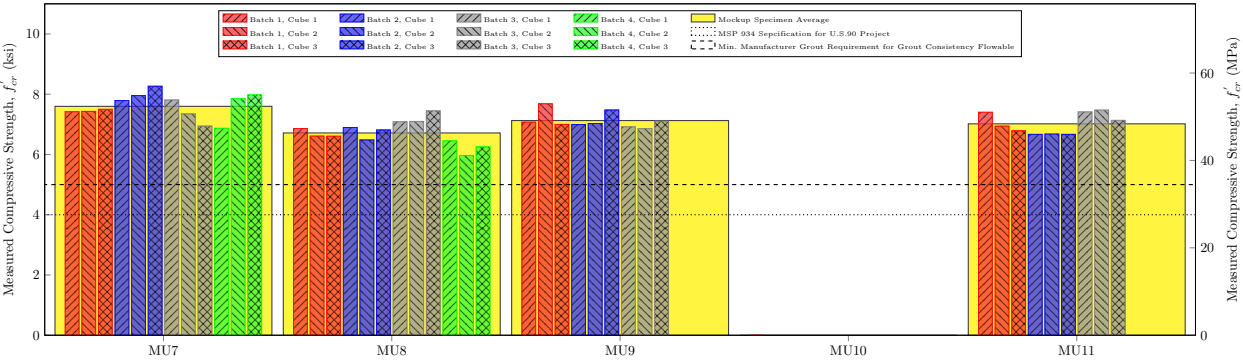


Figure 4.23: Cast cube compressive strength after three (3) days — Task 2

(4.0ksi) or than the values established by BASF (5.0ksi). The highest average specimen strength was 7.60ksi (52.4MPa) for MU7. MU8 measured the lowest one with 6.71ksi (46.3MPa). The results for MU10 could not be obtained at the three (3) day maturity level, due to Hurricane Hermine at the beginning of September 2016.

Figure 4.24 illustrates the compressive strength results after 28 days for all specimens from Task 1 (MU1 through MU6). In total 49 cube samples were tested and all specimens met the lowest requirements provided by FDOT of 6.25ksi (43.1MPa). However, one (1) individual cube from MU6 — Batch 2 — has a lower compressive strength of 8.0ksi (55.2MPa) than necessary due to the manufacturer BASF. In general, the averages of MU1 through MU6 are 1.5 to 2.0ksi (10.4 to 13.8MPa) higher than than requirements from BASF. Finally, Figure 4.25 displays all compressive strength values for cast cubes 28 after the mockup specimen was grouted. The figure shows, that most values were higher than the required FDOT strength of (6.25ksi) (43.1MPa) and than the minimum BASF strength of (8.0ksi) (55.2MPa). Two (2) individual cubes from MU11 did not meet the compressive strength, that is required by BASF. Nevertheless, these two (2) samples reached values that were above the minimum requirements required by FDOT specifications. Analogous to

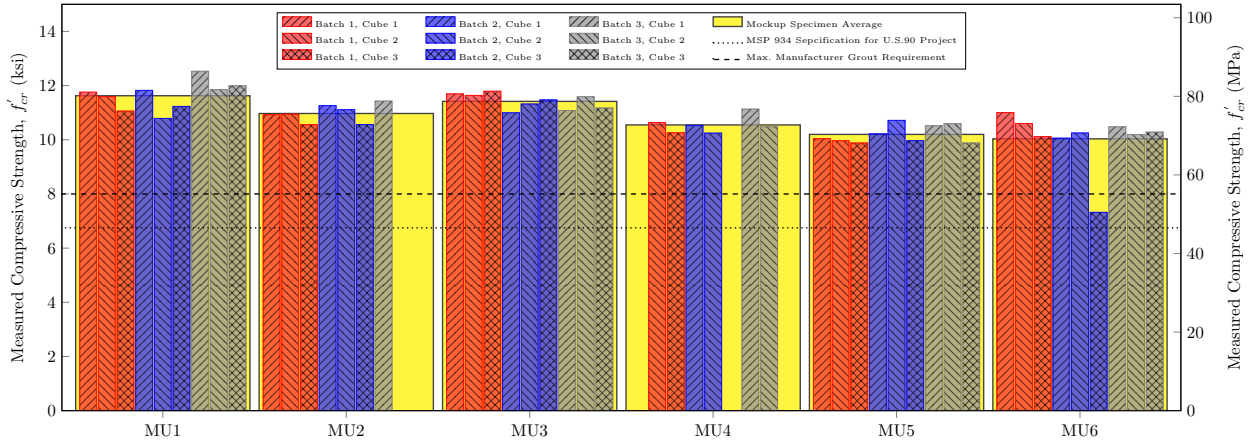


Figure 4.24: Cast cube compressive strength after 28 days — Task 1

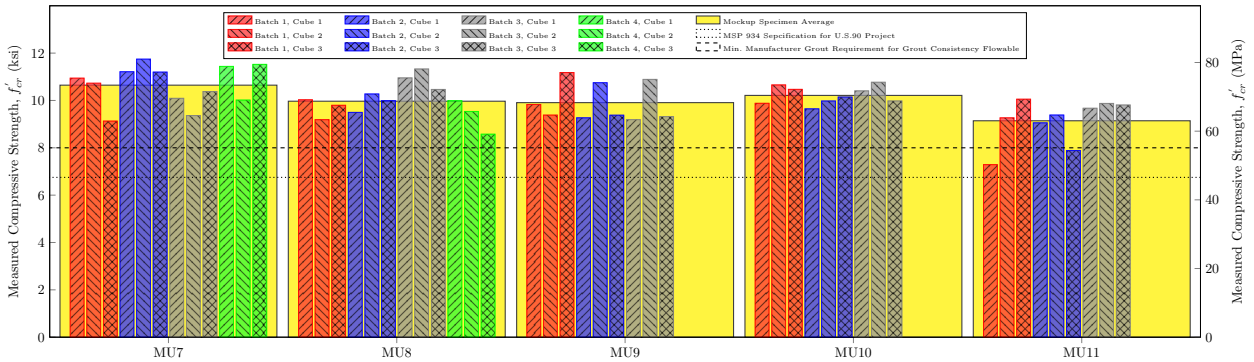


Figure 4.25: Cast cube compressive strength after 28 days — Task 2

the 3 day compressive strength, the highest average mockup specimen strength at 28 days was again noted for MU7 and measured a value of 10.65 ksi (73.5 MPa). However, the lowest average mockup specimen strength was 9.14 ksi (63.1 MPa) for MU11.

To visualize the compressive strength development throughout the monitored period (28 days), Figure 4.26 plots average compressive strengths of each batch against the maturity level. As a random example, MU7 was chosen here but the illustrated trends were similar for all specimens tested in Task 2. The data curves illustrate the average compressive strength developments for each of the four (4) batches that were necessary to fill the formwork of MU7. For each data set, the average from three (3) tested cubes after one (1) day, three (3) days and 28 days were plotted. All curves indicate that the grout gained strength quickly throughout the earlier maturity levels, and that the strength rate slowed significantly after the first 3 days (within the limits of the evaluated maturity levels). Compared to the 28 day strength, the hardened grout reach a strength of approximately 50 % after one (1) day and about 75 % after three (3) days. At later ages, the average strengths deviated further from each other.

To emphasize repeatability, Figure 4.27 plots the individual average batch strength for MU8. It can be seen that Figure 4.26 (for MU7) and Figure 4.27 (for MU8) display very similar trends. The insignificant

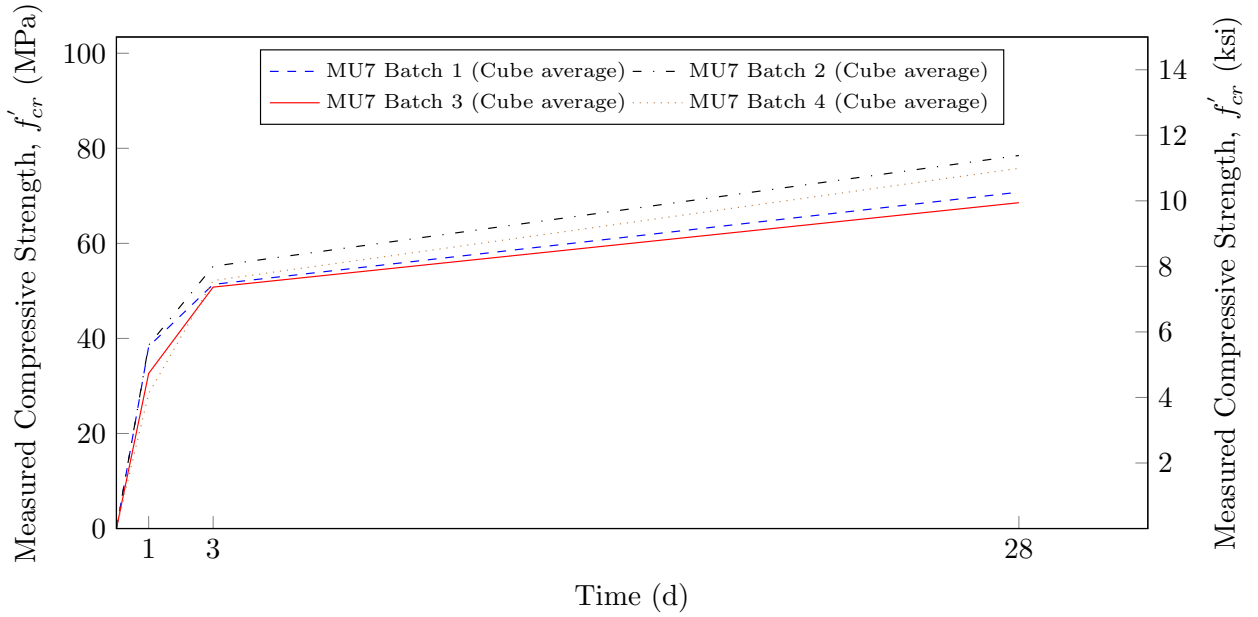


Figure 4.26: Compressive strength development of each batch for MU7 (based on average of cast cubes)

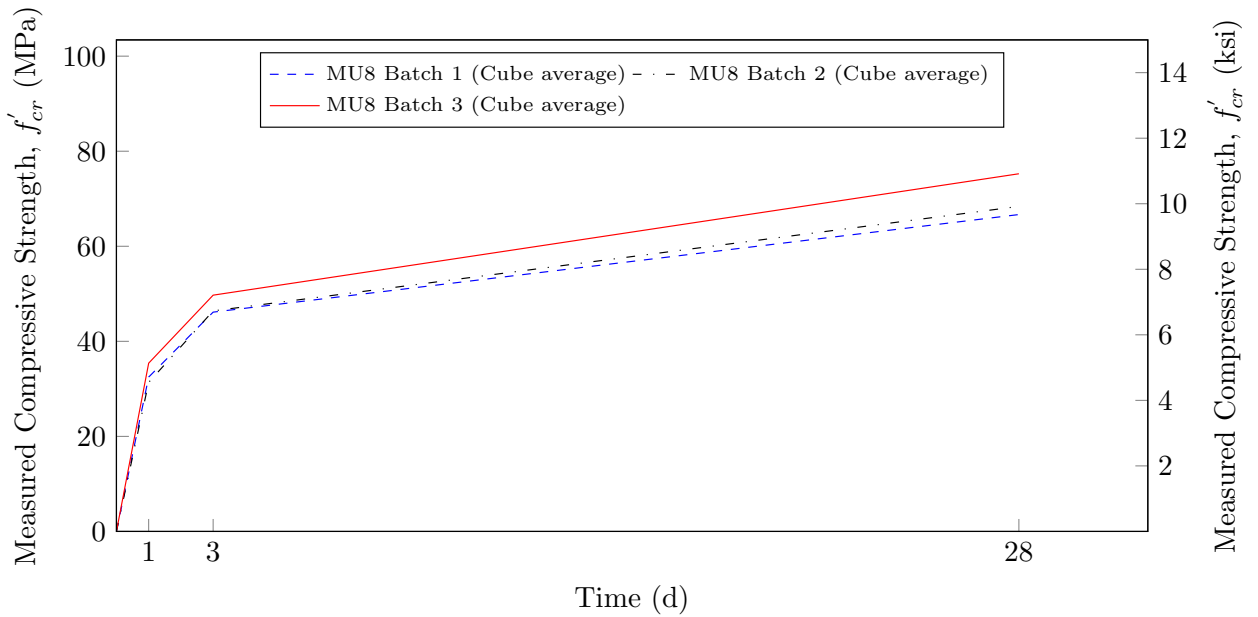


Figure 4.27: Cube Compressive Strength Development MU8

difference between individual batches and the strength gain over time are comparable between both graphs, which demonstrates repeatability between different grout batches and between different mockup specimens with identical vertical grout volume dimensions.

4.5.2 Compressive Strength Results for Extracted Cubes

The previously described results in Subsection 4.5.1 were reflective of the grout compressive strength based on material that was exposed to slightly different conditions than the material that was actually used to fill the pile head-to-bent connection (i.e.; different curing conditions). To obtain further information about the actually cast material, 2.0 in. (50 mm) cubes were cut out of three (3) randomly chosen mockup specimens. Cubes were extracted from MU7, MU9 and MU10. Cubes were cut out 28 days after the mockup specimens were cast, and at least three (3) cubes per (theoretical) layer were obtained. Because the temperature development for the first 48 hours was monitored for all mockup specimens, no cubes were cut out for one (1) day compressive strength testing. Cube specimens for three (3) day compressive strength were not cut out, due to other activities that had to be performed in the laboratory at that time, or due to limited man power. To facilitate a direct comparison, Figure 4.28 through Figure 4.30 plot the measured strength results of the cast cubes on the left, and the measured compressive strength for the extracted cubes on the right.

The bar graph in Figure 4.28 illustrates the strength measurements for MU7. The cubes extracted from

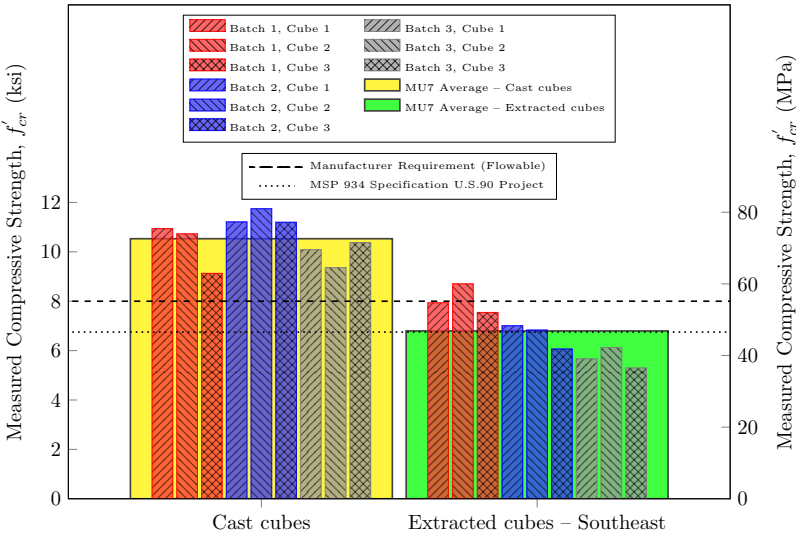


Figure 4.28: Compared Cube Compressive Strength for MU7 after 28 days

MU7 were taken from the vertical volume that was facing the southeast direction to examine the compressive strength at the transition zone between two (2) vertical side volumes. It can be seen in Figure 4.28 that the extracted cubes measured significantly lower strength values than the cubes that were cast. The average of the extracted cubes was 6.80 ksi (46.9 MPa), which was approximately 3.7 ksi (25.5 MPa) lower than the average compressive strength of the cast cubes. Therefore, the relative measured reduction in compressive strength was 35%. Moreover, five (5) extracted cubes met the requirements set by FDOT, while only one (1) out of nine (9) cubes met the manufacturer requirements. On average, the extracted cubes exceeded the FDOT requirements for the US 90 demonstration project prescribed strength value, but did not meet the

manufacturer requirements.

The 28-day compressive strengths for MU9 are illustrated in Figure 4.29. Because two (2) vertical volumes

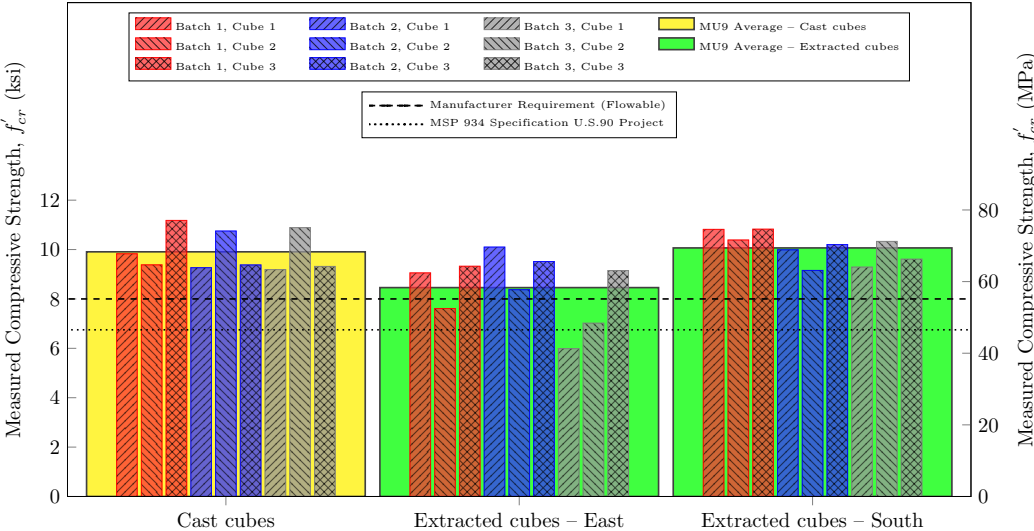


Figure 4.29: Compared Cube Compressive Strength for MU9 after 28 days

(East face and South face) were suitable for cutting out cubes, the graph shows two (2) additional data sets to the right of the previously seen data set for the cast cubes of MU9. Significantly different strength values were measured for the cubes that were cut out from the two (2) different sides. The east side cubes measured an average of 8.5ksi (58.7MPa), while the south side cubes registered an average of 10.0ksi (69.0MPa). For comparison, the cast cubes were 9.9ksi (68.3MPa). Figure 4.29 clearly shows that all average values exceeded the requirements set by FDOT and BASE. However, three (3) individual cubes extracted from the east volume of MU9 did not meet the manufacturer specifications. Furthermore, one (1) of those three cubes did not meet the lower FDOT specifications for the US 90 demonstration project either.

Finally, Figure 4.30 offers a visual comparison between the cast cubes and the extracted cubes for MU10. It can be seen that the extracted cubes did not reach nearly as high compressive strength values as the cast cubes — on average and individually, while the cast cubes clearly exceeded the requirements set by FDOT and the grout manufacturer, most of the extracted cubes did not meet the manufacturer specifications. A few individual extracted cubes did not reach the strength values suitable for the US 90 demonstration project, but on average each tested vertical grout volume met those requirements. The measured average values for the extracted cubes were approximately 2.9ksi (20.0MPa) lower than the conventionally prepared cubes with 10.2ksi (70.4MPa). Therefore, the average results were about 30% lower than the average value for the cast cubes.

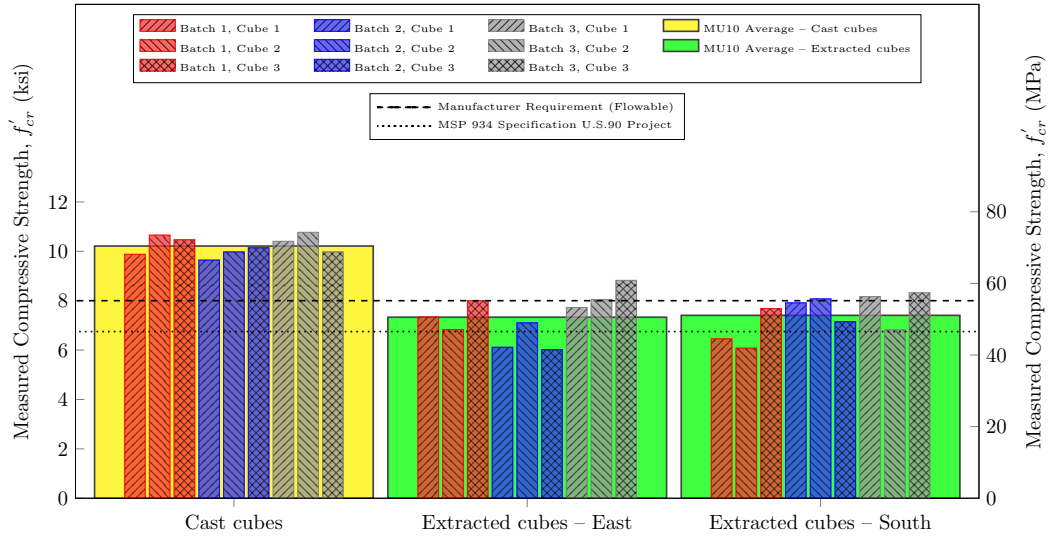


Figure 4.30: Compared Cube Compressive Strength for MU10 after 28 days

4.5.3 Compressive Strength for Cast and Extracted cylinders

Not only cubic sub-specimens were tested, but cylindrical specimens with a 3.0 in. (75 mm) diameter and a length of 6.0 in. (150 mm) were also evaluated for compressive strength. Cylinders were produced in two (2) different fashions; cylinders were molded for all mockup specimens (two (2) per layer), and cores were extracted from mockup specimens that provided grout volumes thick enough to accommodate the required cylinder length. Only MU7 and MU8 offered enough grout volume (thick wall), to extract the cores. Therefore, the compressive strength measurements for the cast cylinders and the extracted cores from those two mockup specimens are detailed below.

The cast and extracted cylindrical specimens for MU7 are visualized in Figure 4.31. The bar graphs show

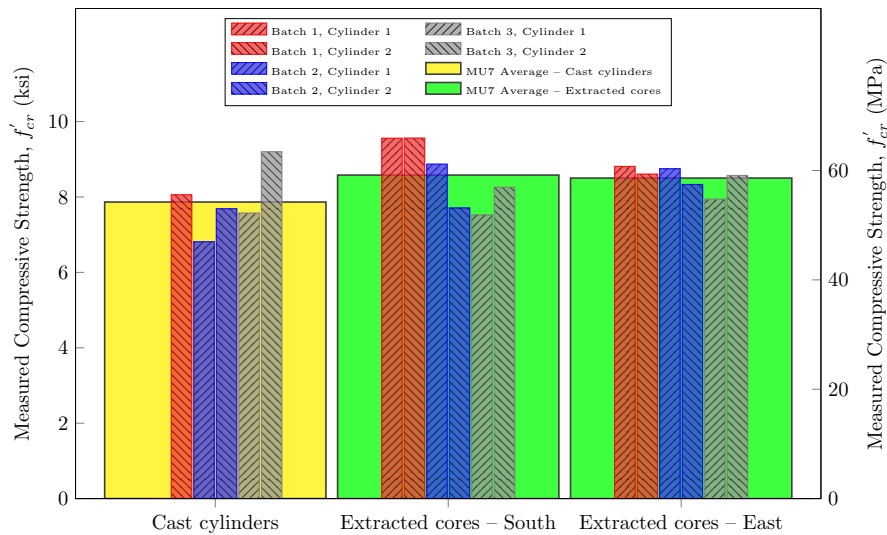


Figure 4.31: Compared Cylinder Compressive Strength for MU7

that the extracted cylinders measured higher strength values (on average) than the cast cylinders. From the figure, it is clear that the extracted cylinders from both vertical volumes of MU7 registered similar averages at approximately 8.50 ksi (58.60 MPa). Therefore both side volumes were 0.65 ksi (4.48 MPa) stronger than the cast cylinders.

The cylindrical specimens for MU8 were also tested for compressive strength and the resulting values are plotted in Figure 4.32. While the cores from one (1) side volume (south) were stronger than the cast

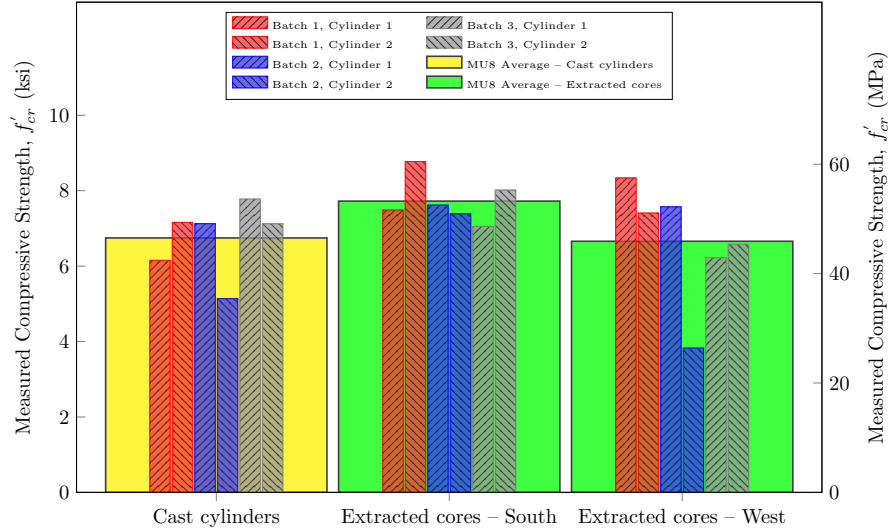


Figure 4.32: Compared Cylinder Compressive Strength for MU8

cylinders (on average) by 1.0 ksi (6.8 MPa), the cores extracted from the west volume were slightly weaker.

Chapter 5

Analysis and Discussion

All eleven (11) mockup specimens that were part of this research project were constructed, tested, and evaluated for distinct properties, as explained in the previous chapters. Throughout the experimental phase and the evaluation of test results, various findings were documented. This chapter aims to provide context for the major and secondary findings, via detailed analysis and an in-depth discussion.

5.1 Significance of Study

The Every Day Count initiative (EDC) that was initialized by the FHWA is responsible for significant developments in the infrastructural systems of the United States. Prefabricated bridge elements and systems (PBES) for use in Accelerated Bridge Constructions (ABC) projects are one of the major developments that lead to improved safety during construction and reduced project periods. For PBES, the connection points are highly critical, because they have to be implemented such that a unified behavior of the structure is guaranteed. To avoid any long-term or durability issues at the bearing interfaces — where forces are transferred from one element to another — specific quality requirements have to be met. The US 90 project demonstrated, that the hot weather conditions in Florida may complicate the construction process, if the strict “preferred temperature range” of 70 °F to 80 °F (21 °C to 27 °C) is enforced by FDOT. The contractor was inexperienced with the material and proper handling (i.e.; store the grout in cooler locations or mix with cold/ice water) under these conditions, and significant quantities of freshly mixed grout were wasted at the construction site. This research project was needed because of those reasons, and due to the fact that on the construction site, the grout flow as well as the final grout volume cannot be visually examined during or after grout placement. To best aid the standardization process for the bent cap-to-pile head interface a square pile cross section — FDOT’s Index D20710 series — was chosen for this study. Multiple boundary conditions were varied throughout this research to better predict the limiting geometric properties and the

specific requirements for the non-shrinkage grout material under Florida conditions.

5.2 Critical Analysis of Major Findings

The fresh grout material — BASF MasterFlow 928, used to connect the individual bridge elements, must meet certain temperature requirements before it can be pumped into the gaps around the pile. The test matrix (see Subsection 3.1.2) shows that all specimens in Task 2 — MU7 through MU11 — targeted temperatures between 85 °F to 90 °F (29 °C to 32 °C), at the upper acceptance level. To reach these temperatures for some mockup specimens, the grout mixture had to be adjusted with additional ice or water; at maximum the mixtures were adjusted twice (under laboratory conditions). In total, all 17 mixtures in Task 2 were prepared with temperatures between 85.4 °F to 90.0 °F (29.7 °C to 32 °C) and no mixture had to be discarded because of high temperatures (see Section 4.1). Throughout the summer months, without air conditioning and open gates in the FDOT structures laboratory, the ambient temperature reached values of up to 95 °F (35 °C), which is comparable to the conditions on the construction sites for hot weather grouting. However, the mixer used in the laboratory was placed in the shade and it was not exposed to direct sunlight. Nevertheless, for grout bags with an initial temperature of approximately 90.0 °F (32 °C), the temperature during mixing increased by as much as 5 °F to 10 °F (2.8 °C to 5.6 °C). While grout mixers on the construction site might be regularly exposed to direct sunlight (for hours — leading to high temperatures inside the mixing drum), for future projects sunlight protection for the mixing drum should be considered. Although it is possible to adjust the fresh grout temperature through the addition of ice, such techniques are inherently limited, because ice can only be added until the target water-to-cement ration has been reached. Further cooling through the addition of ice would not be possible as it compromises other important material characteristics. The pre-tests for this research and the preparation of fresh grout in the laboratory have shown that it is much more effective to control the temperature of the grout bags, rather than adjusting the temperature of the freshly mixed grout through the addition of cold water or ice. It seems good practice to store the dry grout bags in protected areas to avoid high initial temperatures in the grout material — specifically because the grout has a much higher heat capacity and more relative mass than the mixing water. Hence, contractors working on construction projects in Florida (or in hot weather) should be required to properly pre-condition the dry grout powder, to reduce the risk of elevated fresh grout temperatures that cannot be accommodated through the addition of ice.

For materials with a high viscosity, the flowability, and therefore, the efflux time can simply be adjusted through more water. If the material is too fluid, the contractor can add more dry grout powder, as long as the mixer has the appropriate capacity to accommodate the additional volume. It was impossible to precisely meet the “fluid” grout consistency, by exactly following the manufacturer recommended mixing ratios; an

efflux time between 20s and 30s could not be attained without further adjustments to further liquify the mixture. This deviation appears to be a result of the high temperatures that were targeted for the “fluid” mixtures, so that a more viscous material — when following the manufacturer recommendations precisely — during hot weather grouting can be expected. In other words, the manufacturer recommended water-to-material ratios, should be adjusted — towards increased liquidity — for hot weather grouting, to avoid unnecessary adjustments of the grout mixture after initial batching.

The results presented in Sections 4.1.1 and 4.1.2 suggest that the formation of air voids in the grout volumes should be discussed separately for two (2) individual categories; i) for the vertical volumes around the sides of the pile and ii) for the horizontal volume on top of the pile head.

Throughout this research — independent of the efflux time, fresh grout temperature, or gap size opening — the side walls of the grout body did not show any significant air voids, neither on the surface nor internally for the few specimens that were cut open. Video analysis has proven that the grout flew well into the vertical volumes and properly spread into all openings under gravity for all scenarios. The material even filled the smallest gaps of 0.5 in. (12.5 mm) in mockup specimens MU7 and MU8 easily, and therefore, an adequate fillability was documented for all specimens in this research. It was noted, however, that the fillability differs dependent on the relative flow direction. MU5 through MU8 were the only specimens produced with varying vertical gap sizes, and MU7 and MU8 represented the extreme case with two (2) adjacent gap thicknesses of 0.5 in. (12.5 mm) and the other two (2) adjacent gaps with 7.5 in. (187.5 mm). For MU7, the grout was pumped into the mockup specimen through the PVC pipe that was located directly above one of the larger gaps, MU8 on the other hand was filled from above the smaller gap. While the leveling transition times (see Subsection 4.1.1) for specimens with unified gaps were similar, a difference in fillability was observed for specimens with varying gap sizes. Leveling periods were reduced if the material flowed from a smaller gap size opening into a bigger gap size opening (30s for MU8), and increased for the opposite case (60s for MU7). This effect can be traced back to the transition zone where the material accumulates before it can flow from a larger opening into the smaller one; the material stalls and the flow is delayed. If, however, the material flows in the opposite direction, the flow is more consistent and the filling process becomes more uniform, because the material is not blocked at the transition zone (corner). To guarantee better leveling and to promote a uniform grout flow on the construction site, the fresh grout material should always be pumped into the openings from the side with the most narrow opening.

After demolding Mockup Specimens MU1 through MU6 for Task 1, the individual grout batches appeared to form clear layers (see Section 4.4), and the interaction between subsequent (fresh-in-fresh) layers was in question. Accordingly, it was decided to color code the different layers for one specimen in Task 2 (MU8). The color pigments confirmed that two (2) adjacent layers formed a proper connection without any layering

effects, even for the grout material that was prepared to target the highest viscosity in this research — flow cone efflux time of 48 s. No clear separation between differently colored layers was shown, but instead a well mixed grout body was formed. The drilled out cores showed that the intermixing of layers is a three-dimensional phenomenon and that the colored and not colored materials formed a strong bond. Within the 15 min to 20 min time frame between individual batches, the layering effect appears to be unproblematic for the certain grout material evaluated in this research project.

The outside surface (grout bent-cap interface) of all mockup specimens were visually inspected and analyzed for air voids (see Subsection 4.3.1). Generally, no significant air voids were found and all surface voids were smaller than 1/8 in. (3.1 mm) for all mockup specimens, independent of the targeted flow cone efflux times or grout temperatures. It appears that air void development (Park, 2009) on vertical surfaces is not a concern within the boundary conditions evaluated in this research.

The air void development at the top surfaces initially seemed problematic throughout Task 1 — specifically for the material with higher viscosity or high flow cone efflux times (see Subsection 4.3.2) — due to larger air pockets and entrapped air that was pushed towards the corners that were located at the opposite sides of the influent PVC pipe. However, similar to the US 90 demonstration project, the roof of the outer formwork was constructed with a flat and level surface for Mockup Specimens MU1 through MU6. Based on the fact that the vertical surfaces of the grout seemed unproblematic, and because materials with fine aggregates (grout) promote the release of integral air (N/A, 1976), it was assumed that the air void issue was a result of the geometric properties of the outer formwork, and the roof of the pile-pocket model was sloped for all Task 2 specimens — MU7 through MU11 — to further evaluate the formation of air void development at the top surface of the mockup specimen. Although the grout material in Task 2 targeted higher viscosities, it was found that the amount and size of air voids on the top surface was significantly reduced, dependent on the geometric properties of the pile-pocket roof, as an inclined surface — towards the PVC pipes — promotes ventilation and allows the air (that is “wave like” pushed into the open spaces, due to the cyclic pumping mechanism) to escape from the grout that is not 100 % liquid. MU7 and MU8 were constructed with a 3.5 % slope for the pile-pocket roof and a clear improvement, as compared to the horizontal roof, was noted. However, because some bug holes were still found at the corners (opposite to the side from which the grout was fed into the form), it was decided to increase the slope of MU9 through MU11 to realize a 7 % incline. Significant surface improvements were documented for the last three (3) mockup specimens, with no larger entrapped air bubbles at any location on the top surface (grout-to-pile-pocket interface). From the video footage and air void analysis, it can be concluded that the geometric properties of the pile-pocket roof surface have an additional curtail impact on the surface density — which must be considered for durability. It is noted that small air voids on the top surface will always occur, because the mixed in air from the bottom

of the entire grout volume slowly rises to the top (if the material is liquid enough), due to inherent density differences within the Three-Phase-System (Domone and Jefferis, 1994b) described in Subsection 2.5, and because all gaps may be completely filled before the mixed in air has risen completely. Less air might be introduced into the grout body, if the material is pumped into the gaps from the bottom up (see above), which might lead to less small-size air bubbles at the top surface from rising air. However, even for gravity fed grout materials with a high stiffness (48 s cone efflux time), a 7% sloped roof produced high quality surfaces at the grout-to-pile-pocket roof interface. Therefore, for future construction projects that implement FDOT's Index D20710 series or similar connection details, a minimum slope of 7% — towards the influent pipes — should be built into the roof of the pile-pocket, to reduce air entrapment and to promote more durable interface.

Directly after grouting, throughout the initial hydration phase and until the mockup specimens were demolded (24 h for Task 1 and 48 h for Task 2), the temperature development at the center of each grout body was monitored to assess the hydration heat based on the gap size dimensions. The results in Section 4.2, show that i) the relative temperature evolution (shape of temperature curve) follows a similar trend for all grout body dimensions, ii) the temperature development is almost identical for grout elements with equal volume-to-surface ratios, and iii) the peak temperatures increase if the grout element is more massive. All temperature vs. time graphs have shown that the initial dormant period for the tested grout material ranges between 4 h to 5 h, similar to the information found in Mehta and Monteiro (2005). Afterwards, throughout the next 6 h the temperature rapidly increases to reach peak values, which is in agreement with Domone and Jefferis (1994b), who states that grout temperatures increase for about 5 h, before the maximum values are reached and approximately held for 3 h. Then, the temperature reduces quickly until it decreases less rapidly, 24 h after the material was placed, to reach equilibrium with the ambient temperature. This suggests, that grout curing (if possible) is most critical throughout the first day, after placement. In addition, the data showed that the temperature development is similar (nearly identical) for grout volumes of equal size or thickness. While the shape of the temperature curves followed similar trends, it is clear from the graphs in Figures 4.4 through 4.10 that the actual grout temperatures are dependent on the gap size opening, as all curves for one particular grout thickness — 0.5 in. to 7.5 in. (12.5 mm to 187.5 mm) — were almost congruent throughout the entire monitoring periods. Finally, more massive grout bodies reach higher peak values, such that the material in the widest gaps — 7.5 in. (187.5 mm) — reached maximum values of 230 °F (110 °C), as seen in Subsection 4.2.2. According to Domone and Jefferis (1994b); Popovics (1998); Wilson and Kosmatka (2011) these peak temperatures become problematic for the grout structure, because they promote cracking throughout the initial (rapid) cooling phase. However, as demonstrated by the temperature graph for MU5 in Figure 4.7, the temperature inside the grout volumes with a gap size opening of 3.5 in. (88 mm) did not

exceed 195 °F (90 °C). Accordingly, for hot weather grouting, the tolerances on the construction site should be limited, to guarantee that a single gap size does not exceed a certain maximum value. Further research might be necessary to precisely define a maximum allowable grout body thickness, but the temperature measurements in this study suggest a limit of 3.5 in. (90 mm).

Throughout and after the initial hardening process, the compressive strength (Section 4.5) of the grout material must meet certain acceptance requirements. Because companion cast cubes with an edge length of 2.0 in. (50 mm) are mainly used to verify the strength requirements of the grout material, Subsection 4.5.1 details the measurements for Task 1 cubes after 28 days and Task 2 cubes after one (1) day, three (3) days and 28 days. In total, 190 samples — 49 cubes in Task 1 and 141 cubes in Task 2— were evaluated for 35 batches and all eleven (11) mockup specimens. After 28 days, all cast samples for MU1 through MU11 met the FDOT strength specifications for pile-to-bent connections. In addition, all samples for MU7 through MU11 also reached the minimum requirements values after three (3) days, and a FDOT specification for a one (1) day maturity level does not exist for grout cubes. However, at a one (1) day age, two (2) companion specimens in Task 2 did not meet the more rigorous strength requirements set by the grout manufacturer, which means that 96 % of all cast cubes in Task 2 reached satisfactory strength values according to BASF. Also three (3) samples after 28 days — 97 % — measured lower values than required by BASF. However, in total 97 % of all 190 tested samples met both acceptance criteria, provided FDOT and BASF. Due to the fact that grout is made from natural products and and because no two (2) batches are alike, grout composition vary and produce different results for every tested sample (Domone and Jefferis, 1994b). Therefore, the here observed variations in strength measurements fall within the expected standard deviation of compressive strength test results. However, in conclusion, the evaluated grout material performed satisfactory, even under extreme temperature conditions and high viscosity levels.

5.3 Additional Findings

The major objective of this research project was to evaluate the flow and fillability of a specific grout product under hot weather conditions, to supply helpful data for standardizing the bent cap-to-pile-head interface in local PBES projects. The major findings that directly target the research objectives are discussed above in the previous section, however, other observations and discoveries were made throughout the experimental and analysis phase that provide valuable insight on the general topic. These additional findings are discussed below throughout this section.

The temperature developments in all four (4) vertical side volumes for mockup specimens MU1 through MU10 were measured at mid-high, mid-width, and mid-thickness (center) of the grout body. While it was shown (for MU8), that the grout materials of consecutive batches intermix well with each other, it is noted

that only one (1) specific grout batch was in contact with the measuring end of the thermocouple wires — which most often was the second batch. To gain more insight on the temperature behavior of different grout batches and because MU11 was produced with 90 min time delays between each batch, it was decided to monitor the temperature of each individual grout batch for this mockup specimen at the theoretical volumetric center of each of the three (3) needed batches, on two (2) adjacent side walls. The results in Subsection 4.2.3 illustrate that the peak temperatures of each batch occurred at similar times, in spite of the 90 min time delay between placement. Moreover, temperature graph 4.10 shows that the temperature for the first batch rose first, and was followed by the second one, and then the third one — which was expected. However, this appears noteworthy, because the first batch reached the lowest maximum temperature, while the third batch marked the highest maximum values. In general, the temperature differences between the peaks of the first and the last batch of MU11 was about 18 °F(10 °C). These results, therefore, show that a temperature interaction between consecutive layers exists — the initial temperature gain of each batch was reduced, or cooled down, by the (at that instant of time) cooler subsequent batch. And vice versa, the heat of the previous batch supplied additional energy for the temperature gain of the following batch, so that each consecutive batch reached a slightly higher peak temperature than the previous one.

Throughout this research project, cast companion cubes were produced for each grout batch to monitor the strength development throughout the first four (4) weeks and to quality control the grout mixtures. After 28 days, all cast companion cubes exceeded the minimum strength value that was required by FDOT for the US 90 demonstration project, and only three (3) out of 100 cubes for MU1 through MU11 undercut the more conservative manufacturer strength requirement. On average, all mockup specimens clearly exceeded the compressive strength requirements of both — FDOT and BASF. However, besides the cast 2 in. (50 mm) cubes, it was decided to also cast companion 3 in. by 6 in. (75 mm by 150 mm) cylinders, and to extract cores and cubes from selected mockup specimens from Task 2. The 45 extracted cubes were taken from three (3) mockup specimens, from three (3) individual layers of five (5) specific vertical side volumes. Individual and average results in Subsection 4.5.2 showed that cut out cubes measure lower strength values than the cast companion cubes. This may be traced back to i) cube preparation and/or ii) the hydration heat. In agreement with ASTM C109 (ASTM-International, 2016d), the cast cubes were prepared in two (2) layers and each layer was consolidated with a rubber tamper. This compaction action did not take place inside the formwork of the actual mockup specimen, which probably lead to a difference in densities between the cast and the extracted cubes, so that the compressive strength of the less compacted material was lower. In addition, it was shown above that the hydration heat inside more massive grout volumes increases. The 2 in. (50 mm) cubes were not very massive, and compared to the grout inside the mockup specimens, the grout in the cubes molds experienced lower temperatures throughout the first 24 h. This may be substantiated by the

limited number of compressive strength results for the cast vs. extracted cylinders. Compared to the cubes, cast cylinders are more massive, and in this case, the cylinder axis was almost as long as the bigger gaps of MU7 and MU8. It is reasonable to assume that the curing temperature inside the cast cylinders reached higher values than the curing temperature inside the cubes, which may be the reason for better matching results between cast and cored cylinders. However, the limited data in this research is not conclusive and further studies (see below in Section 5.5) would be necessary to validate these findings.

5.4 Limitations

All results and the discussion that are represented in the previous chapters and sections are provided by five (5) mockup specimens produced in the laboratory. There are a few limitations compared to the on site situation and as well as the idea of the research objective itself.

All mockup specimens were produced with one (1) specific type of dry grout powder — BASF’s MasterFlow928 — which is a proprietary product, and the prices of the individual constituents as well as their precise proportions are unknown. Consequently, aside from the water and an uncertain amount of entrapped air, the composition of the fresh grout material cannot be determined, so that different material compositions or dry grout powders from other manufacturers may yield different results. However, MasterFlow 928 is a non-shrink cementitious grout, and it is suggested to use grout materials with such properties for similar applications.

Furthermore the inner box of all mockup specimens — except for MU1 – was made from plywood sheets and the outer formwork was produced with acrylic glass. On the construction site, the pile head and the bent cap are both made from concrete. Comparatively, concrete material has more mass as well as a higher heat capacity than the grout surrounding materials used in this research. To simulate this effect in the laboratory or to retain the hydration heat inside the mockup specimens, insulating blankets were used to cover the mockup specimens after the grout was placed. However, the insulating blankets cannot fully simulate field conditions and the inner formwork (pile head) was hollow, so that the heat exchange between the grout and its surrounding may be different and may lead to different peak temperatures and different peak temperature durations.

Although it is expected that contractors will use similar material for mockup testing, the individual surfaces of the inner and outer formwork were clearly not identical to concrete. The acrylic glass, that was used for the outer formwork was smooth, which appears comparable to the concrete surface inside the pile-pocket — a prefabricated element with a well prepared and smooth surface. However, acrylic glass is non-absorptive or less absorptive than concrete, which may lead to a an improved bond at the grout-to-pile-pocket interface. At the same time, the small surface pores in the concrete pile-pocket will absorb parts of

the liquid grout phase, and withdraw some of the water that is needed for the hydration of the cementitious particles, which might reduce the quality of the grout volume. The inner formwork for all mockup specimens (except for MU1) were made from plywood, which is more absorptive than concrete, and a slightly reduced visual quality of the hardened grout was observed at those interfaces. Under these considerations, it is recommended to pre-soak (and well drain) the connection detail on the construction site, so that all surfaces that interface the fresh grout material are saturated to prevent the loss of hydration water.

The hydration temperatures reached relatively high values for the grout volumes that were more massive. These high temperatures can be problematic from a durability standpoint, because they lead to increased cracking (Domone and Jefferis, 1994a; Neville, 2006). In this particular research project, the high temperatures (and the hydrostatic pressure) lead to deformations in the acrylic glass sheets. This, however, had an insignificant impact on the research activities and the measured results.

Finally, the mockup specimens evaluated throughout this study measured precisely defined dimensions to address a specific connection detail (FDOT Index Series D20710). Other connection types exist to interface intermediate bent caps with piles, and these connections have different requirements and tolerances. While it is assumed that this research provides a general insight and details for most bent cap-to-pile head connections, not all aspects of all possible configurations could be covered by this research. Therefore, it is advisable to closely examine the specifics of an individual connection type, before applying the findings from this research.

5.5 Further and Future Directions

While specific aspects of a certain bent cap-to-pile head connection for PBES were evaluated in this research, and the objectives of the project were addressed, some findings and discoveries suggest future directions to provide more insight into individual details that could not be further examined throughout this study.

The gravity fed grouting method that was used throughout this research lead to a dense grout structure with adequate strength values, the “drop and flow” approach might have entrapped additional air in the fresh grout mixture. It appears that the fresh material was liquid enough to properly deair throughout the filling process, but it is unknown if the material density increases when no additional air is entrapped initially. Specifically from a durability standpoint, an alternative grouting method — in which the grout is pumped into the formwork from the bottom up — might lead to an improved and more dense grout structure. Further analysis of specific feeding techniques could help to enhance the longevity of grouted connections.

The peak temperatures for some mockup specimens with massive grout volumes exceeded 210 °F (100 °C), which may lead to durability issues under longterm considerations (Domone and Jefferis, 1994b; Mehta and Monteiro, 2005). From the test data, it is clear that these high peak temperatures are a result of the gap size opening, as the measured temperature for the more narrow gaps did not exceed 185 °F (85 °C).

Currently, it would be advisable to limit the gap size opening tolerances, so that the grout volume does not exceed undesirable temperatures during hydration. However, the exact temperature development of the grout should be studied in more detail, specifically under longterm durability considerations. In addition, the exact temperature conditions inside the grout as part of a real bent cap-to-pile head connection on a construction site should be monitored, to evaluate the applicability of the temperature measurements obtained from mockup testing.

While a limited number — three (3) per batch per maturity level — of companion grout cubes were cast for all mockup specimens, only a few selected mockup specimens, with thicker grout volumes, were cut and cored to obtain cubes and cylinders from the actually placed material. The cast vs. extracted specimen data in this project is too limited to draw precise conclusions, but the data mostly suggests that the actually placed grout material measures lower strength values than the individually small-size molded material. Due to the inherent variation in hydration heat for differently sized elements (Domone and Jefferis, 1994b; Mehta and Monteiro, 2005; Torrenti et al., 2010), the individually cast specimens (not massive) undergo a different curing process than the placed grout (more massive). Related effects have been studied for concrete mixtures (Ham and Oh, 2013), but literature on the actual size related hydration heat seems rare — specifically for grout mixtures. Similar to the size effect in concrete testing (Kampmann et al., 2013; van Mier and Man, 2009; Bazant, 2000; Gonnerman, 1925), a correlation factor that relates the strength of an individually cast cube to the actually strength of a massive grout element should be established.

Chapter 6

Conclusion

Throughout this research project, the geometric properties of the proposed FDOT's Index D20710 connection — pile-to-bent cap — were evaluated. A non-shrinking hydraulic grout — MasterFlow928 produced by BASF — at various high temperatures and high viscosity levels was used to fill all vertical and horizontal gaps around the pile. Eleven (11) mockup specimens were constructed throughout a two (2) phase (Task 1 and Task 2) experimental program and each one was systematically filled and tested in the laboratory. All results and findings were documented and analyzed, before the discussion lead to the following conclusions:.

- Despite the fact that the manufacturer's recommended water-to-material ratios do not lead to the manufacturer specified viscosities — the material actually becomes more viscous — the quality of the fresh grout is still acceptable with a proper flow behavior and adequate fillability.
- The targeted fresh grout temperatures and viscosities were easily realized in the laboratory. While it was necessary in some cases to incorporate ice into the grout mixture to reach the desired temperatures, the temperature of the grout powder had a more significant impact on the initial fresh grout properties.
- The generally used material for mockup specimens — plywood — performed well and did not impede the flow or fillability properties of the grout material. No significant differences between the control specimen with a concrete pile head and the other pile head models made from plywood were observed.
- The fresh material should always be pumped into the connection detail through the duct that is located above the most narrow opening, to avoid delayed and uneven grout flow, that otherwise may lead to air entrapment.
- To minimize durability issues, a slope of approximately 7% — towards the influent pipes along the centerline of the pile-pocket — should be built into the roof of the pile-pocket, because an inclined top surface reduces air entrapment at the top grout-to-bent cap interface.

- The fresh grout at the upper level of the manufacturer temperature range and an efflux time of up to 48 s according to ASTM C939 appears unproblematic, because even smaller gap size with 0.5 in. (0.5 mm) openings were satisfactorily filled, without significant air voids.
- Within a 15 min to 20 min delay between individual batches, the layering effect appears to be no concern for the evaluated grout material, even under high temperatures and increased viscosity levels.
- If practical and/or feasible, the gap thickness of the grout volume should be limited to a maximum size, for hot weather grouting, to avoid critical curing temperatures throughout the hydration process. While this research study suggests a limiting thickness of less than 4 in. (100 mm), due to high curing temperatures, further research would be necessary to evaluate the durability and long-term issues of thicker grout volumes.
- Within the tested temperature and viscosity ranges, the compressive strength of companion cast grout cubes with a 2.0 in. (50 mm) edge length consistently met the requirements of FDOT Specification Section 934-4.1, as well as the manufacturer target values.

Bibliography

- ASTM-International (2014a). “ASTM C230/C230M-14 — Standard Specification for Flow Table for Use in Tests of Hydraulic Cement. West Conshohocken, PA.
- ASTM-International (2014b). “ASTM C989/C989M-14 — Standard Specification for Slag Cement for use in Concrete and Mortars. West Conshohocken, PA.
- ASTM-International (2015a). “ASTM C1240-15 — Standard Specification for Silica Fume Used in Cementitious Mixtures. West Conshohocken, PA.
- ASTM-International (2015b). “ASTM C618-15 — Standard Specification for Coal Ash and Raw or Calcined Natural Pozzolan for Use in Concrete. West Conshohocken, PA.
- ASTM-International (2016a). “ASTM C494/C494M-16 — Standard Specification for Chemical Admixtures for Concrete. West Conshohocken, PA.
- ASTM-International (2016b). “ASTM C939/C939M-16a — Standard Test Method for Flow of Grout for Preplaced-Aggregate Concrete (Flow Cone Method). West Conshohocken, PA.
- ASTM-International (2016c). “ASTM C1019-16 — Standard Test Method for Sampling and Testing Grout. West Conshohocken, PA.
- ASTM-International (2016d). “ASTM C109/C109M-16a — Standard Test Method for Compressive Strength of Hydraulic Cement Mortars (Using 2-in. or [50-mm]). West Conshohocken, PA.
- Ballantyne, A. (2012). (*Key buildings from prehistory to the present plans, sections and elevations*). Laurence King Pub, London.
- BASF Construction Chemicals UAE LLC (2014). *MasterFlow 928*. Dubai.
- BASF Corporation Construction Systems (2016). *MasterFlow 928 - Technical Data Guide*. 889 Valley Park Drive, Shakopee MN 55379.

- Bazant, Z. P. (2000). “Size effect.” *International Journal of Solids and Structures*, 37(1-2), 69–80.
- Biscopig, D.-I. M. and Richter, D.-I. T. (2013). *Frischbeton, Eigenschaften und Prüfungen*. Verein Deutscher Zementwerke e.V.,.
- Blanks, R. F. and McNamara, C. C. (1935). “Mass concrete tests in large cylinders.” *ACI Journal Proceedings*, 31(1), 280–303.
- Bosold, D.-I. D. and Pickhardt, D.-I. R. (2014). *Zemente und ihre Herstellung*. BetonMarketing West GmbH.
- Bullard, J. W., Jennings, H. M., Livingston, R. A., Nonat, A., Scherer, G. W., Schweitzer, J. S., Scrivener, K. L., and Thomas, J. J. (2011). “Mechanisms of cement hydration.” *Cement and Concrete Research*, 41(12), 1208–1223.
- Do, Q. H., Bishnoi, S., and Scrivener, K. L. (2016). “Microstructural modeling of early-age creep in hydrating cement paste.” *Journal of Engineering Mechanics*, 142(11), 385–388.
- Domone, P. and Jefferis, S. (1994a). *Structural Grouts, Chapter 1 Chemical and physical structure of cement grouts*, (1st Edition). Blackie Academic & Professional, an imprint of Chapman & Hall, Glasgow.
- Domone, P. and Jefferis, S. (1994b). *Structural Grouts, Chapter 2 Fresh properties of Portland cement grouts*, (1st Edition). Blackie Academic & Professional, an imprint of Chapman & Hall, Glasgow.
- Domone, P. and Jefferis, S. (1994c). *Structural Grouts, Chapter 3 Hardened properties of Portland cement grouts*, (1st Edition). Blackie Academic & Professional, an imprint of Chapman & Hall, Glasgow.
- Draganović, A. and Stille, H. (2012). “Bleeding and bleeding measurement of cement-based grout.” *Grouting and Deep Mixing*, 1681–1690.
- Ebbing, C. (2016). “Grout behavior on hot weather conditions - pile pocket specimen tests for accelerated bridge constructions.” mthesis, Fachhochschule Muenster, Münster.
- Florida Department of Transportation (2013). *Specifications Package — Special Provisions*. Financial Project ID(S). 422823-1-52-01.
- Fluke Corporation (2010). *FLUKE 56x Infrared Thermometers Users Manuals*.
- Gonnerman, H. F. (1925). “Effect of size and shape of test specimen on compressive strength of concrete.” *Proceedings of the American Society of Testing Materials*, 25(2), 1–18.
- Ham, S. and Oh, T. (2013). “Effect of mixing and placing in hot weather on hardened concrete properties.” *International Journal of Concrete Structures and Materials*, 7(2), 165–174.

- Indelicato, F. and Paggi, M. (2008). "Specimen shape and the problem of contact in the assessment of concrete compressive strength." *Materials and Structures*, 41(2), 431–441.
- Kampmann, R. (2012). "The influence of the compression interface on the failure behaviour and size effect of concrete," Dissertation, The Florida State University.
- Kampmann, R., Roddenberry, M., and Ping, W. V. (2013). "Contribution of specimen surface friction to size effect and rupture behavior of concrete." *ACI Materials Journal*, 110(2), 169–176.
- Khayat, K. H., Yahia, A., and Sayed, M. (2008). "Effect of supplementary cementitious materials on rheological properties, bleeding, and strength of structural grout." *ACI Materials Journal*, 105(6), 585–593.
- Lea, F. M. (1970). *The Chemistry of Cement and Concrete, Chapter 10 The Setting and Hardening of Portland Cement*, (2rd Edition). Chemical Publishing Company INC., London.
- Malhotra, V. M. (1976). "Are 4 x 8 inch concrete cylinders as good as 6 x 12 inch cylinders for quality control of concrete?." *ACI Journal Proceedings*, 73(1), 33–36.
- Mehta, P. K. and Monteiro, P. J. M. (2005). *Concrete: Microstructure, Properties, and Materials*, (3rd Edition). McGraw-Hill Professional, New York.
- N/A (1976). "Luftlöcher in der betonoberfläche." *Cementbulletin*, 10(1), N/A. supported by Technische Forschungs- und Beratungsstelle der Sschweizerischen Zementindustrie.
- Neville, A. M. (2006). (*Concrete: Neville's Insights and Issue*). Institution of Civil Engineers Publishing, London.
- Padevet, P. and Bittnar, P. (2015). "Creep of cement pastes with content of fly ash one year old." *Applied Mechanics and Materials*, 732, 385–388.
- Park, S.-J. (2009). "A study on the surface air-void reduction of high performance concrete." *Journal of the Korea institute of building construction*, 9(1), 49–55.
- Popovics, S. (1998). *Strength and Related Properties of Concrete: A Quantitative Approach*, (1st Edition). John Wiley & Sons, Inc., New York.
- Rixom, R. and Mailvaganam, N. (1999). *Chemical Admixtures for Concrete*, (3rd Edition). E & FN Spon, London.
- Roddenberry, M., Kampmann, R., Ansley, M. H., Bouchard, N., and Ping, W. V. (2011). "Failure behavior of concrete cylinders under different end conditions." *ACI Materials Journal*, 108(1), 79–87.

- Roddenberry, P. P. M. and Servos, E. J. (2012). “*Prefabricated/precast bridge elements and systems (pbes) for o-system bridges - chapter 1 introduction.*” resreport, FAMU-FSU College of Engineering Department of Civil and Environmental Engineering, Tallahassee. FSU Project ID: 029858.
- Shannag, M. J. (2002). “High-performance cementitious grouts for structural repair.” *Cement and Concrete Research*, 32(5), 803–808.
- Soroka and Ravina (1998). “Hot weather concreting with admixtures.” *Cement and Concrete Composites*, 20(2-3), 129–136.
- Steve Nolan, P. (2015). “PBES — Precast Bent Cap Development and Implementation. Design Training Expo. Presentation.
- Tan, O., Zaimoglu, A. S., Hınıslioglu, S., and Altun, S. (2005). “Taguchi approach for optimization of the bleeding on cement-based grouts.” *Tunnelling and Underground Space Technology*, 20(2), 167–173.
- The QUIKRETE Companies (2016). *Cement Color (Liquid) Product No. 1317 Divison 9*. 3490 Piedmont Rd., NE, Suite 1300, Atlanta, GA 30305.
- Torrenti, J.-M., Pijaudier-Cabot, G., and Reynouard, J.-M. (2010). *Mechanical Behavior of Concrete*, (1st Edition). John Wiley & Sons, Inc., London.
- Toumbakari, E.-E., Gemert, D. V., Tassios, T., and Tenoutasse, N. (1999). “Effect of mixing procedure on injectability of cementitious grouts.” *Cement and Concrete Research*, 29(6), 867–872.
- van Mier, J. G. M. and Man, H.-K. (2009). “Some notes on microcracking, softening, localization, and size effects.” *International Journal of Damage Mechanics*, 18(3), 283–311.
- Vikie Young, P. and Dennis Golabek, P. (2016). “*Full-depth precast deck panel testing.*” resreport, Florida Department of Transportation (FDOT), Tallahassee.
- Wilson, M. L. and Kosmatka, S. H. (2011). *Design and Control of Concrete Mixtures - The guid to applications, methods, and materials*, (15th Edition). Portland Cement Association, Chicago.
- Yazici, S. and Sezer, G. I. (2007). “The effect of cylindrical specimen size on the compressive strength of concrete.” *Building and Environment*, 42(6), 2417–2420.